Elucidating the role of Glycoside Hydrolase 25 in microbial antagonism

Inaugural-Dissertation

zur

Erlangung des Doktorgrades

der Mathematisch-Naturwissenschaftlichen Fakultät

der Universität zu Köln

vorgelegt von

Priyamedha Sengupta

aus Kolkata

Köln, 2022

Die Untersuchungen zur vorliegenden Arbeit wurden von Januar 2019 bis September 2022 am Lehrstuhl für Terrestrische Mikrobiologie an der Universität zu Köln unter der Betreuung von Herrn Prof. Dr. Gunther Doehlemann durchgeführt.

Erstgutachter: Prof. Dr. Gunther Doehlemann

Zweitgutachter: Prof. Dr. Bart Thomma

Tag der mündlichen Prüfung: 23.01.2023

"It's the possibility of having a dream come true that makes life interesting."

— Paulo Coelho, The Alchemist

Summary:

Plant organs are colonized by microorganisms, ranging from beneficial, commensals and pathogenic, which interact among themselves to establish a community. Rhizosphere microbiota is extensively characterized regarding their roles in protection of host plant against pathogenic microbes and in overall plant growth and development. However, the phyllosphere is also enriched with microbial interactions, aiding in plant immunity and protection.

In this study, it was shown how a basidiomycete yeast *Moesziomyces bullatus* ex *Albugo* on *Arabidopsis* (*MbA*) antagonizes the white rust pathogen *Albugo laibachii* by expressing Glycoside Hydrolase 25 (GH25) protein on *Arabidopsis thaliana*. Recombinantly produced *MbA*_GH25 also reduced *A. laibachii* growth *in-planta*, identifying the hydrolase gene to be a major effector of *MbA* mediated antagonism. GH25 proteins are present in various plant-associated fungi, however, their mechanism of action is unknown. To elucidate the mechanism behind *MbA*_GH25 activity, two strategies were employed: firstly, testing purified *MbA*_GH25 as an elicitor of plant immunity and secondly, analyzing the impact of *MbA*_GH25 on bacterial associations of *A. laibachii*.

The potential antagonistic activity of *MbA*_GH25 towards the oomycetes *Hyaloperenospora arabidopsidis* and *Phytophthora infestans* have been investigated as well. Alongside the role of GH25 in related smut pathogen, *U. maydis* has been explored in this study to understand the impact of the hydrolase gene expression on fungal pathogenicity. Taken together, we functionally characterize the role of fungal GH25 proteins to deepen our understanding of microbial interactions in the phyllosphere and carve a path for the development of newer antimicrobials for plant protection.

List of Abbreviations:

°C	Degree Celsius
x g	Gravitational acceleration on earth (9.81m/s2)
µg	Microgram
µl	Microliter
µm	Micrometer
µM	Micromolar
A	Alanine
aa	Amino acid
ABA	Abscisic acid
APS	Ammonium persulphate
BAK1	BRI1-associated receptor kinase 1
bp	Base pair
Carb	Carbenicillin
CAZy	*Carbohydrate-Active Enzyme*
Cbx	Carboxin
cDNA	Complementary DNA
CDS	Coding sequence
CERK1	Chitin receptor kinase 1
Cmu1	Chorismate mutase 1
D	Aspartate
CWDE	Cell Wall degrading enzyme
DMSO	Dimethylsulfoxid
DNA	Deoxyribonucleic acid
dNTP	Deoxynucleoside triphosphates
dpi	days post infection
DTT	Dithiotreitol
E	Glutamate
EDTA	Ethylenediaminetetraacetic acid
Ef1-α	Elongation Factor 1 alpha
ETI	Effector-triggered immunity
EtOH	Ethanol
f.c.	Final concentration

List of Abbreviations

Flg22	Bacterial Flagellin peptide
FLS2	Flagellin-Sensitive 2
g	Gram
Gent	Gentamycin
GH	Glycoside Hydrolase
h	hour
H2Obid	Double distilled water
His	Histidine
HK	Heat-killed
ID	Identifier
ip	Iron–sulphur protein subunit of succinate dehydrogenase
ITS	Internal Transcribed Spacer
JA	Jasmonic acid
Kan	Kanamycin
kb	Kilobases
kDa	Kilodalton
KOH	Potassium Hydroxide
LRR	Leucine rich repeat
LysM	Lysin motif
M	Molar
MAMP	Microbe-associated molecular pattern
MAPK	Mitogen-activated protein kinase
MeOH	Methanol
MgCl2	Magnesium chloride
MgSO4	Magnesium sulphate
min	Minute(s)
ml	Millilitre
mRNA	Messenger RNA
NaCl	Sodium Chloride
ng	Nanogram
Ni	Nickel
NLR	Nucleotide binding leucine rich repeat protein
nm	Nanometer
No.	Number

List of Abbreviations

nt	Nucleotide
NTA	Nitrilotriacetic acid
O/N	Over-night
OD	Optical density
p	Statistical probability value
PAGE	Polyacrylamide gel electrophoresis
PAMP	Pathogen-associated molecular pattern
PCR	Polymerase chain reaction
PCWDE	Plant Cell Wall Degrading Enzyme
Pep1	Protein essential during penetration 1
PGN	Peptidoglycan
PI	Propidium iodide
Pit2	Protein involved in tumors 2
PRR	Pattern Recognition Receptor
PTI	Pattern-triggered immunity
qPCR	Quantitative polymerase chain reaction
qRT-PCR	Quantitative real-time polymerase chain reaction
Rif	Rifampicin
RNA	Ribonucleic acid
rpm	Revolutions per minute
RT	Room temperature
s	Seconds
SA	Salicylic acid
SDS	Sodium Dodecyl Sulphate
TE-buffer	Tris-EDTA buffer solution
TEMED	Tetramethylethylenediamine
Tin2	Tumor inducing 2
U	Unit (Enzyme activity)
V	Volt
v/v	Volume/volume
w/v	Weight/volume
WGA	Wheat germ agglutinin

List of Figures:

1. Introduction:

Figure 1. 1 Oomycetes of different lifestyles ..... - 3 -
Figure 1. 2 Importance of microbial association in the phyllosphere ..... - 8 -
Figure 1. 3 Schematic diagram of Plant Cell-Wall Degrading Enzymes (CWDEs) ..... - 10 -
Figure 1. 4 Life cycle of *Ustilago maydis* ..... - 12 -
Figure 1. 5 Basidiomycete yeast, *MbA* antagonizes *Albugo laibachii* ..... - 14 -

2. Results:

Figure 2. 1 Quantification and visualization of *MbA* antagonism on *A. laibachii* ..... - 17 -
Figure 2. 2 Recombinant expression of *MbA*_GH25 ..... - 18 -
Figure 2. 3 Biochemical Characterization of *MbA*_GH25 ..... - 19 -
Figure 2. 4 Characterization of *MbA*_GH25 effect on Plant immunity ..... - 21 -
Figure 2. 5 Confrontation assay between bacterial strains and *MbA* /*U. maydis* ..... - 23 -
Figure 2. 6 Effect of *MbA* and *MbA*_GH25 on *Hyaloperenospora arabidopsidis* ..... - 25 -
Figure 2. 7 Effect of *MbA* and *MbA*_GH25 on *Phytophthora infestans* ..... - 27 -
Figure 2. 8 *Agrobacterium* based transient expression of *MbA*_GH25 ..... - 28 -
Figure 2. 9 Effect of UMAG_02727 overexpression on *U. maydis* virulence ..... - 30 -
Figure 2. 10 Analysis of maize defense marker gene induction ..... - 31 -

6. Appendix:

Figure 6.2. 1 Visualization of purified *MbA*_GH25 ..... - 101 -
Figure 6.2. 2 Detection of lysozyme activity for commercial Hen-egg white lysozyme (HEWL) ..... - 101 -
Figure 6.2. 3 *Hpa* infection in Col-0 vs *eds1-12* ..... - 102 -
Figure 6.2. 4 Transient expression of *MbA*_GH25 using Myc-epitope ..... - 103 -
Figure 6.2. 5 Functional characterization of UMAG_02727 ..... - 104 -
Figure 6.2. 6 Mechanism of *MbA*_GH25 antagonism ..... - 105 -
Figure 6.2. 7 Difference in gene expression pattern between Pit2 and Actin ..... - 106 -

List of Tables:

Table 4. 1 Chemical reagents and their purpose of use ..... - 46 -
Table 4. 2 Commercial kits ..... - 47 -
Table 4. 3 Media used in this study along with their compositions ..... - 48 -

List of Figures and Tables

Table 4. 4 Antibiotics used for *MbA* and *U. maydis* cultivation ..... - 50 -
Table 4. 5 Antibiotics used for cultivation of *A. tumefaciens* ..... - 51 -
Table 4. 6 *A. laibachii* associated bacteria ..... - 52 -
Table 4. 7 *MbA* strains used in this study ..... - 53 -
Table 4. 8 *U. maydis* strains used in this study ..... - 53 -
Table 4. 9 *P. pastoris* strains used in this study ..... - 54 -
Table 4. 10 *A. tumefaciens* strains used in the study ..... - 54 -
Table 4. 11 Oligonucleotides used in this study ..... - 56 -
Table 4. 12 Antibodies used in this study ..... - 70 -
Table 4. 13 *U. maydis* disease scoring in *Z. mays* ..... - 74 -

Table of contents:

Summary: ..... **I**

List of Abbreviations: ..... **II**

List of Figures: ..... **V**

List of Tables: ..... **V**

1. Introduction: ..... **- 1 -**

1.1 Impact of pathogens in agriculture ..... - 1 -

1.1.1 Oomycetes as Plant pathogens ..... - 2 -

1.2 Host associated microbial communities ..... - 5 -

1.2.1 Importance of the phyllosphere microbiome in plant protection ..... - 5 -

1.2.2 Interaction of phyllosphere microbiome with plant hosts ..... - 6 -

1.2.3 Basidiomycete yeasts as biological control agents ..... - 8 -

1.3 Role of Glycoside Hydrolase proteins in pathogen infection and plant immunity ... - 10 -

1.3.1 Role of GH proteins in biological control of pathogens ..... - 11 -

1.3.2 Role of GH proteins in the smut fungus *Ustilago maydis* ..... - 12 -

1.4 Antagonism of *Albugo laibachii* by basidiomycete yeast, *MbA* ..... - 13 -

1.5 Aim of this study ..... - 15 -

2. Results: ..... **- 17 -**

2.1 Functionally characterizing the role of *MbA*_GH25 in *A. laibachii* antagonism on *A. thaliana* leaves ..... - 17 -

2.2 Elucidating the mechanism behind *MbA*_GH25 activity against *A. laibachii*: ..... - 20 -

2.2.1 *MbA*_GH25 as an elicitor of plant immunity ..... - 20 -

2.2.2 GH25 inhibits bacteria associated with *A. laibachii* ..... - 22 -

2.3 Analyzing the impact of GH25 on oomycetes of different lifestyle ..... - 23 -

2.3.1 Effect of *MbA* and *MbA*_GH25 on *Hyaloperenospora arabidopsidis* (*Hpa*) ..... - 23 -

2.3.2 Effect of *MbA* and GH25 on *Phytophthora infestans* ..... - 26 -

2.4 Functional Characterization of GH25 from *U. maydis*: ..... - 29 -

3. Discussion: ..... **- 35 -**

3.1 *MbA* antagonizes the white rust pathogen *Albugo laibachii* via GH25 protein ..... - 35 -

Table of contents

3.2 Antagonism of *A. laibachii* by *MbA*_GH25 is not explained by activation of host immune responses ..... - 36 -
3.3 Antagonism of *A. laibachii* by *MbA*_GH25 might result from the inhibition of associated bacteria ..... - 37 -
3.4 *MbA* is not antagonizing the downey mildew pathogen *Hyaloperenospora arabidopsidis* ..... - 40 -
3.5 *Phytophthora infestans* is not affected by *MbA* ..... - 41 -
3.6 Overexpression of UMAG_02727 in *U. maydis* leads to reduction of virulence ..... - 42 -
3.7 Conclusion and future directions ..... - 43 -

4. Material and methods: ..... - 46 -
4.1 Material ..... - 46 -
4.1.1 Chemicals ..... - 46 -
4.1.2 Buffers and solutions ..... - 46 -
4.1.3 Enzymes ..... - 46 -
4.1.4 Commercial kits ..... - 47 -
4.2 Media and growth conditions for microorganisms ..... - 48 -
4.2.1 Media ..... - 48 -
4.2.2 Propagation of *A. laibachii* ..... - 49 -
4.2.3 Cultivation of *E. coli* ..... - 50 -
4.2.4 Cultivation of *A. laibachii* associated bacteria ..... - 50 -
4.2.5 Cultivation of *MbA* and *U. maydis* ..... - 50 -
4.2.6 Cultivation of *Pichia pastoris:* ..... - 50 -
4.2.7 Cultivation of *A. tumefaciens*: ..... - 51 -
4.2.8 Determination of cell density: ..... - 51 -
4.3 Microbial Strains and Oligonucleotides: ..... - 51 -
4.3.1. *Albugo laibachii* ..... - 51 -
4.3.2 *Hyaloperenospora arabidopsidis* ..... - 51 -
4.3.3 *Phytophthora infestans* ..... - 52 -
4.3.4 *Escherechia coli* ..... - 52 -
4.3.5 *A. laibachii* associated bacteria ..... - 52 -
4.3.6 *MbA* and *U. maydis* strains ..... - 52 -
4.3.7. *Pichia pastoris* ..... - 53 -
4.3.8 *Agrobacterium tumefaciens*: ..... - 54 -
4.3.9. Plasmids ..... - 55 -

Table of contents

4.3.9.1 Plasmids for transformation in *U. maydis* ..... - 55 -

4.3.9.2 Plasmids for the expression of recombinant proteins in *P. pastoris* ..... - 55 -

4.3.10 Oligonucleotides ..... - 56 -

4.4 Microbiological methods ..... - 61 -

4.4.1 Transformation of *E. coli* ..... - 61 -

4.4.2 Transformation of *U. maydis* ..... - 62 -

4.4.3 Transformation von *P. pastoris* ..... - 63 -

4.4.4 Stress assay of *MbA*/*U. maydis* strains ..... - 63 -

4.4.5 Microbial confrontation assays ..... - 64 -

4.5 Molecular biological methods ..... - 64 -

4.5.1 Isolation of nucleic acids ..... - 64 -

4.5.1.1 Plasmid DNA isolation from *E. coli* ..... - 64 -

4.5.1.2 Genomic DNA extraction of *MbA*/*U. maydis* ..... - 65 -

4.5.1.3 Total RNA extraction from leaf tissue ..... - 66 -

4.5.1.4 DNase-digest after RNA extraction ..... - 66 -

4.5.1.5 Synthesis of cDNA ..... - 66 -

4.5.2 Purification of nucleic acid ..... - 67 -

4.5.3 In vitro modification of nucleic acids ..... - 67 -

4.5.3.1 Restriction enzyme digestion of DNA ..... - 67 -

4.5.3.2 Ligation of DNA fragments ..... - 67 -

4.5.3.3 Gibson Assembly cloning ..... - 67 -

4.5.3.4 Polymerase Chain reaction (PCR) ..... - 67 -

4.5.3.5 Sequencing of DNA ..... - 67 -

4.5.4 Agarose gel electrophoresis for nucleic acid separation and detection ..... - 68 -

4.6 Biochemical methods ..... - 68 -

4.6.1 Separation of proteins via SDS-PAGE ..... - 68 -

4.6.2 Immunological detection of proteins via chemiluminescence (Western blot) ..... - 69 -

4.6.3 Expression of heterologous proteins in *P. pastoris* ..... - 70 -

4.6.4 Biochemical activity assay of *MbA*_GH25 protein ..... - 71 -

4.7 Plant methods ..... - 72 -

4.7.1 Plant material and growth conditions ..... - 72 -

4.7.2 Seed sterilization ..... - 72 -

4.7.3 Infection of *A. thaliana* with *A. laibachii* ..... - 72 -

4.7.4 Infection of *A. thaliana* with *Hpa* ..... - 73 -

Table of contents

4.7.5 Infection of *Z. mays* with *U. maydis* ..... - 74 -
4.7.6 Infection of *N. benthamiana* with *P. infestans* ..... - 74 -
4.8 Microscopy ..... - 75 -
4.8.1 Trypan blue staining to visualize *A. laibachii in planta* ..... - 75 -
4.8.2 WGA-AF488/Propidium iodide staining of *U. maydis in planta* ..... - 75 -
4.8.3 Fluorescence microscopy ..... - 76 -
4.9 Computational analysis ..... - 76 -

5. Bibliography: ..... - 78 -

6. Appendix: ..... - 95 -

Erklärung zur Dissertation: ..... - 109 -

Delimitation of own contribution: ..... - 111 -

Acknowledgements: ..... - 113 -

Curriculam vitae: ..... - 115 -

1. Introduction:

1.1 Impact of pathogens in agriculture

Plants are susceptible to disease outbreaks caused by pathogenic microorganisms like bacteria, fungi, and viruses. Diseases in crop plants, in turn, can affect food availability and human consumption (Savary et al., 2017). A study by Savary et al., (2019) reported 137 pathogens and pests causing yield losses ranging from 17-30% in wheat, rice, maize, potato, and soybean across the world. Higher yield losses were reported from fast growing population and re-emergence of pathogenic strains occurred in several instances (Savary et al., 2019).

Monoculture farming practices and global trading potentially contribute to emergence and spread of pathogens (Fones et al., 2020). Pests and pathogens occupy ecological niches and respond to certain environmental conditions, which in turn, determine their geographical spread and time of infections (Chaloner et al., 2020; Fones et al., 2020). At the same time, climate change is predicted to cause a shift in pathogenic survival and spread resulting in additional hurdles for crop disease management (Chaloner et al., 2021). In fact, a study by (Delgado-Baquerizo et al., 2020) stated that the global distribution of soil borne pathogens is majorly driven by temperature.

Amongst the group of microorganisms, fungal pathogens cause many devastating plant diseases. The rice blast pathogen *Magnaporthe oryzae*, can cause yield loss of up to 50% and increase production cost of the crop (Nalley et al., 2016; Skamnioti and Gurr, 2009). *Botrytis cinerea* is another fungal pathogen that has a broad host range and can cause yield losses of $10 billion to $100 billion annually (Weiberg et al., 2013). Control of *B. cinerea* is heavily dependent on the use of chemical fungicides, consuming 8% of the global fungicide market (De Angelis et al., 2022).

Spraying chemical pesticides are an effective means for curbing plant diseases and increasing crop yield. However, chemical residues in the soil can potentially impact biodiversity and affect human health and environment by groundwater contamination and leaching. At the same time, fungal pathogens either have natural resistance or can rapidly acquire resistance against fungicides, whereby the chemicals are rendered non-functional in the event of diseases. Stable natural resistance has been reported for *Fusarium*, infecting cereal crops such as wheat, barley, oat, and maize (de Chaves et al., 2022; Yerkovich et al., 2020). *Fusarium* shows intrinsic resistance towards a wide group of antifungals such as amphotericin B, itraconazole, fluconazole and echinocandins (Al-Hatmi et al., 2019).

1. Introduction

Several molecular mechanisms have been proposed for fungicide resistance such as 'an altered target site in the fungus, which reduces the binding of the fungicide; synthesis of an alternative enzyme capable of substituting the target enzyme or an overproduction of fungicide target/ metabolic breakdown of fungicide' (Ma and Michailides, 2005). For example, barley powdery mildew *Blumeria graminis* f. sp. *hordei* is insensitive to demethylase inhibitor group of fungicides due to point mutation in *cyp51* gene (Zulak et al., 2018). Fungicide resistance has become a major problem in agriculture since introduction of single-site fungicide (Ma and Michailides, 2005) which target specific residues in the fungal cell walls. As a result, certain group of fungi although initially susceptible, can acquire secondary mechanisms of resistance after exposure to antifungals by selection of resistant clones (Perlin et al., 2017), for e.g., mutation in cyp51A gene in *Aspergillus fumigatus,* which causes resistance to azole group of fungicides.

Therefore, to feed a growing world population, there is a pressing need to introduce sustainable measures of crop protection. Extensive genetic knowledge about plant-microbial interactions can lead to development of sustainable plant protection strategies.

1.1.1 Oomycetes as Plant pathogens

Oomycetes are a taxonomically distinct group of eukaryotic organisms, which cluster together with brown Algae and diatoms in the Phylum Stramenopiles. Many devastating plant pathogens belong to oomycetes, for e.g., *Phytophthora infestans*, the causal agent of late blight disease of potato, that resulted in the Irish famine in 1845. Other species of *Phytophthora*, namely *P. ramorum, P. capsici* and *P. sojae* are known to affect oak trees, solanaceous crops, and Soyabean, respectively (Kamoun et al., 2015).

Oomycetes consist of two major subclasses; first one being Saprolegniomycetidae which consist of Aphanomyces and Saprolegnia, infecting fishes, and other aquatic animals (Phillips et al., 2008). Second major subclass of oomycetes is Peronosporomycetidae, which comprise the plant infecting oomycetes and consist of the orders Rhipidiales, Pythiales, and Peronosporales. Oomycetes mainly reproduce asexually by release of zoospore which germinate on the plant surface to develop appressoria and colonize the host tissue by hyphal branching (Fawke et al., 2015). However, the mode of infection by oomycetes differs depending on their lifestyle. Plant pathogenic oomycetes can have different lifestyles such as biotrophic, hemi-biotrophic and necrotrophic. *Albugo laibachii* and *Hyaloperenospora arabidopsidis (Hpa)* are commonly occurring biotrophic pathogens of *Arabidopsis thaliana*, which require

living host cells to establish infection (Herlihy et al., 2019; Holub, 2008). In contrast, *Phytophthora* exhibits hemi-biotrophic lifestyle where, highly invasive hyphae colonize plant cells and eventually feed on dead plant tissue as necrotrophs (Zuluaga et al., 2016). Some species of *Pythium* (e.g., *P. ultimum*) are necrotrophs, which cause damping off and rot of over 300 plant species including economically important crops like wheat, maize, and soybean (Kamoun et al., 2015).

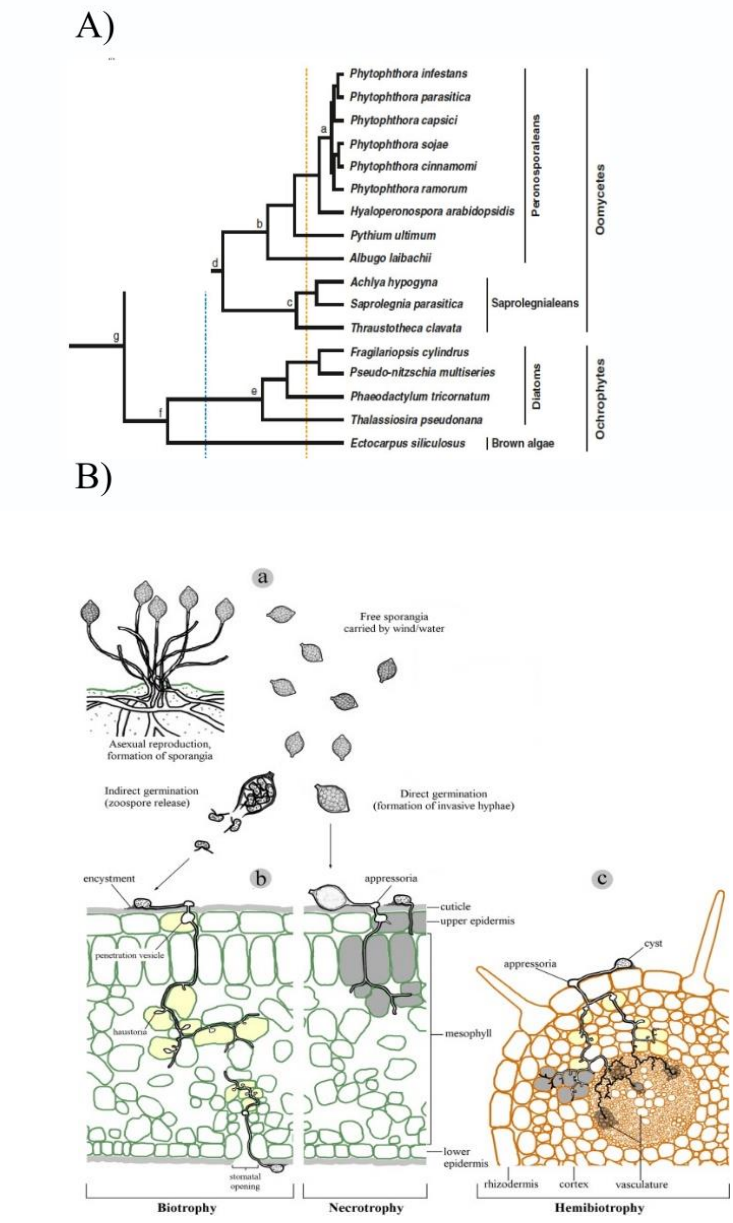

Figure 1. 1 Oomycetes of different lifestyles

A)-Phylogenetic distribution of oomycetes (adapted from Herlihy et al., 2019). B)- Infection strategies and lifestyles of selected oomycetes. (a) Typical asexual *Phytophthora* dispersal structures. (b) Leaf colonization. (c) Root colonization. Two methods of germination (direct germination from sporangia and indirect germination from zoospores) are depicted. Following germination, depending on the species, oomycetes perform biotrophy (e.g., *Hyaloperonospora arabidopsidis* or *Albugo laibachii*, the

latter often entering through stomata and then forming appressoria), necrotrophy (e.g., *Pythium ultimum*), or hemibiotrophy (e.g., *Phytophthora sojae* or *Phytophthora palmivora*). Cells which have been colonized by a biotrophic pathogen are highlighted in yellow, while those that are undergoing cell death because of necrotrophy are shaded gray. In the case of a hemibiotrophic oomycete colonizing a root, the interaction is initially biotrophic, while the oomycete spreads through the cortex, but once the oomycete is established and hyphae have entered the endodermis and vasculature, necrotrophy can be observed (adapted from Fawke et al., 2015).

Plant immunity is essentially a two-tier system which includes Pattern triggered immunity (PTI) and Effector triggered immunity (ETI). During PTI, plants can recognize conserved residues in the pathogen (Pathogen Associated Molecular Patterns-PAMPs) which led to Hypersensitive responses. For example, detection of oomycete elicitin infestin 1 (INF1) triggers programmed cell death (Kamoun et al., 1998) and restricts pathogen growth. Nevertheless, pathogens can evade PTI by releasing effector molecules which suppress host defense responses. Majority of oomycete effectors are proteinaceous, with the except of small RNAs (Dunker et al., 2020). Oomycete effectors can target host transcription factors (TFs) to modify host physiology (Fabro, 2022). Effectors having RXLR motifs have been described for Perenosporales members; for e.g., *Phytophthora infestans* RXLR effector PITG20303 targets potato MAPK cascade protein to promote pathogen colonization (Du et al., 2021). Whereas members of Albuginales encode RxLs and many CHxCs/CGGs effectors (Furzer et al., 2022; Petre et al., 2021).

However, plants can recognize effector molecule by intracellular nucleotide-binding domain/leucine-rich repeat (NLR-LRR) receptors during effector-triggered immunity (ETI) (Bhandari et al., 2019; Jones et al., 2016). In plants, ETI activates several transcription factors including pathogenesis related genes involved in synthesis of salicylic acid (SA), ethylene (ET),and jasmonic acid (JA). ENHANCED DISEASE SUSCEPTIBILITY 1 (EDS1) is a plant specific protein that was identified to be a regulator of SA and in defense against biotrophic pathogens such as *Hyaloperenospora arabidopsidis* (Parker et al., 1996). Later, it was discovered that EDS-1 that forms heterodimeric complexes with PAD4 or SAG101 and act as hubs of plant innate immunity (Dongus et al., 2022; Lapin et al., 2020). Therefore, understanding oomycete effector biology and plant immunity pathways can provide the basis for plant protection against pathogens.

1.2 Host associated microbial communities

The term '*Holobiont*' was coined by Lynn Margulis in 1991 to put forward the concept that animals and plants are not autonomous entities, but rather form a unit together with the associated microbial communities (Bordenstein and Theis, 2015). Rosenberg et al., (2007), while analyzing symbiotic microbial population of corals, proposed the concept of the '*Hologenome*' which states 'microorganisms have an important role in the evolution of animals and plants. 'At the same time, the hologenome is defined as a sum of the 'genetic information of the host and its microbiota' (Zilber-Rosenberg and Rosenberg, 2008). For example, the human hologenome consists of more than 33 million genes compared to human genome which consists of 20,000 genes (Simon et al., 2019).

The first definition of the microbiome was put forward by Whipps et al., working on microbial ecology of the rhizosphere (Whipps J, Lewis K, 1988). The microbiome was initially defined as a "characteristic microbial community" in a "reasonably well-defined habitat which has distinct physio-chemical properties" as their "theatre of activity" (Berg et al., 2020). The microbiome can impact the host's evolutionary potential, as it can increase the genetic repertoire of the host (Henry et al., 2021). The human gut microbiome plays a vital role in host fitness and health and even considered an organ of the human body (Baquero and Nombela, 2012; Valdes et al., 2018).

Plant organs are inhabited by a diverse group of microorganisms which interact with each other, as well as the host on which they reside. Bacteria, fungi, protists, nematodes, and viruses colonize all accessible plant tissues (Trivedi et al., 2020). Beneficial interactions between plants and their associated microbiota have been proposed to play important roles in setting up sustainable cropping system (Cesaro et al., 2021). Recent research has focused largely on the importance of the rhizosphere microbiota in nutrient acquisition, protection from pathogens, and boosting overall plant growth and development (Bulgarelli et al., 2013; Ritpitakphong et al., 2016; Walker et al., 2003). However, the above ground parts of the plant including the phyllosphere are colonized by diverse groups of microbes which also assist in plant protection and immunity (Busby et al., 2016; Mikiciński et al., 2016).

1.2.1 Importance of the phyllosphere microbiome in plant protection

The aerial parts of terrestrial plants, such as leaves, flowers, fruits, buds, and stems, collectively called 'phyllosphere', harbor a complex community of microorganisms (Vorholt, 2012). Microbes colonize the phyllosphere either as epiphytes or endophytes and are collectively

known as Phyllosphere microbiome (Shakir et al., 2021). Epiphytic microbes can help in defense against pathogens, sequester carbon, fix nitrogen, and help in biosynthesis of plant hormones (Andreote et al., 2014; Bulgarelli et al., 2013).

Major colonizers of the leaf surface include bacteria, followed by filamentous fungi, yeasts, protists, and bacteriophages (Balogh et al., 2018; Chaudhry et al., 2021; Stone et al., 2018) There are several sources through which microbes can colonize the phyllosphere with soil, air, seeds, herbivores, and insects being the primary sources (reviewed by Xu et al., 2022). Vertical transmission through seeds plays an important role in shaping the plant microbial community (Bergna et al., 2018; Kusstatscher et al., 2021; Abdelfattah et al., 2021).

The environment has a major impact on the microbial communities of the leaf surface for example high levels of UV exposure, water stress, large shifts in temperature (Lindow and Brandl, 2003; Maignien et al., 2014), ultimately influencing their interactions with the host (Stone et al., 2018). “The direct impact of climate change is likely to be more pronounced on communities that occupy the plant surface (e.g., the phyllosphere), where environmental conditions fluctuate more rapidly as compared to the relatively stable internal plant tissue environments (i.e., the endosphere)” (Trivedi et al., 2022, 2020).

1.2.2 Interaction of phyllosphere microbiome with plant hosts

Host genotype can shape the phyllosphere microbial community (Bodenhausen et al., 2014; Morella et al., 2020). At the same time, microbial populations are instrumental in mediating nutrient exchange between the phyllosphere and the environment (Abril et al., 2005). Reports are available on potential roles of Phyllosphere bacteria / diazotrophs in nitrogen fixation (Bentley, 1987; Carpenter, 1992; Freiberg, 1998; Fritz-Sheridan and Portecop, 1987; Sengupta et al., 1981). A more recent study Abadi et al., (2020) reported high genetic diversity of the N-fixing bacteria in the phyllosphere of maize plants. Cyanobacteria and Proteobacteria dominate the diazotrophic community of Phyllosphere (Bao et al., 2020; Fürnkranz et al., 2008), although, a direct correlation of nitrogen fixing abilities of host plants with the phyllosphere associated diazotrophs has not been ascertained (Fürnkranz et al., 2008). Nevertheless, due to the vast abundance of nitrogen fixing bacteria in plants of tropical forests, there is scope for manipulating the microbiome to enable efficient biological N2 fixation, which in future may serve as a sustainable alternative to application of nitrogen fertilizers.

At the same time, microbial application has immense potential to mitigate abiotic stress responses (reviewed in Shaffique et al., 2022). Leaf associated bacteria have been reported to protect crop plants such as rice and wheat against drought stress (Arun K. et al., 2020; Devarajan

et al., 2021), flooding (Cui et al., 2019; Francioli et al., 2022) and UV radiation (Kumar et al., 2016; Yoshida et al., 2017).

Finally, phyllosphere microbiota have been implicated in defense against biotic stress. In citrus leaves, the microbiome shifts toward recruiting new bacterial species, namely *Pantoea* asv90 and *Methylobacterium* asv41 which help the host plant to restrict the infection of fungal pathogen, *Diaporthe citri* (Li et al., 2022). Diverse phyllosphere microbial community was correlated with a reduced incidence of bacterial wildfire outbreak in tobacco (Qin et al., 2019).

Different mechanisms exist by which phyllosphere microbiome can aid in plant protection. Beneficial microbe combat plant diseases either by inducing systemic resistance in the host, by competing with the pathogen for space and nutrition, or by secreting antimicrobials and secondary metabolites to inhibit the pathogen (Köhl et al., 2019). Direct modes of antagonism include secretion of secondary metabolites such as non-ribosomal peptides and polyketides with antimicrobial properties. *Brevibacillus* sp. Leaf 182 (Helfrich et al., 2018) secreted several non-ribosomal peptides antagonizing Gram-negative bacteria. Commonly found phyllosphere bacterium *Pseudomonas* exhibited biocontrol activity against bacterial and fungal pathogens (*B. cinerea*, *F. graminearum*) by producing phenazines, a group of heterocyclic nitrogen-containing secondary metabolites (reviewed by Legein et al., 2020).

Bacteria utilize QS to act against pathogenic microbes by expressing QS inhibitors (QSIs) to attenuate the activity of AIs, or quorum quenching (QQ) enzymes to disrupt signaling molecules. For example, AHL lactonase enzyme (a potent quorum quencher) present in endophytic bacteria has been reported to inhibit the plant pathogens *Erwinia carotovora* (Dong et al., 2001, 2000), *Bacillus* sp., subspecies of *Bacillus thuringiensis* (Lee et al., 2002; Ulrich, 2004), and *Enterobacter asburiae* (Rajesh and Ravishankar Rai, 2014). (Ma et al., 2013) explored the diversity of tobacco (*Nicotiana tabacum*) leaf-associated strains with QQ activity for disruption of AHL-mediated QS, by using the biosensor reference strain *Chromobacterium violaceum* CV026. These bacterial quorum quenchers can be used as effective biocontrol agents against plant pathogens (Ma et al., 2013).

Alongside, phyllosphere microbes can indirectly antagonize pathogens by upregulating plant defense responses. In an interaction between commensal and pathogenic strains of *Pseudomonas* in *A. thaliana* phyllosphere, host responses were induced by the commensal strain to help in plant protection (Shalev et al., 2021). Soil dwelling bacteria *Streptomyces sp.*, (Vergnes et al., 2020) was able to colonize the leaf surface of *A. thaliana*, leading to inhibition

of fungal pathogen, *Alternaria brassicola* by upregulating plant biosynthesis of salicylic acid (SA).

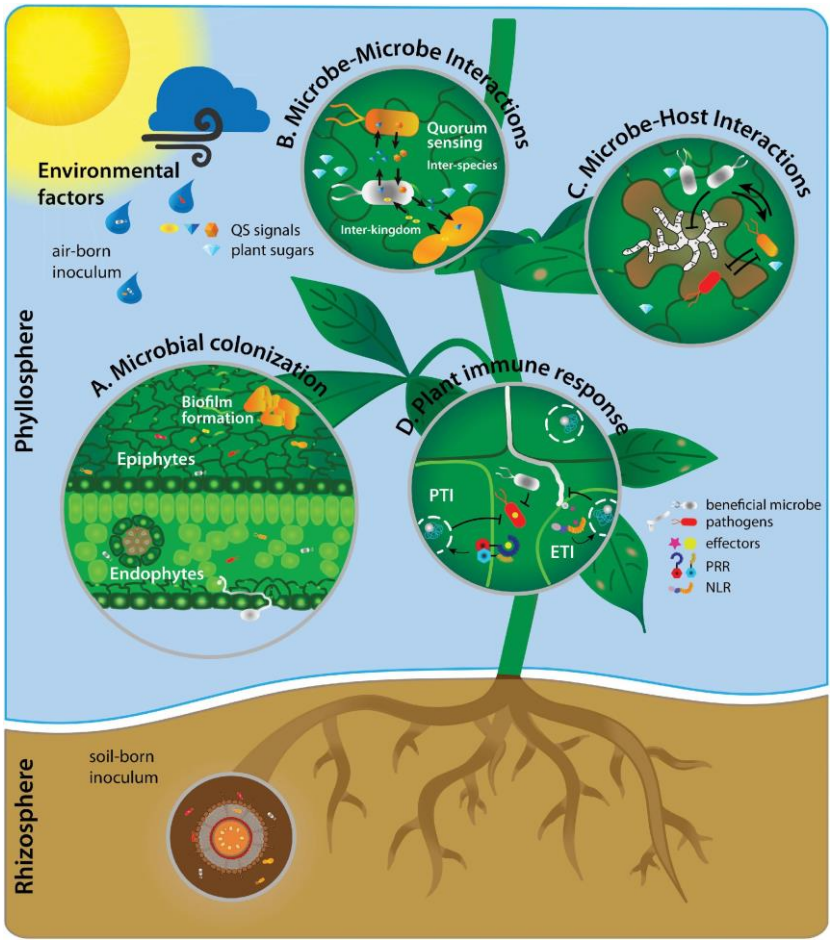

Figure 1. 2 Importance of microbial association in the phyllosphere

(A) Microbial colonization can take place on the leaf surface (epiphytes) from air-borne and soil-borne inocula and the inner leaf part (endophytes). (B) Microbe–microbe interactions occur between interspecies and interkingdoms, referred to as quorum sensing. Quorum-sensing molecules impact microbial recognition and biofilm formation on leaves. (C) Pathogenic microbes colonize host plants by means of their virulence. The genetic make-up of both the host and pathogen contributes to disease progression. However, other microbes in the host phyllosphere can influence this plant–pathogen interaction by either facilitation or antagonism. (D) Plant immune responses are of specific interest as host–microbe interactions shaping the phyllosphere microbiome. Non-host-adapted pathogens are involved in PAMP-triggered immunity (PTI) and recognized via pattern-recognition receptors (PRRs). Host-adapted microbes are recognized via nucleotide-binding leucine-rich repeat receptors (NLRs), summarized in effector-triggered immunity (ETI). (adapted from Chaudhry et al., 2021).

1.2.3 Basidiomycete yeasts as biological control agents

The Ustilaginales, an order of basidiomycete fungi comprises of pathogens of many important crop plants. For example, corn smut, loose smut of oats, barley and wheat are caused by *Ustilago maydis*, *U. avenae*, *U. nuda* and *U. tritici*, respectively all of which fall under the umbrella of Ustilaginales. Basidiomycete yeasts, known as *Moesziomyces* sp. are also present

under Ustilaginales. Ribosomal DNA analysis by Begerow et al., (2017) showed that *Moesziomyces* and Ustilaginales form a monophyletic group. *Moesziomyces* sp. is known to be devoid of any pathogenic sexual morph (Kruse et al., 2017) and is found to epiphytically colonize a wide range of habitats because of its rapid rate of asexual reproduction.

Earlier, *Moesziomyces* was referred to as *Pseudozyma* sp. However, (Wang et al., 2015) showed that due to close phylogenetic relationship between *Moesziomyces bullatus* and four species of *Pseudozyma*, namely *P. antarctica*, *P. aphidis*, *P. parantarctica* and *P. rugulosa*; the latter represent anamorphic and culturable stages of *Moesziomyces* sp. and can be transferred to the genus *Moesziomyces*.

Moesziomyces /*Pseudozyma* has been widely used for biological control of pathogens. The first discovery of biocontrol potential in yeast can be traced back to the late 1980s, when scientists in Southern Ontario, Canada isolated and identified microorganisms as *Stephanoascus flocculosus* and *Stephanoascus rugulosus*, which proved to be antagonistic towards the powdery mildew fungi (Avis and Belanger, 2002). These two species were later renamed as *Pseudozyma flocculosa* and *Pseudozyma rugulosa* (Boekhout, 2011).

Pseudozyma species have since been tested for their biocontrol activity against the powdery mildews of many different crops. Both *P. flocculosa* and *P. rugulosa* were reported to control *Sphaerotheca fuliginea*, the causal agent of powdery mildew disease of cucurbits (Jarvis et al., 1989). *P. flocculosa* has also shown inhibitory effects against rose powdery mildew, *Sphaerotheca pannosa* var. *rosae* (Belanger et al., 1994) and wheat powdery mildew *Erysiphe graminis* var. *tritici* (Hajlaoui and Belanger, 2008). Glycolipids like flocculosin produced by *P. flocculosa* or ustilagic acid characterized in the smut fungus *U. maydis* can destabilize the membrane of different fungi and thus serve as biocontrol agents against powdery mildews or gray mold (Cheng et al., 2003; Mimee et al., 2005; Teichmann et al., 2007)

One of the mechanisms for pathogenic inhibition by *Pseudozyma* sp. is antibiosis (Hajlaou et al., 2008). Different methylated fatty acids like 4-Methyl-7, 11-heptadecadienal and 4-methyl-7, 11- heptadecadienoic acid have been isolated from *P. flocculosa* and *P. rugulosa,* which were shown to inhibit the growth of *Fusarium oxysporum* f. sp. *lycospersici, Trichoderma viride,* and *Bacillus subtilis* (Choudhury et al., 1994), while 6-methyl-9-heptadecenoic acid showed antibiotic activity against *Cladosporium cucumerinum* (Benyagoub et al., 1996). *Pseudozyma aphidis* inhibited the pathogenic bacteria *Xanthomonas campestris pv. vesicatoria, X. campestris pv. campestris, Pseudomonas syringae pv. tomato, Clavibacter michiganensis, Erwinia amylovora*, and *Agrobacterium tumefaciens in-vitro* by secretion of extracellular

metabolites (Barda et al., 2015). Other modes of action also exist for *Pseudozyma* biocontrol strains such as induction of host-defense responses against pathogenic growth. Application of *P. aphidis* triggered induced resistance in tomato plants against *Clavibacter michiganensis* by upregulation of Pathogenesis related (PR) genes in a Salicylic acid independent manner (Barda et al., 2015). *Pseudozyma churashimaensis* was reported to induce systemic defense in pepper plants against *X. axonopodis*, *Cucumber mosaic virus*, *Pepper mottle virus*, *Pepper mild mottle virus*, and *Broad bean wilt virus* (Lee et al., 2017). Direct antagonism has also been proposed for *P. aphidis* which can parasitize the hyphae and spores of *Podosphaera xanthi* (Gafni et al., 2015). A more recent study has suggested multiple modes of antagonism for *P. aphidis* against necrotrophic fungus *Botrytis cinerea* (Calderón et al., 2019). *Pseudozyma aphidis* attaches on to the hyphae of *B. cinerea* and competes for nutrients with the pathogen. Alongside, *P. aphidis* releases antifungal compounds to generate hypersensitive responses and ultimately impairs the colonization and infection ability of *B. cinerea*. Therefore, basidiomycete yeasts *Moesziomyces/Pseudozyma* have dynamic modes of biocontrol activity and immense potential to act as antimicrobial agents.

1.3 Role of Glycoside Hydrolase proteins in pathogen infection and plant immunity

Phytopathogenic fungi and oomycetes have developed an arsenal of Cell Wall Degrading enzymes (CWDE) or carbohydrate-active enzymes (CAZymes) to breach the plant surface by hydrolyzing the different cell wall constituents such as cellulose, hemicellulose, pectin, and xylan (Kubicek et al., 2014). Different groups of CAZymes exist such as glycoside hydrolases (GHs), carbohydrate esterases (CEs), polysaccharide lyases (PLs), glycosyltransferases (GTs), auxiliary activity enzymes (AAs), and carbohydrate-binding modules (CBMs) (Drula et al., 2022; Lombard et al., 2014).

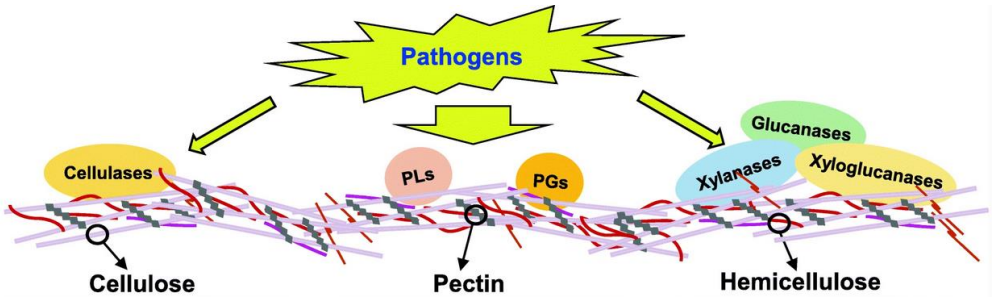

Figure 1. 3 Schematic diagram of Plant Cell-Wall Degrading Enzymes (CWDEs)

Different plant cell wall components such as cellulose, Pectin and Hemicellulose targeted by specialized CWDEs secreted from pathogens during infection **(**adapted from Wan et al., 2021).

1. Introduction

Glycoside Hydrolase is the largest among the group of CAZymes with 172 families and 18 different GH clans (Henrissat and Davies, 1997). Pathogens secrete GH proteins as virulence factors to colonize plants and establish infection (reviewed in Bradley et al., 2022). Deletion of cell wall hydrolyzing enzymes encoded by GH families in fungi *B. cinerea*, *M. oryzae* and *A. alternata* impaired pathogenic virulence (Brito et al., 2007; Ma et al., 2019; van Vu et al., 2012). Nevertheless, pathogens employ GH protein to manipulate plant immunity either by acting as microbe-associated molecular patterns (MAMPs), or through the release of damage associated molecular patterns (DAMPs) because of their enzymatic activity (Bradley et al., 2022). GH12 proteins from oomycete *Phytophthora sojae* and fungi *Verticillium dahliae*, *M. oryzae* and *F. oxysporum* can induce plant immunity by acting as MAMPs (Gui et al., 2017; Ma et al., 2015; Zhang et al., 2021).

1.3.1 Role of GH proteins in biological control of pathogens

Diverse groups of GH proteins target cell wall of fungi and oomycetes have been used in biological control of phytopathogens. Cell wall of fungi is mainly composed of Chitin containing linear residues of ß-1,4 linked N-acetyl glucosamine. Therefore, different groups of bacteria secrete Chitinases (mainly encoded by GH family 18, 19 and 20) to control pathogenic fungi (Berini et al., 2019; Veliz et al., 2017). A recent study showed endophytic microflora of *Brassica rapa* consisted of chitinase producing bacteria, which could be attributed to the resilient nature of the host plant against biotic stressors (Padder et al., 2022)

Other groups of GH proteins such as Glucanases and cellulases have also been reported to function as antimicrobial compounds. Exoglucanase genes from *Pichia anomala* were differentially upregulated in presence of *Penicillium digitatum* and *Botrytis cinerea* (Parafati et al., 2017). Recombinantly produced endo-β-1,3-glucanase (GH64 family) from *Magnaporthe oryzae* inhibited appressoria and germ tube formation in the rice blast pathogen and induced immunostimulatory response in rice by hydrolysis of Pachymaran (Wang et al., 2021).
Widely used biocontrol agent *Trichoderma harzianum* produces a variety of cellulases, that antagonize pathogenic fungi of crop plants (Jensen et al., 1997; Migheli et al., 1998). Saravanakumar et al., (2018) explored the role of cellulose encoding genes from *T. harzianum* in eliciting plant immunity against pathogen *F. graminearum*; cellulase genes trigger the production of DIMBOA and other defense related genes in maize roots to restrict growth of the pathogen.

1.3.2 Role of GH proteins in the smut fungus *Ustilago maydis*

Ustilago maydis is a basidiomycete fungus, under Ustilaginales, which causes corn smut disease of maize and has been developed as a prime model system for studying the impact of genes involved in various biological processes. *U. maydis* can cause symptoms in all parts of the infected plant and results in the induction of anthocyanin biosynthesis and formation of large tumors (Lanver et al., 2017). The filamentous dikaryon produced upon fusion of two haploid cells develops into specialized infection structure known as appressoria and colonizes the host tissue.

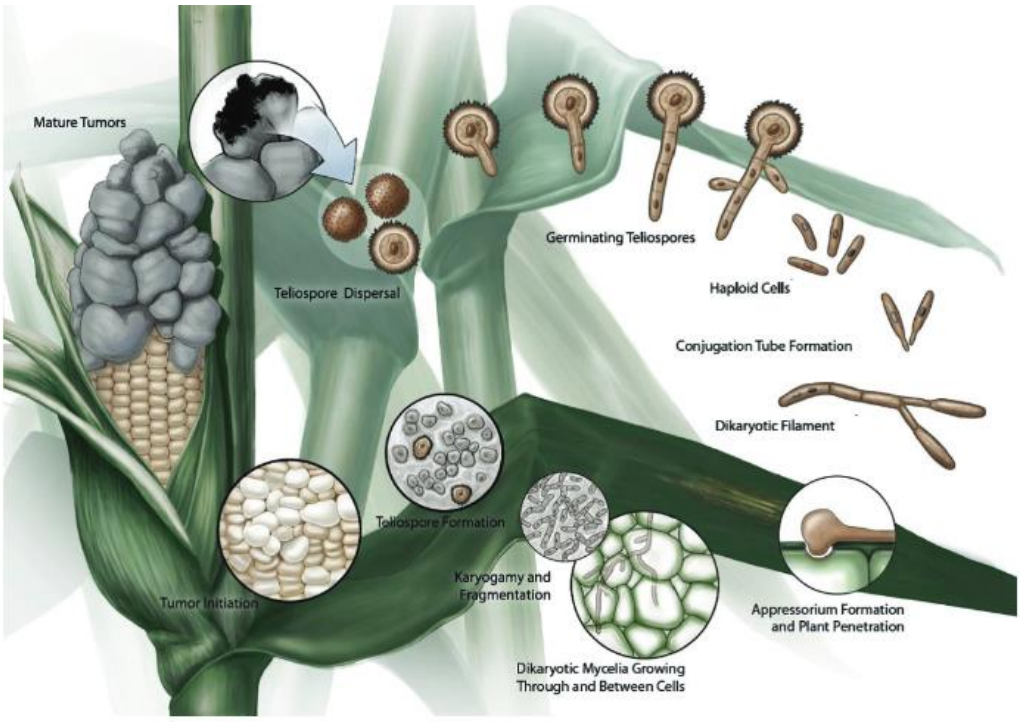

Figure 1. 4 Life cycle of *Ustilago maydis*

Life cycle of *U. maydis* consist of a yeast-like saprophytic and filamentous pathogenic stage. Infection by *U. maydis* causes tumor formation in above ground parts of the plant such as leaves, ear and tassel. Saprophytic stage consists of teliospores which germinate to give rise to haploid sporidia upon meiosis. Two of the compatible haploid sporidia fuse to form a dikaryotic pathogenic filament, which eventually develop appressoria to penetrate host epidermis. Appressoria formation is followed by dikaryotic mycelia colonizing the plant tissue and secreting effectors to modulate host immunity and physiology. Ultimately, tumor formation is initiated, and the fungal hyphae aggregate inside the tumors, which burst open in the later stages of infection to release teliospores (modified from Saville et al., 2012.; Zuo et al., 2019).

During host colonization, *U. maydis* secretes effector proteins which tend to manipulate the entire defense response of the host plant. One such effector protein, Pep1 was reported to be essential in penetration of host plant cells and establishment of primary infection. Pep1 inhibits the production of reactive oxygen species, ultimately leading to suppression of innate plant immunity (Doehlemann et al., 2009; Hemetsberger et al., 2012). Another functionally

characterized effector protein Pit2 was found to inhibit a group of apoplastic plant proteases (papain like cysteine proteases; PLCPs) (Misas Villamil et al., 2019; Mueller et al., 2013a). Additionally, two different effector proteins of *U. maydis*, Cmu1 and Tin2 interfere with salicylic acid (Djamei et al., 2011) and anthocyanin biosynthesis in maize (Tanaka et al., 2014), respectively.

First contact with hydrophobic plant surface leads to activation of CWDEs in *U. maydis* (Lanver et al., 2014). Transcription profile of maize- *U. maydis* interaction has revealed several putative CWDEs, such as GH45 cellulases, hemicellulases, including two arabinofuranosidases, and one pectin lyase, to be activated in *U. maydis* with respect to biotrophic phase (Lanver et al., 2018). Triple deletion of GH45 genes in *U. maydis* did not however impair appressoria and filament formation as well as pathogenic virulence *in planta* (Lanver 2014). A previous study by Doehlemann et al., (2008) showed deletion of genes encoding for pectinolytic enzymes yielded no difference in pathogen colonization or infection efficiency on maize. These results imply a functional redundancy among the different PCWDE in *U. maydis*. Exploring how different class of GH proteins interact with each other and the plant surface, will be important to uncover mechanisms of pathogenicity and host defense.

1.4 Antagonism of *Albugo laibachii* by basidiomycete yeast, *MbA*

Basidiomycete yeast, *Moesziomyces bullatus* ex *Albugo* on *Arabidopsis* (*MbA*) was found to be antagonistic towards the white rust oomycete pathogen *Albugo laibachii* on *A. thaliana* leaves. To test interaction between *MbA* and *A. laibachii*, a gnotobiotic plate assay was performed. Three weeks old *A. thaliana* seedlings growing on ½ MS Agar were spray inoculated with growing culture of *MbA* and two days later with *A. laibachii*. Infection symptoms on *Arabidopsis* was quantified at 14 dpi, where pre-inoculation with *MbA*, almost completely abolished *A. laibachii* spore production (Fig 1.5-A). When the bacterial SynCom was pre-inoculated on leaves 2 days before *A. laibachii* spraying a significant reduction of *A. laibachii* infection by about 50% was observed (Fig 1.5-A).

1. Introduction

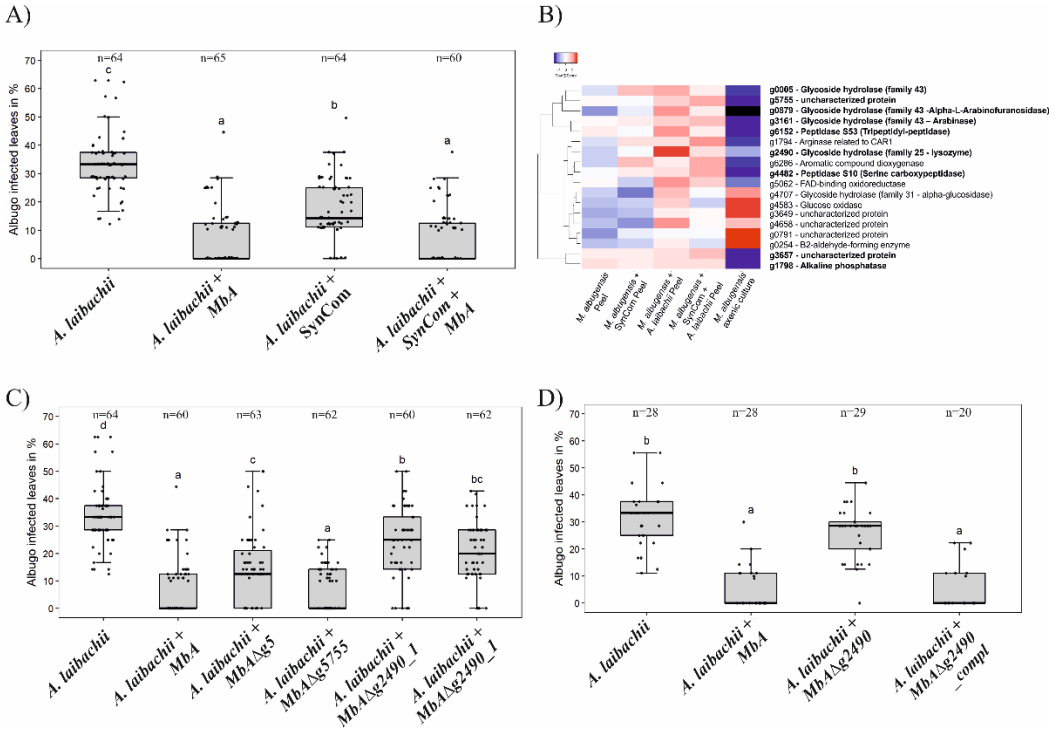

Figure 1. 5 Basidiomycete yeast, *MbA* antagonizes *Albugo laibachii*

A)- Gnotobiotic infection assay on *A. thaliana* seedlings. Addition of a bacterial SynCom reduces the infection symptoms of *A. laibachii* at 14 days dpi. Infection can be almost abolished by spraying *MbA* to the plant, independently of the presence of the bacterial community. Infections were performed in six individual replicates with 12 technical replicates. 'n' indicates the number of infected plants that were scored for symptoms. An analysis of variance (ANOVA) model was used for pairwise comparison of the conditions, with Tukey's HSD test to determine differences among them. Different letters indicate significant differences (p-values <0.05). B)- Hierarchical clustering of the 18 *A. laibachii*-induced *MbA* genes that are predicted to encode secreted proteins. Of these genes, nine were selected as candidate microbe–microbe effector genes, based on their transcriptional upregulation and prediction to encode for extracellularly localized proteins. C)- Three candidate microbe–microbe effector genes (*g5*, *g5755*, and *g2490*) were deleted in *MbA* and deletion strains were individually inoculated on *A. thaliana* together with *A. laibachii*. Inoculation of two independent *g2490 null* strains (*Δg2490_1; Δg2490_2*) resulted in significant and almost complete loss of the biocontrol activity of *MbA*. While deletion of g5 resulted in a marginal reduction of disease symptoms at 14 days post infection, deletion of g5755 had no effect on *A. laibachii.* D)- Genetic complementation of the *g2490* deletion restores the biocontrol activity to wild-type levels. Infections in (C) were performed in six, in (D) in three individual replicates. In each replicate 12 plants were infected. 'n' indicates the number of infected plants that were scored for symptoms. Different letters indicate significant differences (p-values <0.05; ANOVA model for pairwise comparison with Tukey's HSD test) (courtesy: Katharina Eitzen).

Based on the interaction between *MbA* and *A. laibachii*, transcriptomic analysis of *MbA* in response to several biotic interactions was performed (Fig 1.5-B). *MbA* genes that are induced by *A. laibachii*; showing no or low expression in axenic culture and encoding for putative secreted proteins were identified as potential candidates for antagonism towards white rust pathogen. Next, knockout mutation of two glycoside hydrolase genes *g5* and *g2490* (GH43 and GH25) and the gene encoding the uncharacterized protein *g5755* were generated respectively, in *MbA* (Fig 1.5-C).

Only the *MbA*Δg2490 strains lost antagonism towards *A. laibachii*. Whereas, when *g2490* was complemented in the deletion mutant, the resulting complementation strain could inhibit *A. laibachii* growth as before. Therefore, *MbA*_GH25 was selected for functional characterization to provide mechanistic insights into yeast-oomycete antagonism within the phyllosphere community of *A. thaliana*.

1.5 Aim of this study

To establish *MbA*_GH25 as a regulator of *A. thaliana* phyllosphere community and functionally characterize the hydrolase enzyme, the following objectives were carried out in this study:

1. Biochemical characterization of *MbA*_GH25 protein and elucidation of mechanism behind *A. laibachii* antagonism.
2. Exploring the impact of *MbA*_GH25 in oomycetes of varied lifestyle
3. Functionally characterizing GH25 expression in the smut pathogen *Ustilago maydis*

Analyzing the role of glycoside hydrolase enzyme in microbe-microbe interaction will lay the foundation for developing antimicrobial agents and eventually a sustainable measure of pathogen control in agricultural systems.

1. Introduction

2. Results:

2.1 Functionally characterizing the role of *MbA*_GH25 in *A. laibachii* antagonism on *A. thaliana* leaves

My colleague, Katharina Eitzen showed basidiomycete yeast *MbA* to antagonize white rust pathogen *A. laibachii* on *A. thaliana*. The antagonistic effect of *MbA* toward *A. laibachii* was further confirmed by relative biomass quantification of *A. laibachii* at 10 dpi using oomycete Internal Transcribed Spacer (ITS) 5.8s sequence normalized to the *A. thaliana* housekeeping gene EF1-α (Fig 2.1-A). *A. laibachii* biomass was significantly reduced when *MbA* was pre-treated to the leaves. Afterwards, microscopic analysis was performed on Trypan blue stained *A. thaliana* leaves to visualize the impact of *MbA* on *A. laibachii* at 15 dpi A reduction in thick hyphal network was observed in *A. laibachii* with the presence of short, truncated hyphae and an increase in oospores formation (Fig-2.1-B).

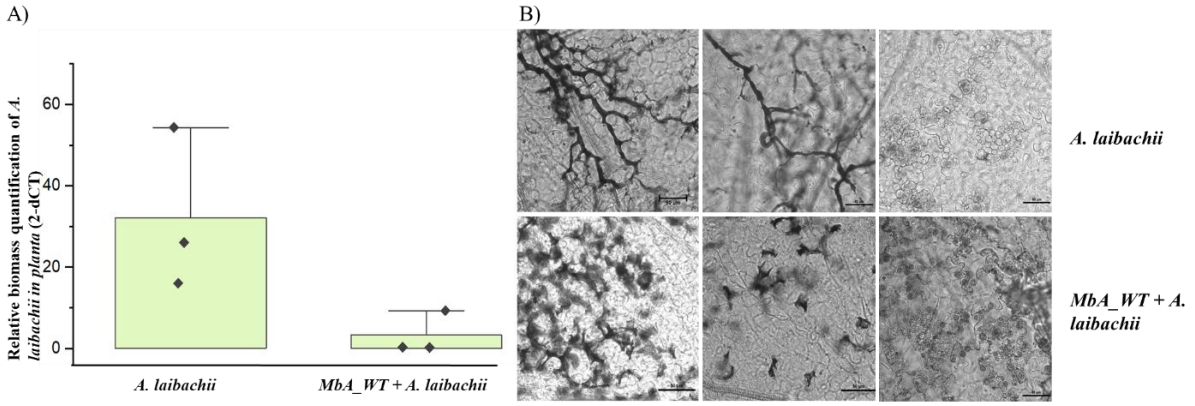

Figure 2. 1 Quantification and visualization of *MbA* antagonism on *A. laibachii*

A)-Relative quantification of *A. laibachii* biomass in response to *MbA* treatment by qPCR. The oomycete internal transcribed spacer (ITS) 5.8 s was normalized to *A. thaliana* EF1-α gene to quantify the amount of *A. laibachii* DNA in the samples at 10 dpi. Error bars indicate outlier (co-eff. 1.5). P values were calculated with an unpaired t-test, *P<0.05. B)- Trypan blue staining of *A. laibachii* (upper row) and *MbA*+ *A. laibachii* (bottom row) infected *A. thaliana* seedling (15dpi). Reduction in thick hyphal network and in increase in oospore formation in *A. laibachii* upon *MbA* treatment.

Katharina identified antagonism of *A. laibachii* to be dependent on GH25 expression in *MbA* (Fig 1.5-D). To further unravel the mechanism behind *MbA* mediated antagonism, heterologous expression of *MbA*_GH25 was carried out in *Pichia pastoris*. The recombinant *MbA*_gh25 gene was driven by constitutively expressed *Pichia*_GAPDH promoter and contained an N- and C-terminal polyhistidine tag for detection of full-length integration in *P. pastoris* genome. Alongside, a highly conserved DXE motif was identified after multiple sequence alignment of GH25 protein from fungi, belonging to a wide range of families such as basidiomycetes,

ascomycetes and chytrids (Fig-2.2-A). Therefore, based on the conserved DXE motif, a mutagenized *MbA*_GH25 (D124E) was cloned in *P. pastoris* for recombinant protein expression.

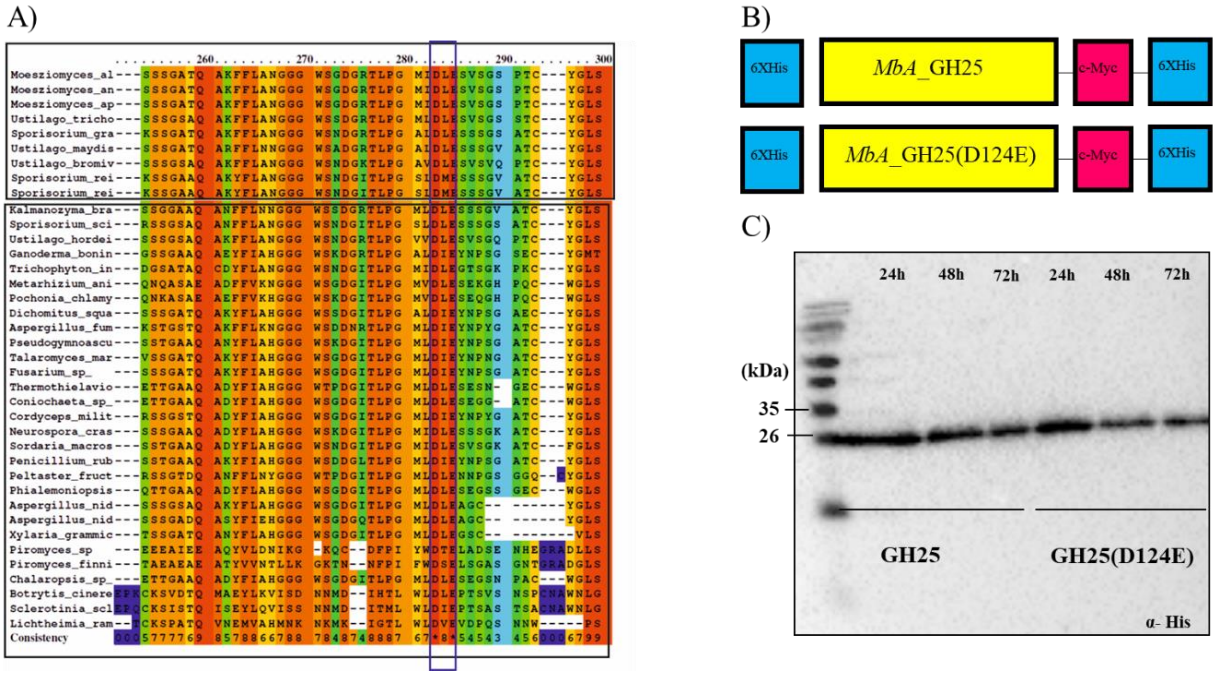

Figure 2. 2 Recombinant expression of *MbA*_GH25

A)-Amino acid alignment of GH25 sequences from different fungal species. The protein sequences were obtained from the NCBI database (Appendix 6.1- can be viewed for full length sequences of GH25 with accession number). Alignment was achieved using the PRALINE multiple sequence alignment program with default parameters. The scoring scheme works from 0 for the least conserved alignment position, up to 10 (indicated by *) for the most conserved alignment position. A conserved active-site DXE motif has been predicted for glycoside hydrolase family 25. Sequences tested from different basiodiomycete, ascomycete, and chytrids have the active site residue conserved (purple box). B)- Schematic diagram of the construct for recombinant expression in the yeast *Pichia pastoris*, where *MbA*_GH25 and *MbA*_GH25(D124E) open reading frames were fused with an N-terminal polyhistidine Tag and a C-terminal peptide, containing the c-myc epitope and a polyhistidine tag. C)- Recombinant *MbA*_GH25 and *MbA*_GH25(D124E) was produced and purified using the *P. pastoris* protein expression system. The purified proteins were subjected to Western Blot using a-His antibody when an expected molecular weight of 27 kDa for His-Tagged GH25 and GH25(D124E) were detected.

Small-scale protein expression of *MbA*_GH25 and *MbA*_GH25 (D124E) in *P. pastoris* was carried out at 24 h, 48 h and 72 h. Supernatants from the *P. pastoris* cultures were harvested and subjected to Western Blot to detect full-length integration of the protein. An expected size of 27kDa of *MbA*_GH25 and *MbA*_GH25 (D124E) protein was visible at all three time points tested (Fig 2.2-C). Eventually, large scale protein expression and purification by Ni-NTA affinity chromatography was performed and the production of full-length protein was confirmed by visualizing in an SDS PAGE (Appendix Fig 6.2.1).

Afterwards, the biochemical functionality of the purified *MbA*_GH25 protein needed to be verified, for which the predicted biological activity of GH25 was considered. *MbA*_GH25 protein shows similarity to *Chalaropsis* type lysozymes. Lysozymes essentially cleave b-1,4-glycosidic bond between N-acetylmuramic acid (NAM) and N-acetylglucosamine (NAG) in the bacterial peptidoglycan.

Biochemical functionality of purified *MbA*_GH25 and *MbA*_GH25 (D124E) was analyzed by a quantitative lysozyme activity assay using the fluorogenic substrate *Micrococcus lysodeikticus* and Hen egg-white lysozyme (HEWL) as a control. Commercial HEWL displayed a steady rise in RFU/min with molar concentration ranging from 1µM to 5.5µM (Appendix Fig 6.2.2) attesting to technical functioning of the assay. For active *MbA*_GH25, an increase in relative fluorescence unit (RFU/min) was recorded with a gradual rise in protein concentration (2µM to 10µM), whereas for similar concentrations of the mutated *MbA*_GH25 (D124E), no significant increase in RFU/min was observed (Fig 2.3-A). Thus, purified *MbA*_GH25 showed activity against bacterial peptidoglycan which requires presence of the conserved DXE motif.

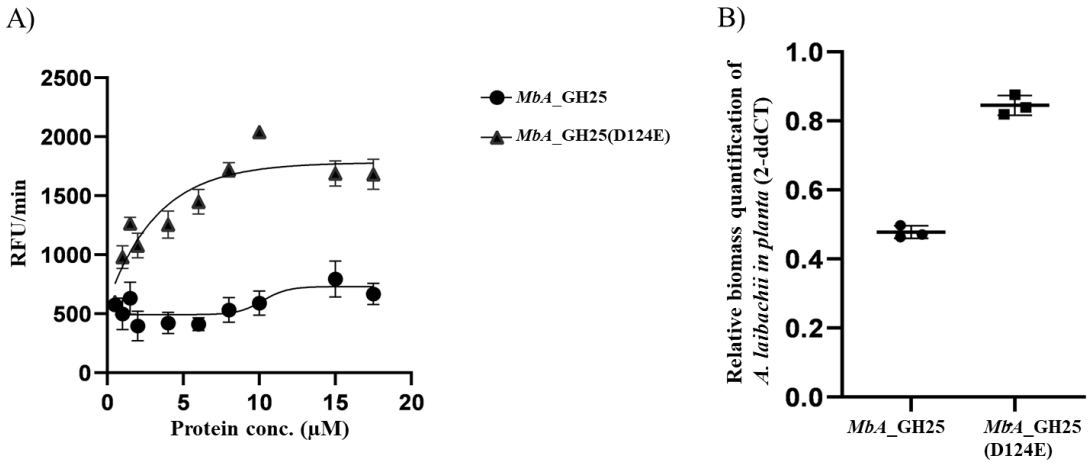

Figure 2. 3 Biochemical Characterization of *MbA*_GH25

A)-Increasing concentrations of purified *MbA*_GH25 and *MbA*_GH25(D124E) were incubated with the DQ lysozyme substrate for an hour at 37°C. The fluorescence was recorded every minute in a fluorescence microplate reader using excitation/emission of 485/530 nm. Relative fluorescence unit (RFU)/min was calculated for each concentration and plotted on the graph. Each data point represents three technical replicates and three independent biological replicates as indicated by the standard error measurement (SEM) bars. An unpaired t-test was performed for the *MbA*_GH25 and *MbA*_GH25(D124E) treatments giving the p-value of <0.0001 and R^2 value of 77.24%. B)-Relative quantification of *A. laibachii* biomass in response to *MbA*_GH25 treatment via qPCR. The oomycete internal transcribed spacer (ITS) 5.8 s was normalized to *A. thaliana* EF1-α to quantify the amount of *A. laibachii* DNA in the samples, 10 days post infection. Relative biomass was calculated comparing control sets (only *Albugo*) with *A. laibachii* treated with *MbA*_GH25 and *A. laibachii* treated with *MbA*_GH25(D124E) by ddCT method. Unpaired t-test gave a p-value of <0.0001 and an R^2 value of 98.88%.

Finally, to determine if GH25 is a main component in the antagonism of *MbA* against *A. laibachii*, *in planta* tests were carried out where 6µM of purified *MbA*_GH25 and *MbA*_GH25 (D124E) proteins were mixed with *A. laibachii* zoospores and sprayed on *A. thaliana* seedlings. *A. laibachii* biomass was quantified at 10dpi, using with oomycete ITS (5.8s) sequence normalized to *A. thaliana* housekeeping gene EF1-α. In accordance with *MbA* treatments, *MbA*_GH25 reduced *A. laibachii* biomass to about 50% compared to GH25(D124E) (p-value of <0.0001 and an R^2 value of 98.88%) (Fig 2.3-B). Therefore, *MbA* holds a strong antagonistic activity toward *A. laibachii*, resulting in efficient biocontrol of pathogen infection by GH25 activity.

2.2 Elucidating the mechanism behind *MbA*_GH25 activity against *A. laibachii*:

2.2.1 *MbA*_GH25 as an elicitor of plant immunity

One possible reason behind the *MbA*_GH25 mediated antagonism could be upregulation of host defense responses. To this end, 2.5-week-old *A. thaliana* seedlings growing on liquid MS media were treated with purified *MbA*_GH25, *MbA*_GH25 (D124A) and heat killed (HK) *MbA*_GH25 protein (2µM conc.), and the seedlings were harvested after 30 minutes to check for activation of several maker genes involved in plant defense pathways. WRKY transcription factors are involved in a plethora of plant developmental processes including defense against biotic and abiotic stressors (Pandey and Somssich, 2009); therefore, wrky30, wrky 33 and wrky53 were chosen for the elicitor assay. Additionally, induction of frk1 gene (involved in early defense signaling) and ics1 gene (involved in Salicylic acid biosynthesis and defense against biotrophic pathogens) were analyzed. *A. thaliana* housekeeping gene EF1-α was used for normalization to quantify relative gene expression levels. Flagellin 22 (flg22), widely recognized bacterial PAMP, was used as a positive control.

All treatments of purified *MbA*_GH25, *MbA*_GH25 (D124A) and HK-*MbA*_GH25 showed weak induction of wrky 33, wrky 53, ics1 and frk1 gene compared to mock treatment (1/2MS media). Flg22 treatment showed significant induction in relative expression levels for all the marker genes tested (Figure 2.4).

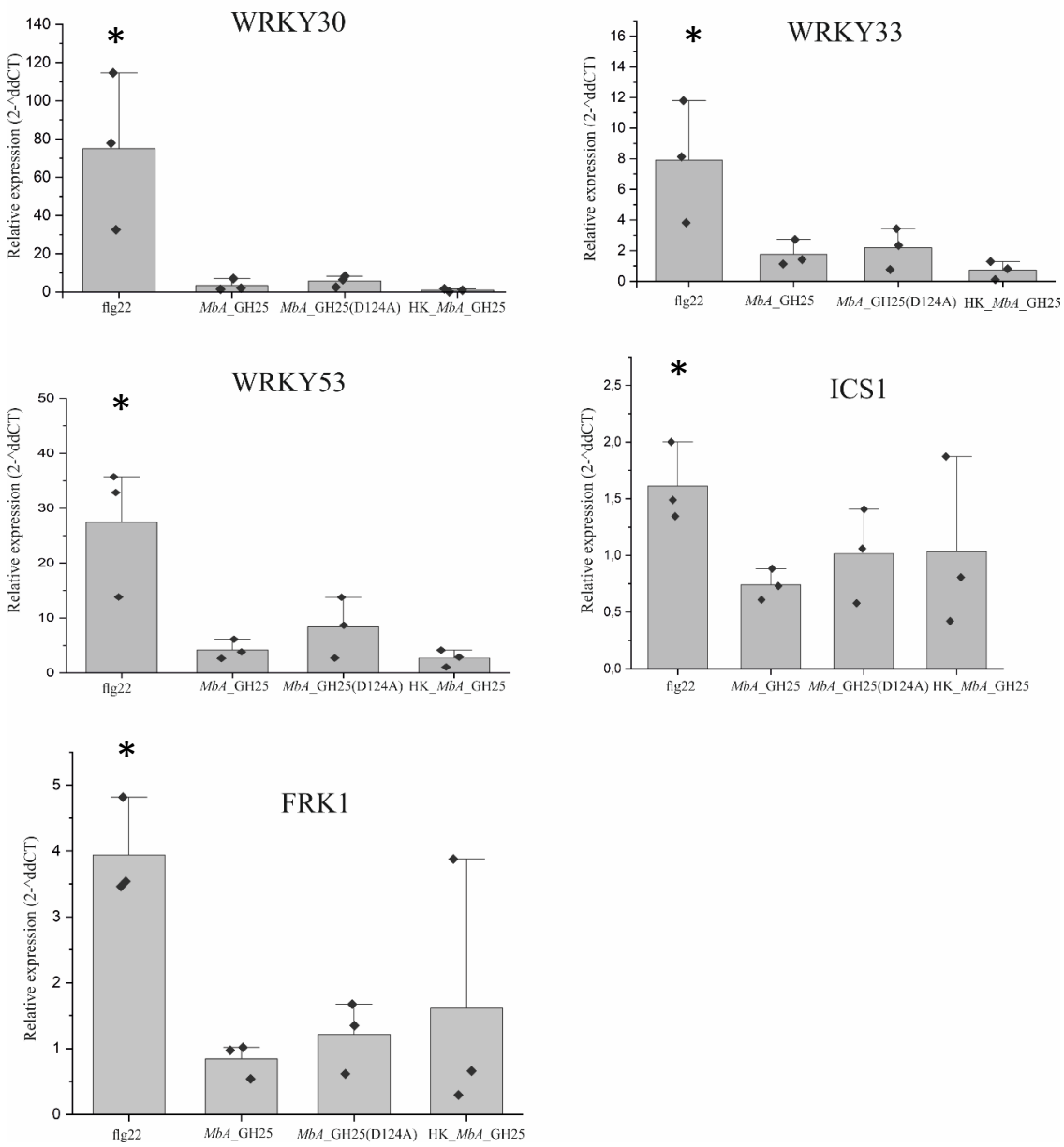

Figure 2. 4 Characterization of *MbA*_GH25 effect on plant immunity

2.5 weeks old *A. thaliana* seedlings treated with purified *MbA*_GH25 and *MbA*_GH25(D124A) (1.5µM conc.) were tested for activation of defense response genes (wrky 33, wrky 53, wrky 30, ics1 and frk1); flg22 (50nM) used as positive control (three biological replicates, error bars indicate outlier). Only flg22 treatment significantly induced compared to *MbA*_GH25, no difference in gene induction between GH25 and GH25 (D124A). P values were calculated with an unpaired t-test, *P<0.05.

The experimental setup to test for host defense activation was appropriate as evidenced by the flg22 treatment. However, no difference in gene induction between active and inactive (mutated and heat-killed) versions of *MbA*_GH25 protein could be ascertained, which indicates that enzymatic activity of *MbA*_GH25 is incapable of eliciting host defense responses.

2.2.2 GH25 inhibits bacteria associated with *A. laibachii*

Another explanation behind *MbA*_GH25 mediated antagonism was inhibition of associated bacterial community of *A. laibachii*. In the laboratory of Eric Kemen (ZMBP, Tübingen) *A. laibachii* NC14 strain was treated with an antibiotic cocktail (Streptomycin, Kanamycin, Rifampicin, Geniticin) to get rid of bacterial population associated with oomycetes. However, 7 bacterial isolates being associated with *A. laibachii* were found to be resistant to the antibiotic treatment and were chosen for confrontation assay with *MbA* (wildtype and deletion mutant of GH25, *MbA*Δg2490). The 7 isolates are as follows:

Collection No. AG Doehlemann	Name of bacteria
#140	*Curtobacterium flaccumfaciens pv. flaccumfaciens* LMG 3645
#143	*Curtobacterium flaccumfaciens pv. flaccumfaciens* LMG 3645
#141	*Pseudomonas brenneri* CFML 97-391
#142	*Pseudomonas veronii* CIP 104663
#137	*Microbacterium luteolum* IFO 15704
#138	*Microbacterium saperdae* IFO 15038
#139	*Microbacterium oxydans* DSM 20578

*MbA*_WT and *MbA* Δg2490 inhibited *Pseudomonas brenneri* and *Pseudomonas veronii* in one-to one confrontation assay on PD plates, as indicated by the halo formation (Fig 2.5). Therefore, expression of *MbA*_GH25 protein was not found to be essential for bacterial inhibition until this point.

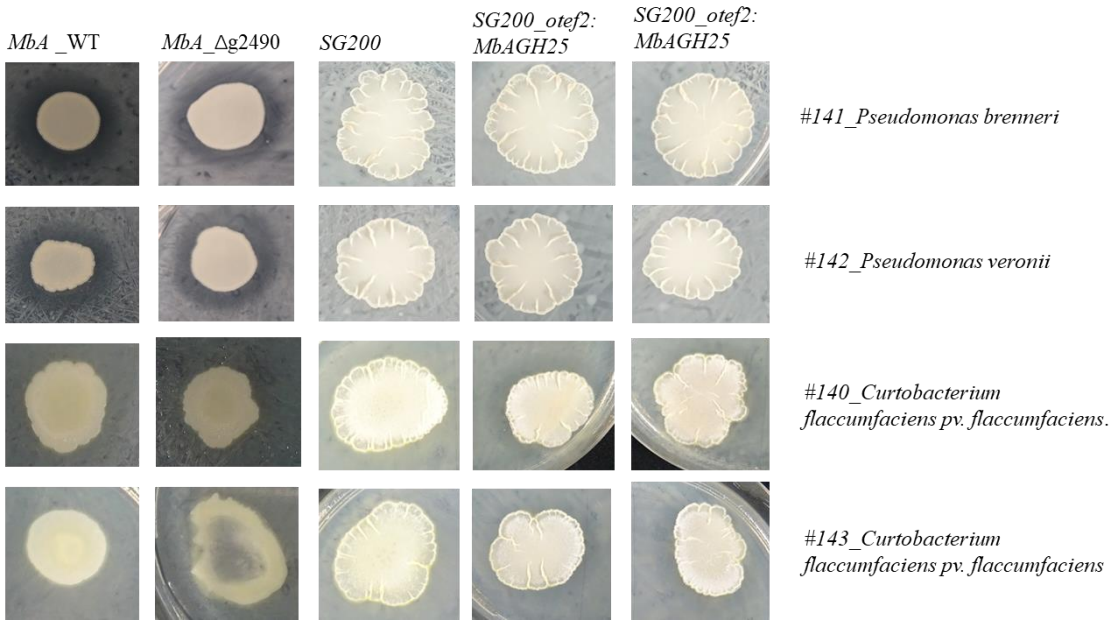

Figure 2. 5 Confrontation assay between bacterial strains and *MbA* /*U. maydis*

A. laibachii associated *P. brenneri* and *P. veronii* were inhibited by both *MbA* WT and *MbA*_Δg2490. Whereas, SG200_otef2:*MbA*GH25 inhibited *Curtobacterium flaccumfaciens pv. flaccumfaciens*, as opposed to the control *U. maydis* SG200 strain.

However, since transcriptional activation of *MbA*_GH25 was previously found (by Katharina Eitzen) to require presence of *A. laibachii* on the plant surface, a fungal strain for constitutive over-expression of *MbA*_GH25 was generated using the efficient transformation system in related smut pathogen, *U. maydis. Ustilago maydis* enabled genomic integration of *MbA*_gh25 gene under constitutively expressed promoter otef (SG200_otef2:*MbA*GH25). Strikingly, *Curtobacterium flaccumfaciens pv. flaccumfaciens* strains (#140 and #143) were inhibited by SG200_otef2:*MbA*GH25. *MbA*_WT, *MbA* Δg2490 and *U. maydis* had no impact on *Curtobacterium* (Fig 2.5).

We have seen in previous section that purified GH25 displays lysozyme activity against bacterial peptidoglycan (Fig 2.3-B). Hence, biochemical activity combined with confrontation assay results points to the fact that *Curtobacterium* sp. is a possible target of GH25 activity.

2.3 Analyzing the impact of GH25 on oomycetes of different lifestyle

2.3.1 Effect of *MbA* and *MbA*_GH25 on *Hyaloperenospora arabidopsidis* (*Hpa*)

After establishing that both *MbA* and purified *MbA*_GH25 can antagonize *A. laibachii*, I wanted to explore if other oomycetes would also be inhibited by the basidiomycete yeast. To this end, collaboration with Jane Parker (MPIPZ, Cologne) was initiated to analyze how the biotrophic

oomycete *Hyaloperenospora arabidopsidis* ***(****Hpa)* interacts with *MbA* and *MbA*_GH25 protein. Infection lifestyle of *Hpa* is similar to *A. laibachii* with an overlapping host range (Ruhe et al. 2016). Therefore, analyzing an interaction between *MbA* and *Hpa*, gives additional insights to the *Arabidopsis* phyllosphere community structure.

To address if *Mba* interferes with *Hpa*, 2.5-week-old Col-0 *A. thaliana* seedlings growing on Jiffy peat pellets were spray inoculated with growing culture of *MbA*, followed by spray inoculation of *Hpa* (15*10^4 spores/ml) two days later. Purified *MbA*_GH25 and *MbA*_GH25(D124A) was mixed directly with *Hpa* spores (6µM conc.) and sprayed on seedlings. 5 days' post pathogen inoculation, release of *Hpa* spores per gram of *A. thaliana* leaves was observed under the light microscope. No significant change in *Hpa* sporulation upon treatment with either *MbA* strains, or GH25 protein on Col-0 (Fig 2.6-A) was observed.

Alongside eds1-12 mutant (on Col-0 background) *A. thaliana* seedlings were used to conduct *Hpa* assay with *MbA* strains and purified *MbA*_GH25 protein. *Hpa* sporulation was significantly higher in eds1-12 mutant line compared to Col-0 (Appendix Fig 6.2.3). Nevertheless, no inhibition of *Hpa* sporulation could be achieved on eds1-12 as well with our treatments (Fig 2.6-B).

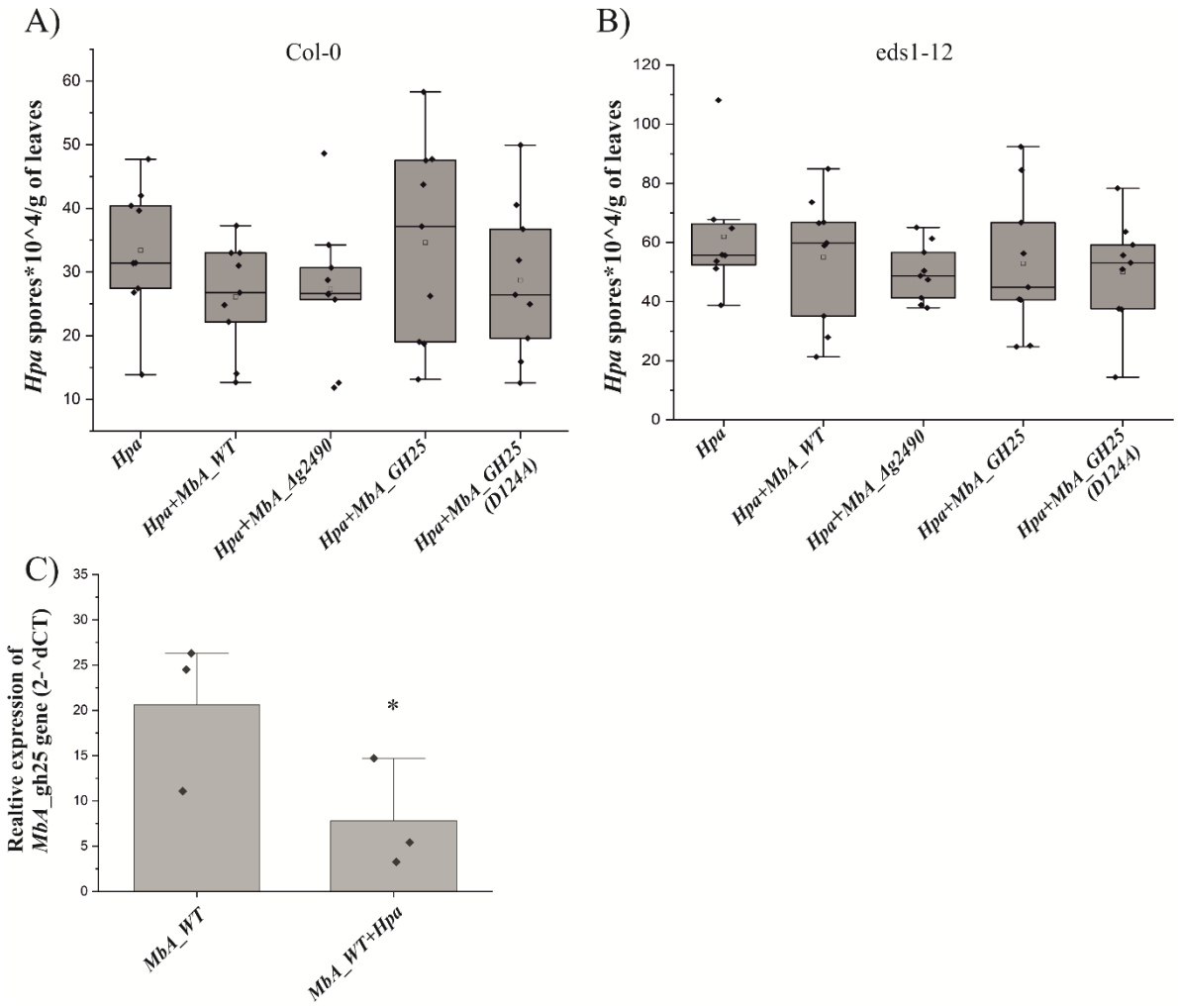

Figure 2. 6 Effect of *MbA* and *MbA*_GH25 on *Hyaloperenospora arabidopsidis*

MbA and purified *MbA*_GH25 do not affect *Hpa* infection in *A. thaliana* (A)- Col-0 and (B)-eds1-12 mutant (Col-0 background). Experiments in (A) and (B) conducted in three biological replicates (consisting of three technical replicates). Quantification of *Hpa* spores *10^4 / g of leaves was performed at 5 dpi. One-way ANOVA and Tukey' HSD (multiple comparisons of means; 95% family-wise confidence level) was performed to find significant difference between treatments. C)-GH25 gene expression analysis in *MbA* WT in response to *Hpa* treatment in *A. thaliana* Col0, normalized to *MbA* housekeeping gene ppi (unpaired t-test, $P<0.05$).

When *MbA* failed to antagonize *Hpa*, relative expression levels of the gh25 gene were quantified. Unlike the transcriptional induction that had been observed for *A. laibachii*, a slight decrease of GH25 expression was observed in presence of *Hpa* (Fig 2.6-C). This suggests that *MbA*_GH25 mediated antagonism was not possible in case of *Hpa* on *Arabidopsis*. Therefore, the presence of the basidiomycete yeast or its secreted hydrolase could not influence the growth of biotrophic oomycete *Hpa*.

2.3.2 Effect of *MbA* and GH25 on *Phytophthora infestans*

In contrast to biotrophic pathogens, such as *A. laibachii* and *Hpa*, *Phytopthora infestans* is known to affect Solanaceous crops and possess hemi-biotrophic lifestyle. In this study, *P. infestans* 88069 strain (Courtesy Francine Govers, WUR, The Netherlands) was used for *in vitro* and *in-planta* assay against *MbA*_WT and *MbA* Δg2490. For *in vitro* analysis, confrontation between *MbA* strains and *P. infestans* was carried out on RSA plates. The experiment was conducted in three individual replicates, and no zone of inhibition was observed between *P. infestans* and *MbA*_WT/ *MbA* Δg2490 (Fig 2.7-A). Nevertheless, *P. infestans* was restricted from growing over the area already colonized by yeast strains.

In planta tests were carried out with detached leaves of 5-6 weeks old *N. benthamiana*. Zoospores of *P. infestans* in 10^5 /ml concentrations were mixed 1:1 with growing culture (0.6-$OD_{600nm)}$ *MbA*_WT and *MbA* Δg2490 and dropped as 10µl on four corners of detached leaf (Fig 2.7-A). Necrotic leaf areas caused by *P. infestans* were quantified with ImageJ and the percentage of necrosis was calculated from three biological replicates (Fig 2.7-B). Both *MbA*_WT and *MbA* Δg2490 could not restrict *P. infestans* growth *in planta* as evidenced by the necrotic lesions.

Further, we tested *Ustilago maydis strain, SG200_otef2:MbAGH25* together with *P. infestans* to check for plant resistance against the oomycete. The overexpressor strains together with *U. maydis*, SG200 could not influence necrotic lesion development by *P. infestans* (Fig 2.7-C&D).

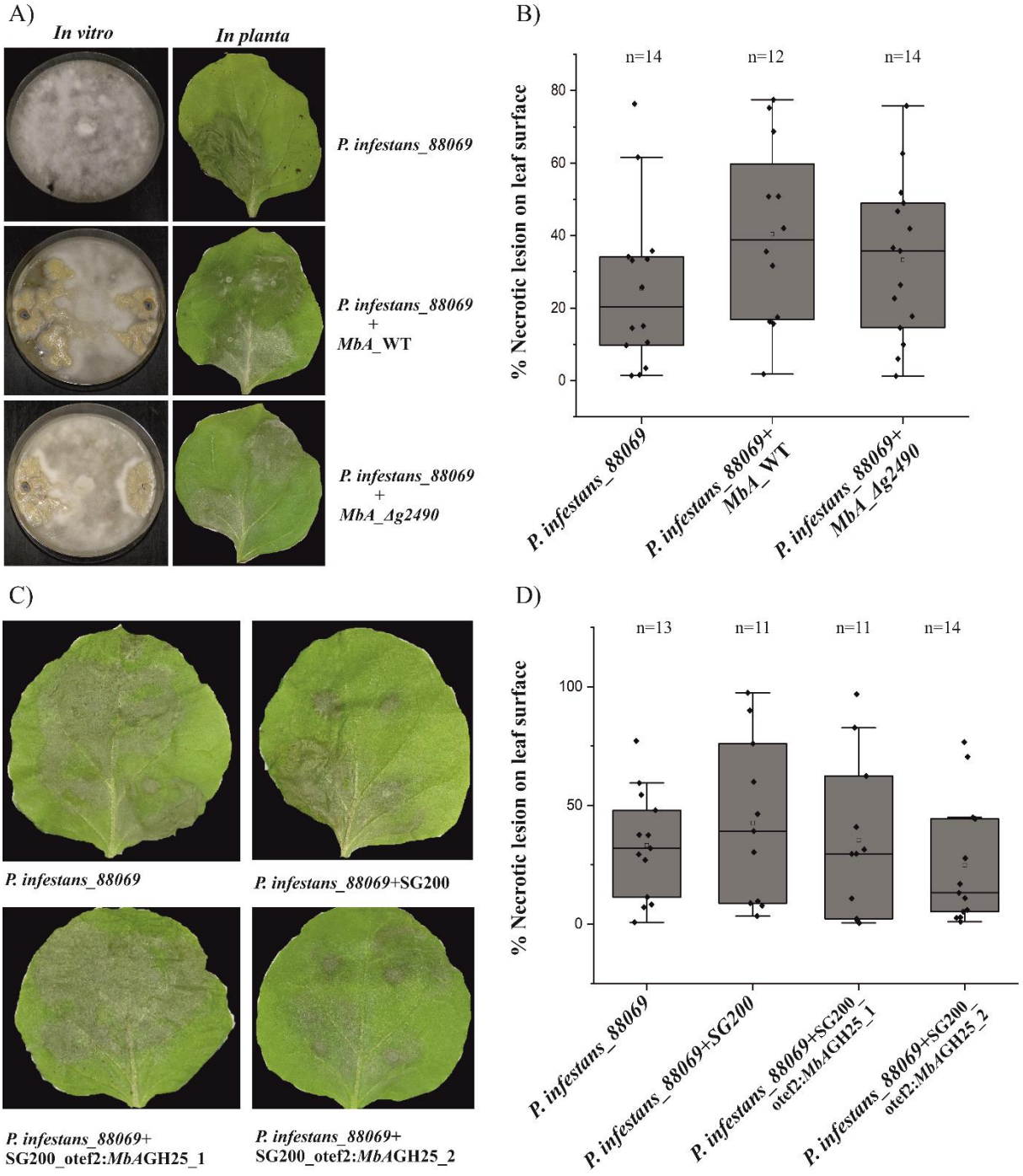

Figure 2. 7 Effect of *MbA* and *MbA*_GH25 on *Phytophthora infestans*

A)-Confrontation assay between *MbA*_WT/*MbA*dgh25 and *P. infestans* _88069 strain: ***in vitro*** on RSA plate where no zone of inhibition is observed and ***in planta*** droplet infection assay on 5-week-old *N. benthamiana* leaves. Necrotic lesion observed on control as well as *MbA*_WT and *MbA*_dgh25 strains. B)-Quantification of necrotic area on leaf surface by ImageJ and percentage of necrosis calculated in 3 biological replicates (n=number of leaves analyzed). One-way ANOVA performed, no significant differences between treatments observed. C)-Droplet infection assay of *P. infestans* on 5 week old *N. benthamiana* leaves. Necrotic lesions observed on control as well as SG200 and *U. maydis*_OE_GH25 strains. D)-Quantification of necrotic areas on leaf surface by ImageJ and percentage of necrosis calculated in 3 biological replicates (n=number of leaves analyzed). One-way ANOVA performed, no significant differences between treatments observed.

Finally, another strategy was employed to test for interaction between *MbA*_GH25 and *P. infestans*. *MbA*_GH25 and *MbA*_GH25(D124E) were transiently expressed in *N. benthamiana* using *Agrobacterium*. Modular cloning assembled the *MbA*_GH25 and *MbA*_GH25(D124E) proteins with N-terminal secretion signal and C-terminal GFP tag into level 1 destination vector. *Agrobacterium* strain GV301 containing the assembled constructs of *MbA*_GH25 was infiltrated into 4 weeks old *N. benthamiana* plants. The infiltrated leaves were further detached and inoculated with droplets of *P. infestans* zoospore suspension. Necrotic lesions were observed in all the *Agrobacterium*-infiltrated strains with GFP signal being detected only for mock inoculated leaf region (Figure 2.8-A).

Nevertheless, western blot was performed to detect GFP expression in total leaf extract. However, while GFP alone was detected in the mock-inoculated leaf at the expected size (28kDa), no band could be visualized for the *MbA*_GH25-GFP fusion protein (Figure 2.8-B).

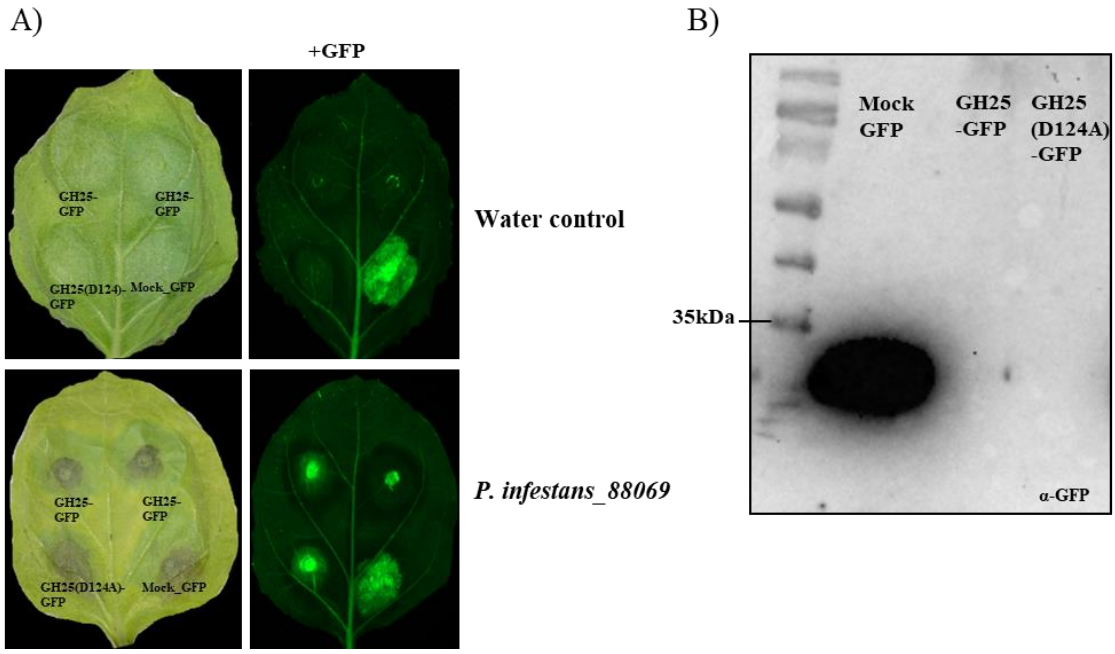

Figure 2. 8 *Agrobacterium* based transient expression of *MbA*_GH25

A)-*Agrobacterium* vector expressing GFP (mock control), GH25-GFP and GH25 (D124A)-GFP were infiltrated in *N. benthamiana*. 3 days post infiltration, the leaves were detached and 10µl of sterile H2O (water control) or zoospore suspension of *P. infestans* were inoculated to the leaves. Necrotic lesions upon *P. infestans* treatment were developed in all infiltrated regions. GFP signal was observed only for mock_GFP infiltrated leaves (Ex. 488 nm, Em. 510 nm). B)-Western blot analysis to detect GH25 expression in planta. 3 days' post infiltration with *Agrobacterium* vector expressing GFP (mock), GH25-GFP and GH25 (D124A)-GFP, leaves were harvested for protein extraction. The total extract of each treatment was loaded in SDS gel to detect expression of respective proteins. Only mock_GFP treatment detected free GFP protein at expected band size of 28kD.

Since GFP is a relatively large tag that might interfere with GH25 protein stability. Therefore, *MbA*_GH25 level 1 construct was assembled using a Myc tag (1.2kD size) in the C-terminal region. However, even for Myc tagged- *MbA*_GH25 *Agrobacterium* construct, no expression was observed *in planta* 3 days post infiltration (Appendix Fig 6.2.4). Transient expression of *MbA*_GH25 protein in *N. benthamiana* needs to be evaluated again and repeated with different tags for detection and localization; at the same time, any potential toxicity of *MbA*_GH25 protein towards *Agrobacterium* itself, needs to be considered.

Therefore, in an interaction between *MbA* and *P. infestans*, antagonism of the oomycete was not observed. *Ustilago maydis* strain, SG200_otef2:*MbA*GH25 was unable to restrict oomycete growth as well, indicating *MbA*_GH25 to be insensitive towards hemi-biotrophic *P. infestans* strain 88069. Nevertheless, since a strong inhibition of *A. laibachii* by *MbA* wildtype yeast and *MbA*_GH25 protein was observed; it could be worthwhile to test for *MbA* antagonism against other isolates of *P. infestans* to identify a potential antimicrobial agent.

2.4 Functional Characterization of GH25 from *U. maydis*:

MbA is phylogenetically close to smut pathogen, *Ustilago maydis*. In the previous section, it is shown that GH25 has a highly conserved DXE motif across the fungal kingdom (Fig 2.3-A) and the GH25 protein sequence from *U. maydis* (gene ID: UMAG_02727) shares 77.87% identity with that of *MbA*. Therefore, it is intriguing to explore the role of GH25 in the pathogenic smut *U. maydis*. Publicly available transcriptome data of *U. maydis* (Lanver et al., 2018) shows that UMAG_02727 is highly expressed between 0.5 and 1 dpi, which correlates with appressoria formation upon host epidermal penetration of the fungus (Appendix Fig 6.2.5-A).

To explore an eventual role of UMAG_02727 during the pathogenic stage, overexpression of the same gene was carried out using promoter of *pit2* (UMAG_01375) gene (SG200_pPit2_02727). Additionally, another construct with UMAG_02727 driven by the actin gene promoter (UMAG_11232) was used to obtain a constitutive expression of *Um*_GH25 (SG200_pActin_02727). Maize inoculation with SG200_pPit2_02727 resulted in a significantly reduced disease symptoms when comparing to of the progenitor strain SG200. Contrary, for SG200_pActin_02727, the disease incidence was similar to that SG200 (Fig 2.9-A). Microscopy performed with infected maize samples shows colonization of SG200 and SG200_pPit2_02727 at 3 dpi (Fig 2.9-B). To determine of any possible growth defects in SG200_pPit2_02727, a series of stress tests on plate was conducted including osmotic stress

(sorbitol, NaCl), cell wall stress (Calcofluor, Congo-red), and oxidative stress (H2O2). SG200_pPit2_02727 displayed no growth defects compared to SG200 (Appendix Fig 6.2.5-B). Alongside, biomass quantification revealed no significant difference in colonization between SG200 and SG200_pPit2_02727 at 4dpi in maize (Appendix Fig 6.2.5-C).

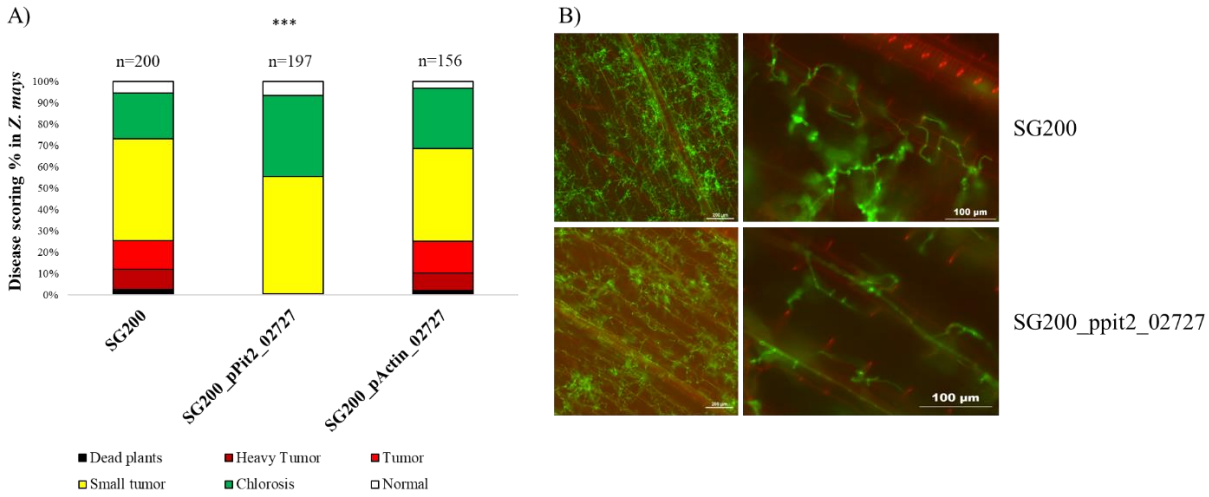

Figure 2. 9 Effect of UMAG_02727 overexpression on *U. maydis* virulence

A)-Disease symptoms on *Z. mays* seedlings showing significant reduction *U. maydis* virulence upon UMAG_02727 overexpression (13 dpi) with *pit2* promoter. No reduction of *U. maydis* virulence with pActin driven umag_02727 overexpression. n indicates the number of maize seedlings across three biological replicates. Asterisks mark significant reduction in *U. maydis* disease index based on the data in (Appendix Table 6.3). (B) To visualize colonization of *U. maydis in planta*, WGA-Alexa flour staining was performed at 3 dpi (fungal hyphae stains green). Both SG200 and SG200_pPit2-02727 strains can colonize plant tissue and cell-cell penetration of hyphae observed. Scale bars: SG200-left (200µm) and right (100µm); SG200_pPit2_02727-left (200µm) and right (100µm).

To further underpin the mechanism of virulence reduction, relative expression of defense marker genes in host plant was analyzed upon infections by SG200 and SG200_pPit2_02727 at 4 and 6 dpi (Fig 2.12-A and B) Maize GAPDH served as a reference for relative gene quantification. The SA associated pathogenesis related genes PR3, PR4, PR5, PRm6b, and the cell-death marker gene hsr203j were analysed, out of which PR5 showed slight upregulation in SG200_pPit2_02727 inoculated maize plant at 4dpi (Fig 2.10-A).

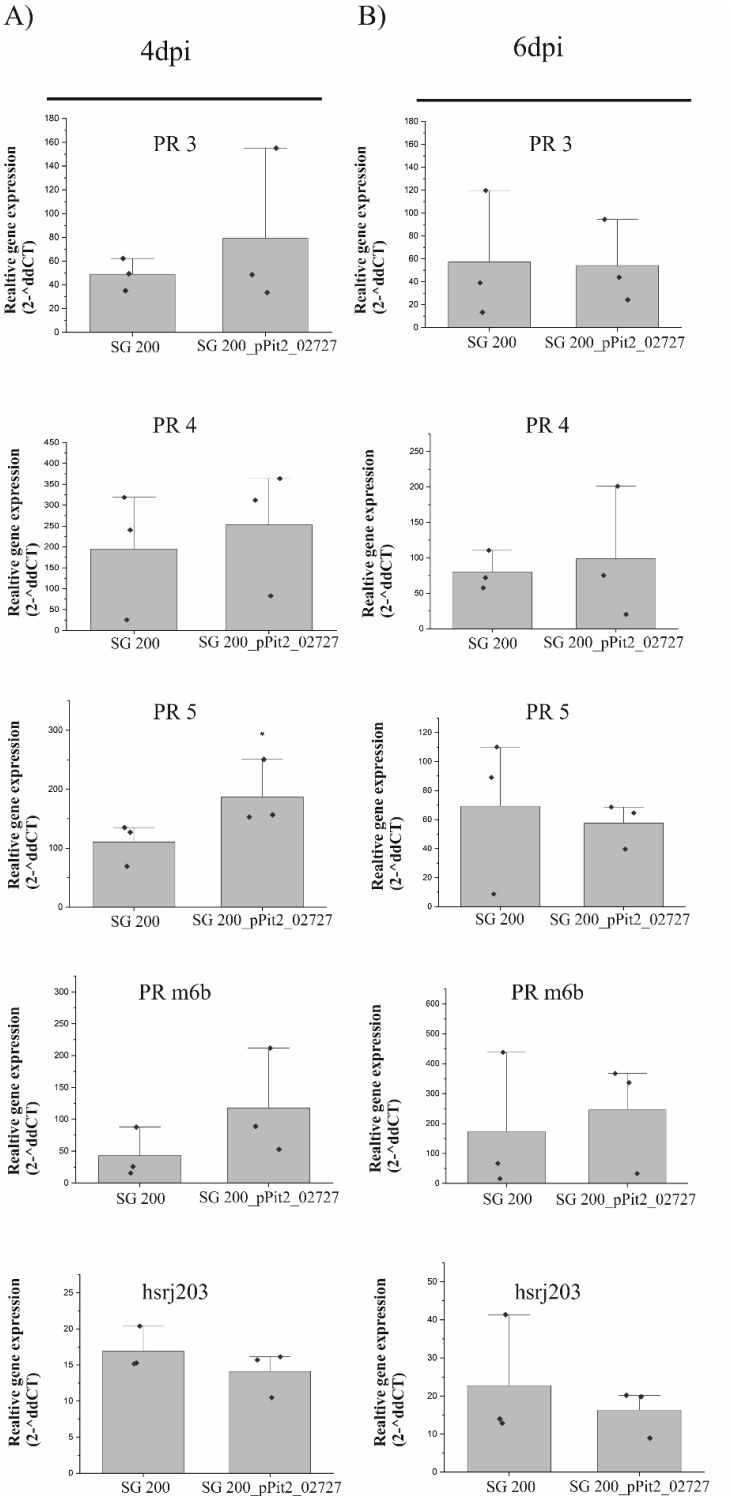

Figure 2. 10 Analysis of maize defense marker gene induction

qRT-PCR analysis of SG200 and SG200_pPit2_02727 infected maize plants at A)-4dpi and B)-6dpi. Fold change of expression of SA- marker genes PR3, PR4; PR5; PRm6b and cell-death marker gene hsr203j was analyzed. Expression was normalised to maize housekeeping gene GAPDH. The experiments were performed in three independent biological replicates (as indicated by the data points on bar graph). Error bars indicate outlier (co-eff. 1.5). P values were calculated with an unpaired t-test, *P<0.05.

Thus, an overexpression of UMAG_02727 leads to a decrease in disease incidence in maize. PR5 upregulation could potentially alert host immune responses to restrict *U. maydis* infection. However, we need to proceed with caution before making a confirmed statement because overexpression of UMAG_02727 with actin promoter would also be expected to reduce disease incidence *in planta*. To address the concern with SG200_pActin_02727, gene expression patterns need to be analyzed for UMAG_02727 in all the overexpressed *U. maydis* strains. Also, a larger repertoire of maize defense marker genes needs to be tested for underpinning the mechanism behind disease reduction. Nevertheless, our results show interesting aspects of GH25 overexpression in smut pathogen, *U. maydis* and could be further explored to dissect plant defense pathways in response to pathogen infection.

3.2 Antagonism of *A. laibachii* by *MbA*_GH25 is not explained by activation of host immune responses

I purified the Glycoside Hydrolase 25 protein from *MbA* after heterologous expression in *P. pastoris*. The purified *MbA*_GH25 was treated to *A. thaliana* seedlings growing on MS media and analyzed for the presence of elicitor activity. Plants can perceive conserved residues in microbes (Microbe associated molecular patterns-MAMPs) by pattern recognition receptors (Jones and Dangl, 2006) and these MAMPs act as elicitors triggering plant immune responses. In the elicitor assay, relative gene expression levels of several marker genes such as WRKY transcription factor encoding genes and genes involved in Salicylic acid synthesis was analyzed.

WRKY transcription factors have been implicated in pathogen defense for a variety of reasons (Zheng et al., 2006). Out of 72 wrky genes were differentially regulated in *Arabidopsis* after treatment with *Pseudomonas syringae* or SA (Dong et al., 2003). Promoters of plant defense related genes such as PR genes and NPR1 contain W-box domain for the *wrky* genes to bind (Yu et al., 2001). Additionally, WRKY22/WRKY29 transcription factor together with plant MAPK cascade leads to resistance against both bacterial and fungal pathogen (Asai et al., 2002). WRKY 53 is one of the important regulators of early leaf senescence, with SA having a positive and JA signaling having a negative impact on expression of wrky53 gene (Zentgraf and Doll, 2019). WRKY33 expression displayed resistance against necrotrophic fungal pathogens such as *Alternaria brassicicola* and *Botrytis cinerea*, however, showed enhanced susceptibility to bacterial pathogen, *P. syringae*. Contrasting responses of wrky33 expression towards bacterial and fungal pathogens was attributed to altered expression of the JA-regulated *PFD1.2* and SA-regulated *PR-1* genes (Zheng et al., 2006). WRKY30 was reported to be involved in defense against Cucumber Mosaic Virus (CMV) in *Arabidopsis* together with being induced in response to abiotic stress, fungal elicitor, SA and ABA treatment (Zou et al., 2019).

Salicylic acid (SA) accumulation is associated with defense against biotrophic pathogens. For e.g., *Ustilago maydis* secretes chorismite mutase 1 (cmu1) to lower SA levels to for host colonization (Djamei et al., 2011). During SA biosynthesis, isochorismate synthase gene 1 (ics1) synthesizes the SA precursor isochorismate. Filamentous pathogens such as *Phytophthora sojae* and *Verticillium dahliae* hijack the SA biosynthesis pathway by secreting isochorismatases which break down isochorismate to 2,3-dihydro-2,3-dihydroxybenzoate (DDHB), promoting pathogen virulence (Lefevere et al., 2020; Liu et al., 2014). *FRK1* (*FLG22*-

INDUCED RECEPTOR-LIKE KINASE 1) encodes for an LRR receptor in *Arabidopsis* which perceives pathogen derived elicitors (PAMP) triggering the PTI response (Asai et al., 2002).

In this study, widely characterized bacterial MAMP, Flg22 was used a positive control, which displayed significant induction of marker gene expression compared to *MbA*_GH25 protein treatment. Although, there was basal level expression in some of the marker genes tested for *MbA*_GH25, *MbA*_GH25(D124A) and Heat-killed *MbA*_GH25 treatments with respect to mock (1/2 MS), no difference in elicitor activity between active and inactive GH25 could be ascertained.

In a recent work by (Wang et al., 2022), phyllosphere yeast *Protomyces arabidopsidicola* displayed an immune priming effect in *Arabidopsis*, whereby the plants resisted further infection caused by *Botrytis cinerea*. The immune priming effect was found to be associated with MAPK activation, together with SA and JA signaling pathways. *Albugo laibachii* does not suppress host-mediated broad-spectrum immune responses and can persist in host plants with altered hormone levels (Ruhe et al., 2016). *A. thaliana* cpr5 mutant accumulating high levels of SA, and PR genes was tested for resistance towards *Hyloperenospora arabidopsidis* (*Hpa*) and *A. laibachii*. While *Hpa* infection was completely abolished in the cpr5 mutant, *A. laibachii* showed in planta colonization at 10 dpi and weak rust symptoms on leaves (Ruhe et al., 2016). Hence, increased plant defense responses had no impact on colonization by white rust pathogen *Albugo laibachii*.

Therefore, the finding that *MbA*_GH25 protein is not significantly activating important regulators of plant immunity such as WRKY transcription factors, SA synthesis precursors support the idea that host immune response activation is not a prerequisite for inhibiting white rust pathogen *A. laibachii*.

3.3 Antagonism of *A. laibachii* by *MbA*_GH25 might result from the inhibition of associated bacteria

To unravel the mechanism behind *A. laibachii* antagonism, I analyzed the impact of *MbA* and *MbA*_GH25 against several *A. laibachii* associated bacteria on *A. thaliana* leaves. Plant leaf surface harbors diverse groups of microbial communities, with an abundance of bacterial members (Vorholt, 2012). Thus, leaf colonization by microbes, in addition to being exposed to host and environmental factors, is influenced by resident microbiota of the phyllosphere (Chaudhry et al., 2021). Biotrophic pathogens are inhibited by host cell death responses, while

necrotrophs benefit from the dead tissue to invade host plants (Glazebrook, 2005). Therefore, necrotrophs can collaborate with hemi-biotrophic pathogens such as *Pseudomonas syringae*, whereby higher SA levels and lower JA accumulation *in planta*, will lead to efficient growth of necrotrophs (Kemen, 2014).

The white rust pathogen *Albugo* is known to suppress non-host resistance in *Arabidopsis thaliana*, (Cooper et al., 2008) and it facilitates the colonization by the hemibiotroph *Phytophthora infestans* (Belhaj et al., 2017). Although *P. infestans* did not induce cell death in *A. thaliana*, it expressed set of effector genes that overlaps with those secreted by *P. infestans* during infection of *Solanum tuberosum* (Belhaj et al., 2017; Larousse and Galiana, 2017). An example of bacterial partnership comes from *Erwinia toletana* which cooperates with the olive knot pathogen *Pseudomonas savastanoi* pv. *savastanoi* by quorum sensing to cause more aggressive disease symptoms on olive plants (Caballo-Ponce et al., 2018). Motile unicellular *Vorticella* helps to disseminate *P. parasitica* propagules, which in turn can promote tobacco black shank disease (Galiana et al., 2011).

Association of beneficial bacteria with *P. infestans* has also been explored to certain extent. An isolate of the soil bacterium *Bacillus megaterium* promoted colonization of 12 *Phytophthora* isolates on Rhododendron (Kong and Hong, 2016). While the importance of beneficial microbes for plant pathogens has not been emphasized (Kemen, 2014), in human pathogens, many such facilitator microbes have been described, such as co-colonized bacterial biofilms assisting in infection of *Candida albicans* (Kojic and Darouiche, 2004), or pre-infection by *Klebsiella aerogenes* making immunocompromised patients susceptible to *Cryptococcus neoformans* (Frases et al., 2006). Analyzing beneficial associations of pathogenic microbes can provide meaningful insights into disease proliferation and pathogenicity (Kong and Hong, 2016) as well as how new pathogens emerge and how pandemics occur (Kemen, 2014).

From the laboratory of Eric Kemen (ZMBP, Tübingen), I received 7 bacterial member consortia, closely associated with *A. laibachii* Nc14 strain which were found to be present even after antibiotic treatment and repeated propagation of Nc14 on *A. thaliana*. Bacterial members comprised of both gram-positive and gram-negative strains and *in vitro* confrontation assays with *MbA* resulted in the inhibition of *Pseudomonas brenneri* and *Pseudomonas veronii*. However, the *MbA* knockout strain of GH25 (*MbA*_∆g2490) similarly inhibited the same *Pseudomonas* strains, therefore, this antagonism of *MbA* is probably caused by other means. For example, anamorphic yeasts such as *Moesziomyces antarcticus* are known to produce bio-

surfactants and secondary metabolites (Morita et al., 2007), which could potentially serve as antimicrobials.

At the same time, interaction patterns during *in vitro* and *in planta* tests can vary, and the transcriptomic analysis by my colleague Katharina Eitzen, showed low expression of *gh25* gene in axenic culture and differential upregulation in presence of *A. laibachii in planta*. Therefore, to test for inhibition of *Albugo* associated bacteria, the gh25 gene was heterologously expressed in related smut fungus *U. maydis*. Interestingly, the recombinant *U. maydis* strains overexpressing *MbA*_GH25 inhibited *Curtobacterium flaccumfaciens pv. flaccumfaciens*, but not the *Pseudomonas* strains. This shows that *MbA* displayed antimicrobial activity against *Pseudomonas* independent of GH25 secretion. Purified *MbA*_GH25 also inhibited *Curtobacterium flaccumfaciens pv. flaccumfaciens* in an *in vitro* plate assay as opposed to the mutant *MbA*_GH25(D124A) (Appendix Fig 6.2.6-A). Therefore. *Curtobacterium* is likely a target for GH25 activity.

Furthermore, it will be of interest to find out if any specific cell wall residues are cleaved in *Curtobacterium.* NMR spectroscopic analysis revealed that in cell wall of *Curtobacterium* glycopolymer rhamnan is present, which has been correlated with bacterial adhesion, biofilm formation and pathogenicity (Zaychikov et al., 2021). Therefore, rhamnan could be a potential substrate for *MbA*_GH25 by which *Curtobacterium* is inhibited.

Nevertheless, to test if GH25 directly targets *A. laibachii* cell wall, an additional experiment was performed. In results section 2.1, it was shown that purified *MbA*_GH25 protein showed lysozyme activity against bacterial peptidoglycan in fluorogenic assay. Although the cell walls of oomycetes are mainly composed of β-1,3, and β-1,6 glucans (Aronson et al., 1967), Mélida et al., (2013) reported that oomycete cell walls contain varying levels of N-acetyl Glucosamine (NAG)-the building blocks of bacterial peptidoglycan. Therefore, I isolated *A. laibachii* cell walls from harvested zoospores using a protocol from (Mélida et al., 2013) , and checked for activation of *MbA*_gh25 gene expression. However, no significant induction of the gh25 expression was detected in growing *MbA* culture (Appendix Fig 6.2.6-B). Since, it is challenging to isolate cell wall from an obligate biotroph such as *A. laibachii*, there is the possibility that adequate cell wall material was not present to induce gh25 gene expression in *MbA.* Therefore, a direct activity of *MbA*_GH25 on *A. laibachii* cell wall could not be established in this study.

3.4 *MbA* is not antagonizing the downey mildew pathogen *Hyaloperenospora arabidopsidis*

Hyaloperenospora arabidopsidis (*Hpa*) is a biotrophic oomycete similar to *Albugo* and is a frequently occurring foliar pathogen of natural *A. thaliana* populations (Herlihy et al., 2019; Holub, 2008). However, microbial associations of *Hpa* differ from that of *A. laibachii*. In a recent study by Almario et al., (2022), *Hpa* comprised of core taxa and its relative abundance increased throughout the winter season until March. Interestingly, the sampled leaves were asymptomatic due to the presence of plant beneficial bacterium such as *Sphingomonas* and *Variovorax* (Almario et al., 2022). Mainly bacterial members have been identified to be antagonistic towards *Hpa*. Berendsen et al., (2018) reported three bacterial taxa (*Stenotrophomonas* sp., *Xanthomonas* sp., and *Microbacterium* sp. to become enriched in the *A. thaliana* rhizosphere upon infection with *Hpa*. The antagonism of *Hpa* by yeasts have not been explored greatly.

In this study, *MbA* strains and purified *MbA*_GH25 protein had no impact on *Hpa* sporulation. Importantly, the gh25 gene expression was not induced in *MbA* when in contact with *Hpa*. Therefore, the presence of yeast could not influence the growth of downey mildew pathogen compared to the reduction of white rust pathogen on the same host. At the same time, since purified *MbA*_GH25 was unable to induce *ics1* gene involved in SA biosynthesis, the inhibition of *Hpa* would not be possible.

While screening of mutant lines in *A. thaliana* for resistance to biotrophic pathogen *Hpa,* EDS1 protein was identified (Parker et al., 1996). In this study, the eds1-12 mutant (in Col-0 background) of *A. thaliana* was also treated to analyze the impact of *MbA* and purified GH25 on *Hpa* infection (Fig 2.6-B). Sporulation of *Hpa* was significantly higher in *eds1-12* than Col-0 (Appendix Fig 6.2.3), however, *MbA* and *MbA*_GH25 could not influence *Hpa* sporulation in anyway. Therefore, even under host immunity deficient conditions, *MbA*_GH25 did not act as a non-specific elicitor to provide any additional defense responses against *Hpa* infection in the plant.

Hpa is less abundant in wild *Arabidopsis thaliana* populations (Ruhe et al., 2016), because it is strongly affected by altered hormonal levels in the host. ABA mutant lines of *A. thaliana* are accompanied by decreased JA levels and increase in SA biosynthesis and is therefore resistant to *Hpa* infection (Adie et al., 2007; Léon-Kloosterziel et al., 1996; Ruhe et al., 2016). On the other hand, the *sid2-2* mutant, defective in Isochorismate Synthase 1 and unable to accumulate

SA, is highly susceptible to *Hpa* (Bernsdorff et al., 2015; Nawrath and Metraux, 1999; Ruhe et al., 2016). Nevertheless, *A. laibachii* growth was unaltered when analyzed with *A. thaliana* hormone mutant lines. The above results led (Ruhe et al., 2016) to hypothesize that *Hpa* could outcompete *A. laibachii* for a short span of time, by taking advantage of suppressed plant immune system, but eventually *A. laibachii* will persist because it is well adapted to an active host immune system, which gives *Albugo* an edge over other microbes when competing for limited resources in the phyllosphere. Nevertheless, *A. candida* is known to suppress broad spectrum host innate immunity and increases susceptibility of the plant to downey (Cooper et al., 2008; Prince et al., 2017). Therefore, it will be interesting to explore a tripartite interaction among *MbA, A. laibachii* and *Hpa* on *Arabidopsis;* whether *MbA* could inhibit both *A. laibachii* and *Hpa* growth and which genetic components would be involved behind the antagonism.

3.5 *Phytophthora infestans* is not affected by *MbA*

Phytophthora infestans is a hemi-biotrophic pathogen of solanaceous crops. Although, *P. infestans* does not naturally infect *Arabidopsis thaliana*, a mutation of the gene *pen3*, involved in cell wall defense, allowed the pathogen to establish infections *in planta* (Stein et al., 2006). Later, it was shown that *A. laibachii* infections help *P. infestans* to colonize and sporulate on *Arabidopsis* (Belhaj et al., 2017), which could result from *Albugo* infections in Brassicaceae promoting a host jump by certain pathogens (Thines, 2014).

Prompted by *MbA* antagonism of *A. laibachii*, I investigated the interaction of the basidiomycete yeast with other oomycetes which have evolved independently to develop different lifestyles (Kemen and Jones, 2012). To test whether there is a direct antagonism between *MbA* and *P. infestans*, confrontation assays on plate were carried out. However, any zone of inhibition between the two interacting microbes was not observed, although *P. infestans* was unable to grow over *MbA* on plate. *In vitro* assays were followed by *in planta* experiments; however, a growing culture of *MbA* was unable to restrict necrotic lesions on *N. benthamiana* caused by *P. infestans* (Fig 2.7).

In a study by de Vries (2018), ascomycetous fungal endophytes were tested for inhibition against *P. infestans*, out if which, *Monosporacu*s sp. inhibited *Phytophthora* under culture conditions but not *in planta* which suggests conditional activation of inhibitory compound by the ascomycete fungus. In this study, the niche competition between the yeast and *Phytopthora* was not observed. Nevertheless, to test for an eventual impact of *MbA*_GH25 on *P. infestans*, recombinant *Ustilago maydis*, SG200_otef2:*MbA*GH25strains (earlier used for bacterial

confrontation assay in Results section 2.2.2) were utilized. Also in this case, there was no reduction of necrotic lesions caused by *P. infestans*. Therefore, *P. infestans* is not a target for *MbA*_GH25 antagonism.

Biological control of *Phytophthora* has been achieved by various means. Some reports have highlighted the inhibitory effect of potato associated bacteria against *Phytophthora* (de Vrieze et al., 2019), or by the application of bacterial volatiles on potato leaf surface (Gfeller et al., 2022). Biocontrol fungi such as *Trichoderma* and *Penicillium* have also been involved in antagonizing *Phytophthora* (reviewed by Oubaha et al., 2021); either by emission of volatile organic compounds or by induction of host defense responses. Currently, there are not many reports that show the inhibiton of *P. infestans* by yeasts or secreted CWDEs. Nevertheless, other *Phytophthora* isolates can be potentially screened for antagonism by *MbA* to chance upon a target antimicrobial agent that could be useful in agricultural practices.

3.6 Overexpression of UMAG_02727 in *U. maydis* leads to reduction of virulence

MbA is phylogenetically close to the group of pathogenic smuts which comprises *Ustilago maydis*, *U. hordei*, *U. avenae* which are pathogens of maize, barley, and oats respectively. Therefore, given the highly conserved nature of GH25 protein in the fungal kingdom (Fig 2.2-A), it is intriguing to explore function of the GH25 expression in a smut pathogen. To this end, GH25 gene from *U. maydis* (UMAG_02727) was overexpressed with *pit2* promoter in the solopathogenic strain of *U. maydis* called SG200. Pit2 (UMAG_01375) is a secreted effector of *U. maydis* which is essential for fungal virulence and is highly expressed *in planta* throughout the entire infection cycle (Mueller et al., 2013; Skibbe et al., 2010). Further experiments revealed a significant reduction of fungal virulence on maize plant together with upregulation of SA associated pathogenesis related gene PR5.

To observe any toxicity in SG200 cells due to overexpression of UMAG_02727, another recombinant strain with promoter of the actin gene was constructed. Actin (UMAG_11232) is highly expressed in axenic culture as well as *in planta* (Lanver et al., 2018). Nevertheless, no reduction of *U. maydis* virulence was observed in maize for pActin_02727 overexpression strain, which could be due to pit2 promoter having a much stronger *in planta* activity than pActin as evidenced by the difference in expression levels of Pit2 and Actin genes (Appendix Fig 6.2.7).

Necrotrophs have a much larger secretome than biotrophs and encode a larger number of CWDEs (Bradley et al., 2022; Hane et al., 2020). Nevertheless, many recent studies have focused on exploring the role of CWDEs or GH proteins in biotrophic pathogens such as *U. maydis*. Glycoside Hydrolases from *U. maydis* have been characterized in a recent study by Moreno-Sanchez et al. (2021), where xylanase encoding genes from GH10 and GH11 families were necessary for fungal proliferation. However, single, and multiple deletion of xylanase genes reduced *U. maydis* infection to similar levels. Other GH proteins such as ß1-3 glucanases from *U. maydis* were found to be involved in fungal cell remodelling (Reyre et al., 2022) and cell to cell expansion (Ökmen et al., 2022).

In this study, UMAG_02727 overexpression led to an increased expression of the maize defense marker gene PR5. This may indicate either a direct recognition of GH25 by a plant receptor or could result from cleaving ß-glucans from the fungal cell wall, which in turn could act as a PAMP to induce pattern triggered immunity. Interestingly, in the transcriptomic analysis by Lanver et al., (2018) UMAG_02727 is only expressed between 0.5 and 1 dpi, which corresponds to which correlates with appressoria formation upon host epidermal penetration of the fungus. Therefore, *U. maydis* switches off the production of UMAG_02727 before the biotrophic colonization of host begins. A recent study by Gámez-Arjona et al., (2022) has also shown how loss of a cellulose degrading gene leads to an enhancement of virulence in *Fusarium oxysporum*, highlighting the fact that biotrophic pathogens perform better with loss or downregulation of certain CAZymes which helps them to evade recognition by host immune pathways.

Therefore, what could be the purpose of *U. maydis* having UMAG_02727 in their genetic repertoire, if overexpression of the same gene leads to a reduction of virulence? In this study, it is shown that GH25 from *MbA* antagonizes the pathogenic oomycete *A. laibachii*. Hence, expression UMAG_02727 could be advantageous for yeast cells of *U. maydis* and other pathogenic smuts to compete against other microbes on the plant surface.

3.7 Conclusion and future directions

In this study, I have shown the importance of basidiomycete yeast, *MbA* in regulating phyllosphere community of A. thaliana by antagonizing white rust pathogen, *A. laibachii*. From an ecological perspective, functional investigation of such interactions can provide meaningful insights as to why certain yeasts prefer to colonize certain environments. Glycoside Hydrolase 25 protein from *MbA* specifically antagonized *A. laibachii* by targeting associated bacterial

strain, which brings forth the importance of microbial network analysis in plant protection. Further studies can be conducted to gain deeper insight into impact GH25 on leaf microbiome assembly. At the same time, evolutionary conservation of GH25 mediated antagonism can be analyzed in microbial interactions to understand the importance of hydrolase genes in the fungal kingdom.

To explore the role of *MbA*_GH25 against oomycetes of different lifestyles, I tested *Hpa* strain Noco2 and *P. infestans* strain 88069, both of which were not inhibited by *MbA* and purified *MbA*_GH25. Nevertheless, it could be worthwhile to screen other economically important plant pathogens such as *Botrytis cinerea* to develop GH25 as an antimicrobial agent.

Exploring the function of GH25 expression in biotrophic pathogens such as *Ustilago maydis* can help identify mechanisms of fungal pathogenicity. Alongside, detailed investigation on plant immune pathway upon perception of hydrolases can open new avenues for generation of resistant plant varieties.

Finally, to broaden the understanding of microbial antagonism in basidiomycete yeasts, the function of Glycoside hydrolases beyond GH25 could potentially be investigated. Plant-microbial interactions are a treasure trove for generating sustainable strategies of crop protection and more studies performed in this direction will help in boosting agricultural productivity and achieve food security.

3. Discussion

4. Material and methods:

4.1 Material

4.1.1 Chemicals

All chemicals used in this study were purchased from Biozym (Hessisch Oldendorf, Germany), Becton Dickinson (Heidelberg, Germany), GE Healthcare (Munich, Germany), Invitrogen (Darmstadt, Germany), Merck (Darmstadt, Germany), Roche Diagnostics (Mannheim, Germany), Roth (Karlsruhe, Germany), and Sigma-Aldrich (Deisenhofen, Germany) unless otherwise stated.

4.1.2 Buffers and solutions

Buffers and solutions were prepared according to (Sambrook et al., 1989; Ausubel, 2002) if not otherwise stated in the respective method description. Sterilization of buffers and solutions was done at 121 °C, 5 min or via a sterile filter, if solution was heat sensitive (Pore size 0.2 µm, Merck, Darmstadt, Germany).

4.1.3 Enzymes

All enzymes used in this study is summarized below in Table 4.1.

Table 4. 1 Chemical reagents and their purpose of use

Reagent/Purpose	Supplier
Restriction enzymes	• New England Biolabs (NEB, Frankfurt/Main, Germany) • Thermo (Thermo Fisher Scientific Inc., Bonn, Germany)
DNA polymerases	• Phusion® Hot Start High-Fidelity DNA-Polymerase (Thermo Fisher Scientific Inc., Bonn, Germany) • KOD Xtreme™ Hot Start DNA Polymerase (Novagen®/Merck Millipore, Darmstadt, Germany) • GoTaq® Green Master Mix (Promega, Walldorf, Germany)
Ligation of DNA molecules	• T4 DNA ligase (NEB, Frankfurt/Main, Germany)

Enzymatic degradation of RNA	• RNaseA (Serva, Heidelberg, Germany)
Enzymatic degradation of DNA	• TURBO DNA-free™ Kit (Ambion®/ Thermo Fisher Scientific Inc., Bonn, Germany)
Enzymatic degradation of fungal cell walls	• Lysing enzymes from *Trichoderma harzianum*/ Glucanex® (Sigma-Aldrich, Deisenhofen, Germany)

4.1.4 Commercial kits

All commercial kits used in this study is summarized below in Table 4.2

Table 4. 2 Commercial kits

Purpose	**Supplier**
Plasmid DNA extraction	QIAprep® Mini Plasmid Kit (Qiagen, Hilden, Germany)
Purification of PCR products/ Extraction of nucleic acid from agarose gel	NucleoSpin gel and PCR Clean-up kit (Machery-Nagel, Düren, Germany)
cDNA synthesis	RevertAid H Minus First Strand cDNA Synthesis Kit (Thermo Fisher Scientific Inc., Bonn, Germany)
Gibson assembly	2x Hifi DNA assembly mix (NEB, Frankfurt/Main, Germany)
Site-directed mutagenesis	Quickchange (Multi) Kit (Agilent Technologies, Santa Clara, USA). 4.2 Media and growth conditions for microorgan
Purified GH25 activity assay	EnzChek Lysozyme Assay Kit (E22013, Invitrogen, Fisher Scientific GmbH - Im Heiligen Feld 17, Germany
Ni-NTA matrix for protein purification	Ni-Sepharose 6 Fast-Flow, GE-Healthcare; Freiburg, Germany
Protein Desalting or Buffer Exchange	Zeba Spin Desalting Columns 7K MWCO (Thermo Fisher Scientific Inc., Germany)

4.2 Media and growth conditions for microorganisms

4.2.1 Media

Table 4. 3 Media used in this study along with their compositions

Name	Composition	Remarks
1/2 Murashige and Skoog (MS)	0.2 % (w/v) MS basal salt mixture 0.8 % (w/v) Agar	in H2Obid. pH 5.7
Potato-Dextrose (PD)-Agar	2.4 % (w/v) PD broth 2.0 % (w/v) Agar	in H2Obid.
PDA- Charcoal	Addition of 1 % (w/v) Charcoal to PD-Agar media	in H2Obid.
YEPSL	1.0 % (w/v) Yeast extract 0.4 % (w/v) Peptone 0.4 % (w/v) Sucrose	in H2Obid.
Regeneration Agar	1.0 % (w/v) Yeast extract 0.4 % (w/v) Peptone 0.4 % (w/v) Sucrose 18.22 % (w/v) Sorbitol 1.5 % (w/v) Agar	in H2Obid.
dYT	1.6 % (w/v) Tryptone 1.0 % (w/v) Yeast extract 0.5 % (w/v) NaCl	in H2Obid.
YT-Agar	0.8 % (w/v) Tryptone 0.5 % (w/v) Yeast extract 0.5 % (w/v) NaCl 1.3 % (w/v) Agar	in H2Obid.
YPD	1 % (w/v) Yeast Extract 2 % (w/v) Peptone 2 % (w/v) Dextrose	in H2Obid. Addition of 100 ml of 20 % (w/v) Dextrose after autoclaving
YPD Agar	Addition of 2.0 % (w/v) Agar to YPD medium	
YPDS Agar	Addition of 1 M sorbitol to YPDA medium	
King's B	2.0 % (w/v) Peptone 0.15 % (w/v) K2HPO4 0.5 % (v/v)	in H2Obid. pH to 7.2 with HCl (If MgSO4 is added

	1M MgSO4 1.5 % (w/v) Glycero	before autoclaving, the medium becomes cloudy)
King's B Agar	Addition of 1.5 % (w/v) Agar to Kings-B medium	
Rye Sucrose Agar	Detailed recipe is given below	

Rye Sucrose agar media

Protocol adapted from lab of Prof. Laura Rose, HHU, Düsseldorf. For 2.5l media: 150g rye kernels, 50g sucrose, 37.5g agar. Rye kernels are incubated in 2.5% NaOCl for 4 minutes and washed under a sieve, until the smell of chlorite is no longer detected. The kernels are transferred to a tray and covered with a layer of VE water. The tray is covered with a plastic lid with perforations, and kept for 24 hours at RT. The germinated kernels are grinded in a blender, 25 sec at low, so not to completely crush the grains. The blended portion is incubated at 55°C for 3 hours. Mixture is transferred to a sieve and flow through is collected in a beaker; for ca. 10 min try by adding little amounts of VE water. Agar and sucrose is added and volume adjusted to 2.5l; a portion of the blended kernel is also added to the final mixture. Media is autoclaved at 120°C for 20 minutes.

4.2.2 Propagation of *A. laibachii*

Albugo laibachii is an obligate biotroph and was therefore, maintained on *A. thaliana* Col-0 accession. 3 weeks old *A. thaliana* seedlings were sprayed every two weeks with *A. laibachii* zoospore suspension (15*10^4 spores/ml concentration). For this, 10-12 infected leaves were harvested in 20 ml H2Obid (vortexed for 1 min at highest speed to release the spores) and incubated on ice for 1 h. Afterwards, the spore suspension was sieved through Miracloth (Millipore/ Merck, Darmstadt, Germany) to remove leaves and mycelia and centrifuged at 2000 x g for 10 min at 4°C. The pellet was dissolved in sterile water, ready to be sprayed. Infected plants were incubated at 4 °C and high humidity (inside a plastic bag) overnight and afterwards transferred to the growth chamber having 22°C on a short-day period (8 hr light) with (33–40%) humidity. To maintain a high humidity, plants were covered with the plastic bag for one additional day.

4.2.3 Cultivation of *E. coli*

E. coli served as a host for amplification of plasmid DNA. The cultures were grown at 37°C overnight in dYT media, with shaking at 200 rpm. For long term storage, the overnight cultures were placed in screw cap vials together with Glycerol (25% f.c) and stored at -80°C cryogenic freezer. For selection, dYT agar media were supplied with carbenicillin (100 µg/ml) or kanamycin (40 µg/ml).

4.2.4 Cultivation of *A. laibachii* associated bacteria

The bacterial strains were grown in dYT liquid media at 22°C overnight in a rotary shaker (200 rpm). For long term storage, the overnight cultures were placed in screw cap vials together with Glycerol (25% f.c) and stored at -80°C cryogenic freezer. The strains were streaked on to dYT Agar plates from the long-term storage.

4.2.5 Cultivation of *MbA* and *U. maydis*

Wild-type *MbA* (at 22°) and *U. maydis* (at 28°) strains were grown in liquid YEPS light medium overnight in a rotary shaker (200 rpm). For long term, storage, overnight grown cultures were diluted to an optical density (OD600nm) of 0.2 and grown at respective temperatures until OD600nm of 0.6-0.8 is reached. The cultures were then placed in screw cap vials together with Glycerol (25% f.c) and stored at -80°C cryogenic freezer. The strains were streaked on to Potato Dextrose Agar plates from the long-term storage. For selection of transformed strains regeneration agar (Table 3) plates were supplied with the appropriate antibiotics (Table 4.4)

Table 4. 4 Antibiotics used for *MbA* and *U. maydis* cultivation

Antibiotic	**Working concentration(µg/ml) *MbA/U. maydis***
Carboxin	8/2
Hygromycin	400/400
Nourseothricin	300/-

4.2.6 Cultivation of *Pichia pastoris:*

P. pastoris cultures were grown on a rotary shaker at 28°C and 200 rpm in liquid YPD medium. For long term, storage, overnight grown cultures were diluted to an optical density (OD600nm) of 0.2 and grown at respective temperatures until OD600nm of 0.6-0.8 is reached. The cultures

were then placed in screw cap vials together with Glycerol (25% f.c) and stored at -80°C cryogenic freezer. The strains were streaked on to YPDS Agar plates with Zeocin (25µg/ml) from the long-term storage.

4.2.7 Cultivation of *A. tumefaciens*:

A. tumefaciens cultures were grown on a rotary shaker at 28°C and 200 rpm in dYT liquid media with respective antibiotics (Table X). For long term storage, the overnight cultures were placed in screw cap vials together with Glycerol (25% f.c) and stored at -80°C cryogenic freezer. The strains were streaked on to dYT Agar plates, containing appropriate antibiotics from the long-term storage.

Table 4. 5 Antibiotics used for cultivation of *A. tumefaciens*

Antibiotic	**Working concentration(µg/ml)**
Carbenicillin (Carb)	100
Gentamycin (Gent)	50
Rifampicin (Rif)	40

4.2.8 Determination of cell density:

The cell density was determined by measuring the absorption at 600 nm (OD600) in a Genesis 10S VIS spectrophotometer (Thermo Fisher Scientific Inc., Bonn, Germany) and taking the corresponding culture medium as reference value. Cultures were diluted to absorption values below 0.8 to ensure a linear dependence of the measurements.

4.3 Microbial Strains and Oligonucleotides:

4.3.1. *Albugo laibachii*

All multipartite experiments were performed with the *A. laibachii* Isolate Nc14 which was isolated in Norwich, UK and kindly provided by the Group of E. Kemen at the University of Tübingen.

4.3.2 *Hyaloperenospora arabidopsidis*

All experimental assays were performed with *Hpa* isolate Noco2 in the laboratory of J. Parker at Max Planck Institute of Plant Breeding, Cologne.

4.3.3 *Phytophthora infestans*

P. infestans strain 88069 was kindly provided by Prof. Francine Govers, WUR, The Netherlands.

4.3.4 *Escherechia coli*

For plasmid amplification during normal cloning procedures E. coli K-12 Top10 [F– mcrA Δ(mrr-hsdRMS-mcrBC) φ80lacZΔM15 ΔlacX74 recA1 araD139 Δ(ara-leu)7697 galU galK λ– rpsL(StrR) endA1 nupG] ((Grant et al. 1990)/ Invitrogen Karlsruhe) and E. coli K-12 DH5α [F– φ80lacZΔM15 Δ(lacZYA-argF)U169 recA1 endA1 hsdR17(rK –, mK +) phoA supE44 λ– thi-1 gyrA96 relA1] ((Glover 1985)/ Gibco/BRL Eggenstein) were used.

4.3.5 *A. laibachii* associated bacteria

Bacterial strains isolated from *A. laibachii* Nc-14 were used for confrontation assays. They are listed below (Table 4.6).

Table 4. 6 *A. laibachii* associated bacteria

Collection No. AG Doehlemann	Name of bacteria
#140	*Curtobacterium flaccumfaciens pv. flaccumfaciens* LMG 3645
#143	*Curtobacterium flaccumfaciens pv. flaccumfaciens* LMG 3645
#141	*Pseudomonas brenneri* CFML 97-391
#142	*Pseudomonas veronii* CIP 104663
#137	*Microbacterium luteolum* IFO 15704
#138	*Microbacterium saperdae* IFO 15038
#139	*Microbacterium oxydans* DSM 20578

4.3.6 *MbA* and *U. maydis* strains

MbA wildtype strain (a1mfa1bW1bE1) was isolated from *A. laibachii* infected *A. thaliana* leaves. The *U. maydis* FB2 and solopathogeneic SG200 strains have been used. All plasmids generated for transformation of *MbA* and *U. maydis* are listed in chapter 4.3.9.2. A summary of all *MbA* strains used in this study are listed below:

Table 4. 7 *MbA* strains used in this study

Name	Genotype	Resistance	Reference
WT	a1mfa1 bW1bE1	-	(Agler et al., 2016)
MbA_dg2490	a1mfa1 bW1bE1 ΔMbAg2490::hph	Hygromycin	By Katharina Eitzen

Table 4. 8 *U. maydis* strains used in this study

Name	Genotype	Resistance	Reference
FB2	a2mfa2 bW2bE2	-	(Banuett und Herskowitz 1989)
SG200	*a1 :: mfa2* *bW2bE1::ble*	Ble (Phleomycin)	Bölker et al. 1995
SG200_pPit2_02727	*a1 :: mfa2* *bW2bE1* pPit2:umag_02727:Tnos:Cbx	Carboxin	This study
SG200_pActin_02727	*a1 :: mfa2* *bW2bE1* pActin:umag_02727:Tnos:Cbx	Carboxin	This study
SG200_otef2:MbAGH25	*a1 :: mfa2* *bW2bE1* pOtef:MbA_g2490:Tnos:Cbx	Carboxin	This study

4.3.7. *Pichia pastoris*

For protein expressions the *P. pastoris* strain KM71H (Invitrogen, Karlsruhe, Germany) was used, as it enables a selection of Zeocin-resistant expression vectors to generate strains with MutS phenotype. All plasmids generated for transformation of this strain are listed in chapter (4.3.9.3).

Table 4. 9 *P. pastoris* strains used in this study

Name	Genotype	Resistance	Reference
KM71H	aox1::ARG4, arg4	-	Lab of G.Doehlemann
pGAPzA-His-g2490-His	aox1::ARG4, arg4, pgap::MbA_g2490	Zeocin	By Katharina Eizen
pGAPzA-His-g2490(D124E)-His	aox1::ARG4, arg4, pgap::MbA_g2490(D124E)	Zeocin	This study
pGAPzA-His-g2490(D124A)-His	aox1::ARG4, arg4, pgap::MbA_g2490(D124A)	Zeocin	This study

4.3.8 *Agrobacterium tumefaciens*:

The strain used in this study for *A. tumefaciens*-mediated transformation of *N. benthamiana* was GV3101 (Koncz and Schell, 1986). This strain contains a chromosomal rifampicin resistance, the Ti-plasmid pMP90 with vir-genes and a gentamycin resistance as well as a Ti-helper plasmid bearing a tetracycline resistance. All strains used for expression in *N. benthamiana* are listed in Table D below

Table 4. 10 *A. tumefaciens* strains used in the study

Name	Background	Resistance
pL1M-F3-2x35S-p19- pterm	GV3101	Carb; Rif; Gent; (Tet)
pL1M-F2-2x35S-eGFP	GV3101	Carb; Rif; Gent; (Tet)
pL1_F1-p2x35s:::MbA_GH25-GFP:::35ster	GV3101	Carb; Rif; Gent; (Tet)
pL1_F1-p2x35s:::MbA_GH25(D124A)-GFP:::35ster	GV3101	Carb; Rif; Gent; (Tet)
pL1_F1-p2x35s:::MbA_GH25-c-Myc:::35ster	GV3101	Carb; Rif; Gent; (Tet)

4.3.9. Plasmids

4.3.9.1 Plasmids for transformation in *U. maydis*

#2165_potef_g2490_cbx

The plasmid was used to generate *U. maydis* strains expressing the *MbA*_GH25 protein. The plasmid carries a Cbx resistance cassette, enabling integration into the *U. maydis* ip locus via homologous recombination. MbA_g2490 gene is under control of the o2tef promoter (Po2tef) and is terminated by the *Agrobacterium tumefaciens* nos terminator (Tnos). Selection of this plasmid in *E. coli* was based on Ampicillin resistance.

#2451_pActin_umag_02727_cbx

The plasmid was used to generate *U. maydis* strains overexpressing UMAG_02727 protein under the control of *U. maydis* actin-promoter (obtained from Regine Kahmann, MPI Marburg, 2019) and terminated by Tnos. Plasmid carries Cbx resistance cassette and selection in *E.coli* was based on Ampicillin resistance.

#2860_ppit2_umag_02727_cbx

The plasmid was used to generate *U. maydis* strains overexpressing UMAG_02727 protein under the control of *U. maydis* pit2-promoter (Doehlemann et al., 2011) and terminated by Tnos. Plasmid carries Cbx resistance cassette and selection in *E. coli* was based on Ampicillin resistance.

4.3.9.2 Plasmids for the expression of recombinant proteins in *P. pastoris*

pGAPZα (Thermo Fisher Scientific Inc., Bonn, Germany)

This plasmid was used to constitutively express recombinant proteins under control of the GAP promoter. It carries the S. cerevisiae α-factor secretion signal, which is fused N-terminally to the recombinant protein, to secrete the protein into the supernatant. Recombinant proteins are C-terminally fused to a Myc epitope and a Polyhistidine-Tag, which can be visualized by western blot. Selection of this plasmid is based on the selectable marker Zeocin™.

pGAPZα-His-MbA_g2490(D124E)-Myc-His

Plasmid constructed by Katharina Eitzen was subjected to site directed mutagenesis where Aspartate at position 124 was changed to Glutamate in *MbA*_g2490 gene (without secretion signal) in the pGAPZα vector.

Another mutated version of *MbA*_g2490 (D124A) was constructed in the same vector.

The plasmids were used to express mutant version of *MbA*_GH25 protein in *P. pastoris*.

4.3.10 Oligonucleotides

All oligonucleotides used in this study were purchased from Sigma-Aldrich (Deisenhofen, Germany). A list of the oligonucleotides can be found in Table 4.11

Table 4. 11 Oligonucleotides used in this study

Name	Sequence	Use
g2490_fw_NcoI	GCTACCATGGCACATCTGCCCATCCTCATC	Amplification of *MbA*_gh25 gene for cloning into vector with otef promoter
g2490_rv_NotI	AATTGCGGCCGCTAGGAGGGCGCACTGTTTTG	Amplification of *MbA*_gh25 gene for cloning into vector with otef promoter
g2490_mut_fw	CTCCCAGGAATGATCGAACTCGAAAGCGTTAGTGG	Site directed mutagenesis of *MbA*_GH25(D124E)
g2490_mut_rv	CCACTAACGCTTTCGAGTTCGATCATTCCTGGGAG	Site directed mutagenesis of *MbA*_GH25(D124E)
umag_02727_ovrexp_fw	GTAGACCATGGCGCTCTCCACAAGTCACATC	Amplification of *U. maydis* GH25 gene (with introns)

umag_02727_ovrexp_rv	ATAAGGCGCGCCGTGCCCGTAAACTGGATAGG	Amplification of *U. maydis* GH25 gene (with introns)
EFIa_fw	AAGGAGGCTGCTGAGATGAA	qPCR amplification of house-keeping gene of *A. thaliana*
EFIa_rv	TGGTGGTCTCGAACTTCCAG	qPCR amplification of house-keeping gene of *A. thaliana*
ITS_oomycete_fw	ACTTTCAGCAGTGGATGTCTA	qPCR amplification of *Albugo laibachii* ITS sequence
ITS_oomycete_rv	ACTTTCAGCAGTGGATGTCTA	qPCR amplification of *Albugo laibachii* ITS sequence
Mut_g2490_asp_ala_fw	ACTAACGCTTTCGAGGGCGATCATTCCTGGGAG	Site directed mutagenesis of *MbA*_GH25(D124A)
Mut_g2490_asp_ala_fw	CTCCCAGGAATGATCGCCCTCGAAAGCGTTAGT	Site directed mutagenesis of *MbA*_GH25(D124A)

WRKY33_fw	GGTCACAACAATCCGGAAGA	qPCR analysis of *A. thaliana* wrky33 gene relative expression
WRKY33_rv	GGAGAGACAAGAGAAGGAGAGA	qPCR analysis of *A. thaliana* wrky33 gene relative expression
WRKY53_fw	TCACCGAGCGTACAACTTATTCC	qPCR analysis of *A. thaliana* wrky53 gene relative expression
WRKY53_rv	CGTTTATCGATGCCGGAGATT	qPCR analysis of *A. thaliana* wrky33 gene relative expression
WRKY30_fw	CGGAGCCAAATTTCCAAGAGG	qPCR analysis of *A. thaliana* wrky30 gene relative expression
WRKY30_rv	GACGGAGAGTTTGATGCTGAG	qPCR analysis of *A. thaliana* wrky30 gene relative expression

frk1_at_fw	GCCAACGGAGACATTAGAG	qPCR analysis of *A. thaliana* frk1 gene relative expression
frk1_at_rv	CCATAACGACCTGACTCATC	qPCR analysis of *A. thaliana* frk1 gene relative expression
Ics1_at_fw	CTTTTCAGTCCCTCAGGTTG	qPCR analysis of *A. thaliana* Ics1 gene relative expression
Ics1_at_rv	AGTTCATCATCCCAAGCAAT	qPCR analysis of *A. thaliana* Ics1 gene relative expression
SDM_umag_02727_fw	CGATGACTCGAGGGCAAGCGCACCAGG	Site directed mutagenesis of *U. maydis* GH25(D124A)
SDM_umag_02727_rv	CCTGGTGCGCTTGCCCTCGAGTCATCG	Site directed mutagenesis of *U. maydis* GH25(D124A)
pL0_TK61_g2490_fw	TTGAAGACAAAGGTTGCTCCCTTGGAGAAGCGCG	Level-0 cloning of *MbA*_gh25 gene for expression in *Agrobacterium* vector

pL0_TK61_g2490_rv	GAAGACAACGAAGGGCCGGTGGCGAACTTCTTGA	Level-0 cloning of *MbA*_gh25 gene for expression in *Agrobacterium* vector
L0_BsaI_dom_new_fw	CGCCCACCTGCTATGGTCTTAGCCAGAGCG	Domestication of BsaI site in MbA_gh25 gene for expression in *Agrobacterium* vector
L0_BsaI_dom_new_rv	GCACCTACCCCGGCGACCAGGACACTT	Domestication of BsaI site in MbA_gh25 gene for expression in *Agrobacterium* vector
umag02727_OE_ppit2_fw	CGCCCACCTGCTATGGTCTTAGCCAGAGCG	Amplification of *U. maydis* GH25 gene for cloning in vector with pit2 promoter
umag02727_OE_ppit2_rv	GCACCTACCCCGGCGACCAGGACACTT	Amplification of *U. maydis* GH25 gene for cloning in vector with pit2 promoter

*Curtobacterium*_fw	CAACAAGCTGATAGGCCGCG	qPCR analysis of *Curtobacterium* sp. biomass
*Curtobacterium*_rv	TCGAACGATGATGCCCAGCT	qPCR analysis of *Curtobacterium* sp. biomass

4.4 Microbiological methods

4.4.1 Transformation of *E. coli*

- **Production of competent cells:**

  100 ml dYT medium supplemented with 10 mM MgCl2 and 10 mM MgSO4 was inoculated with 1 ml of a freshly grown overnight culture and incubated at 37 °C at 200 rpm until OD600 reached 0.5. Cells were then cooled on ice for 30 min and centrifuged for 8 min at 4°C and 1250 ×g. The supernatant was discarded, and the cells were resuspended in 1/3 of the initial culture volume of RF1-solution, followed by incubation at 4 °C for 30 min. The cells were then centrifuged for 8 min at 4 °C and 1250 ×g. The supernatant was again discarded, and the cells were resuspended in 1/20 of the initial culture volume of RF2- solution and incubated at 4 °C for at least 30 min. The cells were finally aliquoted to 50 µl in pre-chilled reaction tubes, shock-frozen with liquid N2 and stored at-80 °C until further use.

RF1 solution	100 mM RbCl
	50 mM MnCl2 x 4 H2O
	30 mM potassium acetate
	10 mM CaCl2 x 2 H2O
	15% (w/v) Glycerol
	pH 5.8
RF2 solution	10 mM MOPS
	10 mM RbCl
	75 mM CaCl2 x 2 H2O
	15% (w/v) Glycerol
	pH 5.8

- **Heat-shock transformation of *E. coli***

  50 µl of competent cells of E. coli K-12 Top10/DH10β or E. coli K-12 DH5α were used for transformation with 1.5 ng of plasmid DNA. The mixture was incubated in ice for 15-30 minutes, then the cells were subjected to heat shock at 42°C for 45 sec, and immediately transferred to ice for 2 minutes. Afterwards, 500µl of dYT media was added to the cells for regeneration and incubated at 37°C for 30 minutes with shaking at 200 rpm. The cells were plated on YT solid plates containing the appropriate antibiotic for selection and incubated at 37 °C overnight.

4.4.2 Transformation of *U. maydis*

- **Preparation of protoplast**

  U. maydis strains were grown in YEPSL at 22°C in a rotary shaker at 200 rpm until an O.D. of 0.6 is reached and centrifuged for 15 mins at 2000 x g. The cells are washed in in 20 ml of SCS, and further centrifuged for 10 minutes at 2000 x g, before being treated with 3ml SCS solution with 20mg/ml of Glucanex (Lysing Enzyme from *Trichoderma harzianum*, # L1412, Sigma). After 20 minutes of incubation at room temperature, protoplasts start to come out from the cells. Cold SCS is added to the mix, and spun down for 10 minutes at 1300 x g. The cells are washed twice with SCS and then resuspended with 10 ml STC to be centrifuged at 1300 x g for 10 minutes. Finally, the pellet is dissolved in 500 ul STC, and stored in aliquots of 50 ul at -80°C.

- **Transformation of protoplast**

  5ug of plasmid DNA along with 15 µg Heparin was added to 50 ul protoplasts. After incubation on ice for 10 minutes, STC/40%PEG (500 ul) was added to it and mixed gently by pipetting up and down; this step was followed by another 15 minutes on ice. The transformation mix was added to 10 ml of molten regeneration (reg) agar and poured over a layer of already solidified reg agar containing appropriate antibiotic solution. For 10 ml of Agar, 400 µg/ml Hygromycin/ 8 µg/ml Carboxin/ 300 µg/ml nourseothricin (NAT) were used for selection of transformed colonies.

SCS solution	20 mM Na-Citrate, pH 5.8
	1 M Sorbitol in H2Obid., sterile filtered
STC solution	10 mM Tris-HCl, pH 7.5
	100 mM CaCl2

	1 M Sorbitol in H2Obid., sterile filtered
STC/PEG solution	15 mL STC
	10 g PEG4000

4.4.3 Transformation von *P. pastoris*

- **Production of competent cells:** Competent cells were produced following the protocol by Invitrogen Corporation (Catalog nos. V200–20 and V205–20). *P. pastoris* strain grown overnight, diluted to 0.2 OD600 in the morning, and incubated with shaking at 200rpm till and OD600 of 0.8-1 is reached. *P. pastoris* cells were centrifuged at 1500 × g for 5 minutes at 4°C. Next, the pellet was resuspended in sterile water and centrifuged at 1500 × g for 5 minutes at 4°C, twice. Finally, the cells were dissovled in 1ml (1/5 volume of overnight culture) of ice-cold 1M Sorbitol and aliquoted to 50µl in pre-chilled tubes, and stored at -80°C.
- **Transformation of *P. pastoris* by electroporation:** 1-5µg of linearized plasmid DNA was added to 50µl of competent cells and incubated in a pre-chilled cuvette for 5 min at 4°C. The cells were pulsed at 1500V for 5ms, followed by an addition of 1ml of 1M ice-cold Sorbitol. Cuvette contents were transferred to an 15ml falcon tube and incubated at 30°C for 1-2 h. Next, 1ml of liquid YPD media was added to the tube and incubated at 30°C for 1 h on a rotary shaker (200 rpm). Cells were plated on a YPDS media containing 100µg/ml of Zeocin^{TM} and incubated for 2-3 days at 30°C.

4.4.4 Stress assay of *MbA*/*U. maydis* strains

Transgenic *MbA* and *U. maydis* strains were tested for their fitness and axenic survivability. Strains grown to an optical density (600 nm) of 0.6-0.8 were centrifuged at 2000 x g for 10 minutes and suspended in sterile water to reach an OD of 1.0. Next, a dilution series from 10^0 to 10-4 was prepared in sterile H2O. In the end, 5 µl of each dilution are spotted on CM plates having components of different stress conditions. The plates are incubated for 2 days at 22°C.

CM media	2 g (0.25 %) (w/v) Casaminoacids (Difco)
	0.8 g (0.1 %) (w/v) Yeast extract
	8 ml (1 %) (v/v) Vitamine solution (Holliday ’74)
	50 ml (6.25 %) (v/v) Salt solution (Holliday ’74)
	0.4 g (0.05 %) (w/v) DNA degradation free (Sigma)

1.2 g (0.15 %) (w/v) NH4NO3
10 ml (1 %) (v/v) 1 M Tris-HCl pH 8.0
16 g (2 %) (w/v) Agar

The components are mixed in 784 ml ddH2O, and autoclaved. After autoclaving, 16 ml 50 % Glucose (sterile filtrated) is added to get a final concentration of 2% glucose.

CM-Supplements:

CM + 2 % Glucose (Control)

CM + 2 % Glucose + 100 µg/ml Calcofluor (cell wall stress)

CM + 2 % Glucose + 150 µg/ml Calcoflour (cell wall stress)

CM + 2 % Glucose + 1 mM H2O2 (oxidative stress)

CM + 2 % Glucose + 1.5 mM H2O2 (oxidative stress)

CM + 2 % Glucose + 45 µg/ml Congored (cell wall stress)

CM + 2 % Glucose + 1 M NaCl (osmotic stress)

CM + 2 % Glucose + 1 M Sorbitol (osmotic stress)

4.4.5 Microbial confrontation assays

At first, *MbA/ U. maydis* and bacterial strains are grown to an O.D of 0.6. *MbA*/ *U. maydis* (10ul) were dropped in four quadrants of a PD Agar plate, spread previously with 100µl of bacterial culture. Plates were incubated for 2-4 days at 22°C.

For *P. infestans* confrontation assay, RSA plates supplemented with 100µg/ml Ampicillin were used. A mycelial plug of *P. infestans* was placed in the centre of the plate and growing culture of *MbA* (10µl) was placed as droplets on two corners of the plate.

4.5 Molecular biological methods

4.5.1 Isolation of nucleic acids

4.5.1.1 Plasmid DNA isolation from *E. coli*

NucleoSpin® Plasmid Kit (Macherey-Nagel, Düren, Germany) was used for isolation of plasmid DNA by alkaline lysis according to the manufacturer's instructions.

4.5.1.2 Genomic DNA extraction of *MbA*/*U. maydis*

Genomic DNA was isolated using phenol-chloroform extraction protocol (Kämper et al., 2006). 2ml of overnight grown *MbA*/*U. maydis* culture was centrifuged at 12000*g for 2 min in a 2 ml microcentrifuge tube. About 0.3g of (0.4-0.6mm) glassbeads was added to the pellet, followed by 500µl of Phenol-Chloroform-Isoamyl alcohol (25:24:1; Roth, Karlsruhe, Germany) and 400µl of Usti-lysis buffer. The microcentrifuge tube was placed in Vibrax- VXR shaker (IKA, Staufen, Germany) at 2500 rpm for 15 min. For phase separation, the tube was spun down at 12000*g for 15 min. The upper aqueous phase containing the extracted genomic DNA was placed in a fresh 1.5ml microcentrifuge tube and precipitated with 400µl of Isopropanol and centrifuged at 12000*g for 10 min. The supernatant was discarded, and 1ml of 75% EtOH was added to the tube followed by another centrifugation step. The pellet was left to air dry for 5 min, and eventually dissolved in 50µl of TE-buffer containing 20 µg/ml RNaseA by incubation in a Thermomixer (Eppendorf, Hamburg, Germany) at 55 °C, 1200 rpm, 30 min. The extracted DNA was stored at -20 °C.

***Ustilago* lysis buffer**	50 mM Tris-HCl, pH 7.5
	50 mM Na2-EDTA
	1 % (w/v) SDS
	in H2Obid.

Genomic DNA extraction from *A. thaliana*/*Z. mays*:

Leaf tissue was frozen in liquid N2 and homogenized using a mortar and pestle under constant liquid N2 cooling. Extraction buffer was added to the ground tissue and incubated at 37°C for 30 minutes (Ruhe et al., 2016) for *A. thaliana* and at 65°C for 10 min for *Z. mays*. Genomic DNA extraction was then carried out following the Phenol-Chloroform method.

Extraction buffer	0.5M EDTA 100 ml
	1M Tris∗Cl 100 ml
	NaCl 29.2 g
	SDS 15 g
	ddH20 added to 1L
	Autoclaved and 3ml of ß-mercaptoethnol added before use

4.5.1.3 Total RNA extraction from leaf tissue

Leaf tissue was frozen in liquid N2 and homogenized using a mortar and pestle under constant liquid N2 cooling. RNA was isolated by using TRIzol® reagent (Invitrogen, Darmstadt, Germany) following the recommended instructions. The ground leaf material was filled into a 2 ml reaction tube and 1 ml TRIzol® reagent was immediately added and sample vortexed for 5 min. Then, 200µl of chloroform was added to it, and vortexed for 2 min. The tube was centrifuged at 12000 x g for 15 min at 4 °C, and the upper aqueous phase was transferred to a fresh tube and mixed with 400µl of Isopropanol. After incubation at 4°C for 10 min, and centrifugation at 12000*g for 10 min at 4°C, the supernatant was discarded. Pellet was washed with 1 ml 75% EtOH at 7500 x g for 5 min and then dried for 5 min at room temperature. The pellet was finally dissolved in 50 µl RNase-free H2O at 55 °C for 10 min. Extracted RNA was immediately processed for DNase digest or stored at -80°C.

4.5.1.4 DNase-digest after RNA extraction

Turbo DNA-Free™ Kit (Thermo Fisher Scientific Inc., Bonn, Germany) was to remove any DNA contamination in the extracted RNA. 5 µl 10x DNase buffer and 1 µl DNase were added to the extracted RNA and the mixture was incubated at 37 °C for 30 min. Afterwards, 5µl of DNase inactivation enzyme was added to the mixture and incubated at room temperature for 5 min. Finally, sample was centrifuged at 7500 x g for 2 min and supernatant was transferred to a fresh 1.5 ml reaction tube. The amount of RNA was assessed by photometric measurement on a NanoDrop 2000c spectrophotometer (Thermo Fisher Scientific Inc., Bonn, Germany) and quality was afterwards assessed by loading 1 µg of RNA on a 1 % Agarose gel.

4.5.1.5 Synthesis of cDNA

Synthesis of cDNA was performed using First Strand cDNA Synthesis Kit (Thermo Scientific, Bonn, Germany) according to recommended instruction. 10µg RNA was transcribed into cDNA in a total volume of 12µl, where initially, 0.5 µl oligo(dT)18 primer was added and incubated at 65 °C for 5 min. Then the reaction tube was placed on ice for 2 min, after which 4 µl 5x Reaction buffer, 1 µl RiboLock RNase Inhibitor (20 U/µl), 2µl 10 mM dNTP Mix and 1 µl RevertAid H Minus M-MulV Reverse Transcriptase (200 U/µl) was added to the sample. Reaction was incubated at 42 °C for 60 min and terminated by heating at 70 °C for 5 min. The cDNA was stored at -20 °C until further use.

4.5.2 Purification of nucleic acid

NucleoSpin gel and PCR Clean-up kit (Machery-Nagel, Düren, Germany) were used for purification of plasmid DNA and restriction enzyme digested PCR fragments respectively. The purification was done according to the manufacturer's instructions.

4.5.3 In vitro modification of nucleic acids

4.5.3.1 Restriction enzyme digestion of DNA

Enzymatic digestion of DNA was carried out using type II restriction endonucleases (NEB, Frankfurt/Main, Germany) with DNA concentration ranging from 1-5µg. The reaction was set up according to manufacturer's instruction.

4.5.3.2 Ligation of DNA fragments

Gene of interest was ligated into a vector backbone using T4 DNA (Thermo scientific, Bonn, Germany) ligase in molar ratio of 3:1. Reaction performed using manufacturer's instruction.

4.5.3.3 Gibson Assembly cloning

Gibson Assembly cloning is an exonuclease-based method to assemble DNA. DNA fragments were designed to have 20 nt overlap to assemble them via homologous recombination. NEBuilder® HiFi DNA Assembly Master Mix (NEB, Frankfurt/Main, Germany) was used to perform Gibson assembly reaction following manufacturer's instuction.

4.5.3.4 Polymerase Chain reaction (PCR)

Amplification of DNA was performed using various polymerases. For ampliying gene from all organisms used in this study the Phusion® Hot Start High Fidelity DNA-Polymerase (Finnzymes/Thermo Scientific, Bonn, Germany) and Q5 Polymerase (NEB, Frankfurt/Main, Germany) were used owing to their proof-reading ability. For the cloning long DNA-fragments (>5kb) or amplying products from cDNA, KOD Xtreme™ Hot Start DNA Polymerase (Merck Millipore, Darmstadt, Germany) was used. For Colony PCR, GoTaq® Green Master Mix (Promega, Walldorf, Germany) was used. PCR reactions were set up according to manufacturer's instruction.

4.5.3.5 Sequencing of DNA

Sequencing reactions were performed by Eurofins (formerly GATC, Cologne, Germany) and analyzed using Clone Manager 9 software (SciEd, Denver, US).

4.5.4 Agarose gel electrophoresis for nucleic acid separation and detection

Separation of DNA fragments by size was done by agarose gel electrophoresis. Depending on the size of the DNA fragment of interest, the agarose concentration of the gel was 0.8-2% (w/v) with 0.25 µg/ml ethidium bromide in 1x TAE buffer. Samples were mixed with 6X loading dye in ratio of 5:1 and together with a DNA ladder of defined size, loaded into the wells of Agarose gel and were run in a chamber containing 1x TAE buffer. Separation of DNA was done at constant voltage of 80-120 V depending on the size and percentage of the gel. DNA bands were visualized by UV radiation at 365 nm using a gel documentation unit (Peqlab/VWR, Langenfeld, Germany).

50x TAE-buffer	2 M Tris-Base
	2 M Acetic acid
	50 mM EDTA pH 8.0
6x DNA loading dye	50 % (w/v) Sucrose
	0.13 % (w/v) Bromophenol blue

4.6 Biochemical methods

4.6.1 Separation of proteins via SDS-PAGE

Sodium dodecyl sulfate polyacrylamide gel electrophoresis (SDS-PAGE) was used for separation of denatured and negatively charged proteins based on their molecular weight. To denature the proteins, samples were boiled for 5 min at 99 °C in 1x SDS gel loading buffer containing 100 mM DTT. The gels for SDS-PAGE composed of an upper stacking and a lower separating gel and were casted using the Mini Protean System (BioRad, Munich, Germany). The gel was placed in the chamber (Invitrogen, Carlsbad, California, USA), which was then filled with SDS running buffer (4.34). The protein samples as well as 4 µl of protein ladder (Thermo Fischer scientific,Bonn, Germany) were loaded into the wells of SDS gel and were run in 1x SDS running buffer in a gel chamber at a constant voltage of 120-160V for 1 h. The SDS gel was further used for protein staining or Immunoblot.

6x SDS loading buffer	4M Tris-HCl, pH 6.8
	6 % (w /v) SDS
	0.15 % (w /v) Bromophenol blue
	60 % (v /v) Glycerol
SDS running buffer	25 mM Tris-HCl, pH 8.3
	192 mM Glycine
	4 mM SDS
Stacking gel	5 % (v/v) Acrylamide
	0.1 % (w/v) SDS
	in 125 mM Tris-HCl, pH 6.8
	0.1 % (w/v) Ammonium persulfate
	0.1 % (v/v) Tetramethylethylenediamine (TEMED)
Separating gel	12 % (v/v) Acrylamide
	0.1 % (w/v) SDS
	in 375 mM Tris-HCl, pH 8.8
	0.1 % (w/v) Ammonium persulphate
	0.04 % (v/v) TEMED

Staining of SDS gel: Instant blue reagent™ (Expedeon, San Diego, California, USA) was added to the SDS gel for staining; protein bands can be visualized after 15 min. Samples can be destained with H2Obid. to remove background signals until desired stain is reached.

4.6.2 Immunological detection of proteins via chemiluminescence (Western blot)

After separation by SDS-PAGE, the proteins were blotted to a Polyvinylidene fluoride (PVDF; Amersham Hybond P 0.45 PVDF blotting membrane, GE Healthcare, Munich, Germany) membrane and desired tagged proteins were detected using specific antibodies. Prior to blotting, the PVDF membrane was activated by adding pure MeOH and Whatman paper were soaked in transfer buffer. SDS gel was washed in transfer buffer. The blot was assembled from bottom to top as follows: Whatman paper, activated PVDF-membrane, SDS-gel, Whatman paper. The blot was transferred to a Trans-Blot Turbo Transfer system (BioRad, Munich, Germany) and proteins were transferred by adding a constant voltage of 25 V and 1 Ampere (A) for 25 - 30 min, depending on the size of the desired protein. Afterwards, the membrane was incubated with blocking solution (4% Bovine serum albumin in 4.41) for 1 h at RT or O/N at 4°C. Antibodies were diluted in blocking solution according to manufacturer instructions. After

blocking, the membrane was incubated with the primary antibody, specific to the tag of the desired protein, for 1 h at RT or at 4 °C overnight. The membrane was washed three times with TBST to get rid off excess and unbound antibodies. Next, the secondary antibody, specific to primary antibody was added to the membrane, and incubated at RT for 1 h. After, another 3x washing with TBST, the tagged proteins were visualized by enhanced chemiluminescence reagent SuperSignal™ West Pico (Thermo Fisher Scientific Inc., Bonn, Germany). The enhanced chemiluminescence reagent is processed by the Horseradish peroxidase, which is bound to the secondary antibody and releases a chemiluminescent signal (475 nm) which is documented using a ChemiDoc™ MP system (BioRad, Munich, Germany).

Transfer Buffer	39 mM glycine
	48 mM Tris-base
	0.0375 % SDS
	20 % Methanol
TBST	50 mM Tris-HCl, pH 7.5
	150 mM NaCl
	0.1 % (v/v) Tween-20

Table 4. 12 Antibodies used in this study

Antibody	Organism	Working dilution	Supplier
His	Mouse	1/10000	Sigma-Aldrich (Deisenhofen, Germany)
Mouse IgG	Goat	1/3000	Thermo Fisher Scientific Inc., (Bonn, Germany)
GFP	Mouse	1/1000	Roche Diagnostics (Mannheim, Germany)
c-Myc	Mouse	1/5000	Sigma-Aldrich (Deisenhofen, Germany)

4.6.3 Expression of heterologous proteins in *P. pastoris*

The *Pichia pastoris* KM71H-OCH gene expression system was used to produce *MbA*_GH25 domain tagged with an N-terminal Polyhistidine tag (6xHis) and a C-terminal peptide containing the c-myc epitope and a 6xHis tag. The His-MbA_GH25 cloned into pGAPZαA vector (Invitrogen, Carlsbad, CA, USA) under the control of a constitutive promotor with an α-

factor signal peptide for secretion. Expression and purification of recombinant proteins were performed according to manufacturer's instructions (Invitrogen Corporation, Catalog no. K1710-01): YPD medium supplemented with 100 µg ml−1 zeocin was used for initial growth of P. pastoris strains at 28°C and 200 rpm (for liquid cultures). Production of the recombinant protein was performed in 1 L buffered (100 mM potassium phosphate buffer, pH 6.0) YPD medium with 2% sucrose at 28°C for 24 hr with 200 rpm shaking. Next the protein was subjected to affinity purification with a Ni-NTA-matrix according to manufacturer's instructions (Ni-Sepharose 6 Fast-Flow, GE-Healthcare; Freiburg, Germany). After purification, the His-*MbA*_GH25 protein was dialyzed in an exchange buffer (0.1 M NaPi, 0.1 M Nacl, pH = 7.5). The purified protein was kept in 100 µl aliquots at 4°C.

4.6.4 Biochemical activity assay of *MbA*_GH25 protein

Purified glycoside hydrolase of *MbA* from *P. pastoris* was quantified according to a sensitive fluorescence-based method using Molecular Probes EnzChek Lysozym-Assay-Kit (ThermoFisher Scientific, Katalognummer: E22013). DQ lysozyme substrate (Micrococcus lysodeikticus) stock suspension (1.0 mg/ml) and 1000 units/ml HEWL stock solution were prepared according to the manufacturer's instruction. Molar concentration of the HEWL stock solution was calculated using the following website (https://www.bioline.com/media/calculator/01_04.html) and was found to be 11 µM. Protein concentration of *MbA*_GH25 and *MbA*_GH25(D124E) was measured in the Nanodrop 2000c spectrophotometer (Thermo Fischer scientific, Bonn, Germany) according to the manufacturer's instructions using 100 µl of sample after using 100 µl of the appropriate buffer as a blank control in glass cuvette. The molar concentrations of recombinant proteins were also calculated as above.

At the start of the reaction 50 µl of the DQ lysozyme substrate working suspension was added to each microplate well containing reaction buffer with either HEWL (in molar concentrations ranging from 0.1 to 5.5 µM) or *MbA*_GH25 (in molar concentration from 0.5 to 17.5 µM). Fluorescence intensity of each reaction was measured every 5 min to follow the kinetic of the reaction at 37°C for 60 min, using fluorescence microplate reader with fluorescein filter Tecan Infinite 200 Pro plate reader (Tecan Group Ltd., Männendorf, Switzerland). Digestion products from the DQ lysozyme substrate have an absorption maximum at ~494 nm and a fluorescence emission maximum at ~518 nm.

4.7 Plant methods

4.7.1 Plant material and growth conditions

A. thaliana plants were grown in Phyto-chambers having 22°C on a short-day (8 h light) and long dark (18°C) period with 40% humidity. For gnotobiotic plate preparation, A. thaliana seedlings were grown in 12-well plates on ½ MS agar.

Zea mays was grown at 28 °C on a long day period (16 h light) with 80% humidity and a 8 h night period at 22 °C in greenhouse.

Nicotiana benthamiana was grown at 23°C on a long day period (16 h light) and at 20°C for 8 h dark period with 30 – 40% humidity in greenhouse.

4.7.2 Seed sterilization

A. thaliana seeds (ecotype Col-0) were sterilized, by addition of 600µl of 1.5% NaClO/0.02% Triton in a 1.5 ml EP tube containing the seeds. The tube is shaken vigorously at room temperature for 4-5 minutes, and then the seeds are washed 5 times with ddH2O. Seeds were stored in 500 µl 0.1 % agar in dark at 4 °C for 1 week for stratification.

Maize seeds (Golden Bantam) were sterilized by incubation in 2% Chloramine T for 15 mins. Afterwards, the seeds were washed 3-4 times with ddH2O. The sterilized seeds were immediately sown in soil.

4.7.3 Infection of *A. thaliana* with *A. laibachii*

Sterilized and stratified *Arabidopsis thaliana* seeds (3-4) were sown on ½ MS agar prepared on 12 well plates. The plates were placed in the Phyto-chamber having 22°C on a short-day (8 h light) and long dark (18°C) period with 40% humidity. After 2 weeks, additional seedlings were removed under sterile conditions, so that only 1 seedling remained per well. After another week, the seedlings were sprayed with yeast and fungal strains. Overnight grown liquid cultures of *MbA* and *U. maydis* were diluted and grown to an OD600 = 0.6. Cultures were centrifuged at 2000x g for 10 min and pellet dissolved in 10mM MgCl2. 500 ul of each culture is eventually sprayed on three-week old *A. thaliana* seedlings using airbrush guns (Conrad Electronics GmbH, Hirschau, Germany). Two days later, a spore solution of *A. laibachii* was prepared as described in Propagation of *A. laibachii* and the zoospores were pelleted at 2000 x g for 10 min. The supernatant was removed, and the spores were treated with 2 ml of an antibiotic mix (Kanamycin 500 µg/ml, Rifampicin 500 µg/ml, Streptomycin 625 µg/ml and Gentamycin 250

µg/ml) for 25 min at room temperature in darkness. Afterwards, spores were washed 3x with sterile ddH2O and dissolved in 10mM MgCl2 with a spore concentration of 15 x 104 spores/ ml. 500 µl of *A. laibachii* spore solution was sprayed on each *A. thaliana* seedling. 10 days later A. laibachii relative biomass was calculated with respect to the treatments.

Quantification of *A. laibachii* biomass:

After 10 dpi, the seedlings were harvested, frozen in liquid nitrogen, and kept at −80°C. For DNA extraction, the frozen plant material was ground into a fine powder with mortar and pestle and treated with extraction buffer (50 mM Tris pH 8.0, 200 mM NaCl, 0.2 mM ethylenediaminetetraacetic acid [EDTA], 0.5% SDS, 0.1 mg/ml proteinase K [Sigma–Aldrich]). This was followed by centrifugation after the addition of one volume phenol/chloroform/isoamylalkohol, 25:24:1 (Roth). The top aqueous layer was removed and added to one volume of isopropanol to precipitate the nucleic acids. DNA pellet obtained after centrifugation was washed with 70% EtOH and finally dissolved in 50 µl nuclease-free water. For qPCR measurements, 10 µl of GoTaq qPCR 2× Master Mix (Promega, Waltham, Madison, USA), 5 µl of DNA (~50 ng), and 1 µl of forward and reverse primer (10 µM) up to a total volume 20 µl were used. Samples were measured in triplicates in a CFX Connect real-time PCR detection system (Bio-Rad) following the protocol of Ruhe et al., 2016. Amount of *A. laibachii* DNA was quantified using the following oligonucleotide sequences: *A. thaliana* EF1-α: 5′-AAGGAGGCTGCTGAGATGAA-3′, 5′-TGGTGGTCTCGAACTTCCAG-3′; Oomycete internal transcribed spacer (ITS) 5.8 s: 5′-ACTTTCAGCAGTGGATGTCTA-3′, 5′-GATGACTCACTGAATTCTGCA-3′. Cq values obtained in case of the oomycete DNA amplification was normalized to *A. thaliana* DNA amplicon and then the difference between control (only *Albugo*) and treatment (*Albugo*+ GH25/Mut_GH25) was calculated by ddCq. The relative biomass of *Albugo* was analyzed by the formula (2^{-ddCq}).

4.7.4 Infection of *A. thaliana* with *Hpa*

A. thaliana (ecotype Col-0) and *A. thaliana* eds1-12 mutant (in Col-0 background) were used in this study performed at MPIPZ, Köln at Laboratory of Prof. Jane Parker. Plants were grown on soil in a controlled environment under 10-h light/14-h dark regime at 22°C and 60% relative humidity. The *Hpa* isolate Noco2 (4 x 10^4 spores/ml ddH2O) was sprayed onto 3 weeks old *A. thaliana* seedlings, two days after spraying with *MbA* strains. After 5 days poat Hpa infection, the seedlings were harvested in a falcon tube, their fresh weight measured followed by addition of 5 ml of ddH2O. The samples were vortexed for 10 sec to release the conidiospore. To

determine the *Hpa* sporulation in planta, the conidiospores released from each treatment was calculated in a Neubar chamber under light microscope.

4.7.5 Infection of *Z. mays* with *U. maydis*

6 days old maize seedlings were used for infection assay with *U. maydis*. Overnight grown *U. maydis* strains were diluted and grown to an OD600 = 0.8.-1. Next, the fungal cells were centrifuged at 2400xg for 10 min and the pellet dissolved in ddH2O to an OD600=1. 300–500 µl of the *U. maydis* cell suspension were injected into 6-day old seedlings at the stem region (approx. 1 cm from the soil). Disease symptoms on maize seedlings were scored after 6 dpi and 12 dpi, based on the scoring system below (Table 4.13).

Table 4. 13 *U. maydis* disease scoring in *Z. mays*

Disease symptom	Description
No symptom	No disease symptoms or sign of infection in the plant
Chlorosis	Chlorotic areas around the infection site on the infected leaf and younger leaves
Small tumor	Tumors around the infection area are ≤ 1 mm on the infected leaf and younger leaves
Heavy tumor	Tumors around the infection area are ≥ 1 mm on the infected leaf and younger leaves
Dead	Death of plant due to *U. maydis* infection.

4.7.6 Infection of *N. benthamiana* with *P. infestans*

N. benthamiana seedlings were grown under green house conditions for 4-5 weeks. Subsequently, the 3rd or 4th leaf was detached and placed on moist tissue paper. *P. infestans* spores were harvested by addition of ddH2O to mycelium growing on plate. After 3-4 h incubation at 4°C, the zoospores were released by scratching the mycelium with a sterile tip. The zoospore concentration was adjusted to 10^5 spores/ml of water.10µl of *P. infestans* spore suspension was dropped on detached leaves. After 6 days, the necrotic lesions were evaluated using ImageJ.

4.8 Microscopy

4.8.1 Trypan blue staining to visualize *A. laibachii in planta*

Leaves of *A. thaliana* treated with *A. laibachii* were harvested and placed in a 15 ml falcon tube. To the tube, working solution of Trypan blue stain was added to cover all the leaf material. The samples were boiled in a water bath for 1-2 minutes, and removed from heat as soon as the liquid inside the tube started to boil. The staining solution is left overnight and then discarded, followed by the addition of Chloral hydrate solution, which can be changed several times, until the sample solution turns transparent. The leaf material can be stored in Chloral hydrate for several months.

Trypan blue stock solution	10 ml phenol, 10 ml glycerol, 10 ml lactic acid, 10 ml water and 10 mg of trypan blue Working solution: Dilution of stock solution with 96% EtOH (1:1 v/v)
Chloral hydrate solution	2.5 g Chloral hydrate / ml of ddH2O (needs to be stirred overnight to dissolve)

4.8.2 WGA-AF488/Propidium iodide staining of *U. maydis in planta*

Zea mays leaf material infected with *U. maydis* was harvested and placed in 100 % EtOH for bleaching. Afterwards, the samples are placed in 10% KOH at 85°C for 2-3 hours, and then washed 3-4 times with 1 x PBS until the pH of the solution turns neutral. Eventually, WGA/PI solution is vacuum infiltrated to the samples (3 times at 250 mbar for 5 minutes). Samples can be stored in 1x PBS at 4°C until microscopy.

10% KOH	11,8g of 85% KOH-Pellets in 100 ml
10X PBS	8.9 g of Na2HPO4, 19.7 g KH2PO4, 0.9 g of MgCl2 x 6H2O, 2 g of KCl and 80 g of NaCl in 1 L ddH2O (adjust to pH-7.2 with HCl).

WGA-AF/PI staining solution	20 µg/ ml Propidium iodide, 10 µg/ml WGA-AF 488, 0.02 % Tween20 in 1x PBS

4.8.3 Fluorescence microscopy

Nikon Eclipse Ti inverted microscope (Nikon Instruments Microscopes and Digital Imaging Systems, Alzenau, Germany) with Hamamatsu C11440 ORCA-flash4.0LT camera (Hamamatsu Photonics, Herrsching am Ammersee, Germany) was used for fluorescence microscopy.

4.9 Computational analysis

MEGA software used for multiple sequence alignment of GH25 protein. For statistical analysis, to identify significant differences between treatments, an analysis of variance (ANOVA) model with Tukey's HSD test was used for pairwise comparison. R- studiov3.5.1 (RStudio Inc., Boston, Massachusetts, USA), Origin 2018 (OriginLab, Northampton, MA) and GraphPad Prism 6 (GraphPad Software, San Diego, USA) was used to generate data plots. ImageJ 1.53K version (Wayne Rasband and Contributers National Institute of Health, USA) was used to calculate necrotic lesions of *P. infestans* and zone of inhibition by fungal and yeast strains.

5. Bibliography:

Abadi VAJM, Sepehri M, Rahmani HA, Zarei M, Ronaghi A, Taghavi SM, Shamshiripour M. 2020. Role of Dominant Phyllosphere Bacteria with Plant Growth–Promoting Characteristics on Growth and Nutrition of Maize (Zea mays L.). *J Soil Sci Plant Nutr* **20**:2348–2363. doi:10.1007/S42729-020-00302-1/TABLES/2

Abdelfattah A, Fellow MC, Wisniewski M, Schena L, Tack AJM. 2021. Experimental evidence of microbial inheritance in plants and transmission routes from seed to phyllosphere and root. doi:10.1111/1462-2920.15392

Abril AB, Torres PA, Bucher EH. 2005. The importance of phyllosphere microbial populations in nitrogen cycling in the Chaco semi-arid woodland. *J Trop Ecol* **21**:103–107. doi:10.1017/S0266467404001981

Adie BAT, Pérez-Pérez J, Pérez-Pérez MM, Godoy M, Sánchez-Serrano J-J, Schmelz EA, Solano R. 2007. ABA Is an Essential Signal for Plant Resistance to Pathogens Affecting JA Biosynthesis and the Activation of Defenses in Arabidopsis. *Plant Cell* **19**:1665–1681. doi:10.1105/tpc.106.048041

Agler MT, Ruhe J, Kroll S, Morhenn C, Kim ST, Weigel D, Kemen EM. 2016. Microbial Hub Taxa Link Host and Abiotic Factors to Plant Microbiome Variation. *PLoS Biol*. doi:10.1371/journal.pbio.1002352

Al-Hatmi AMS, Sybren de Hoog G, Meis JF. 2019. Multiresistant Fusarium Pathogens on Plants and Humans: Solutions in (from) the Antifungal Pipeline? *Infect Drug Resist* **12**:3727. doi:10.2147/IDR.S180912

Almario J, Mahmoudi M, Kroll S, Agler M, Placzek A, Mari A, Kemen E. 2022. The Leaf Microbiome of Arabidopsis Displays Reproducible Dynamics and Patterns throughout the Growing Season. *mBio* **13**:e0282521. doi:10.1128/mbio.02825-21

Andreote FD, Gumiere T, Durrer A. 2014. Exploring interactions of plant microbiomes. *Sci Agric* **71**:528–539. doi:10.1590/0103-9016-2014-0195

Aronson JM, Cooper BA, Fuller MS. 1967. Glucans of oomycete cell walls. *Science* **155**:332–335. doi:10.1126/science.155.3760.332

Arun K. D, Sabarinathan KG, Gomathy M, Kannan R, Balachandar D. 2020. Mitigation of drought stress in rice crop with plant growth-promoting abiotic stress-tolerant rice phyllosphere bacteria. *J Basic Microbiol* **60**:768–786. doi:10.1002/JOBM.202000011

Asai S, Rallapalli G, Piquerez SJM, Caillaud MC, Furzer OJ, Ishaque N, Wirthmueller L, Fabro G, Shirasu K, Jones JDG. 2014. Expression Profiling during Arabidopsis/Downy Mildew Interaction Reveals a Highly-Expressed Effector That Attenuates Responses to Salicylic Acid. *PLoS Pathog* **10**:e1004443. doi:10.1371/JOURNAL.PPAT.1004443

Asai T, Tena G, Plotnikova J, Willmann MR, Chiu W-L, Gomez-Gomez L, Boller T, Ausubel FM, Sheen J. 2002. MAP kinase signalling cascade in Arabidopsis innate immunity. *Nature* **415**:977–983. doi:10.1038/415977a

Avis TJ, Belanger RR. 2002. Mechanisms and means of detection of biocontrol activity of Pseudozyma yeasts against plant-pathogenic fungi. *FEMS Yeast Res* **2**:5–8. doi:10.1111/J.1567-1364.2002.TB00062.X

Balogh B, Nga NTT, Jones JB. 2018. Relative level of bacteriophage multiplication in vitroor in phyllosphere may not predict in planta efficacy for controlling bacterial leaf spot on tomato caused by xanthomonas perforans. *Front Microbiol* **9**:2176. doi:10.3389/FMICB.2018.02176/BIBTEX

Bao L, Cai W, Cao J, Zhang X, Liu J, Chen H, Wei Y, Zhuang X, Zhuang G, Bai Z. 2020. Microbial community overlap between the phyllosphere and rhizosphere of three plants from Yongxing Island, South China Sea. *Microbiologyopen* **9**. doi:10.1002/MBO3.1048

Baquero F, Nombela C. 2012. The microbiome as a human organ. *Clinical Microbiology and Infection* **18**:2–4. doi:https://doi.org/10.1111/j.1469-0691.2012.03916.x

Barda O, Shalev O, Alster S, Buxdorf K, Gafni A, Levy M. 2015. Pseudozyma aphidis induces salicylic-acid-independent resistance to Clavibacter michiganensis in tomato plants. *Plant Dis*. doi:10.1094/PDIS-04-14-0377-RE

Begerow D, Stoll M, Bauer R. 2017. A phylogenetic hypothesis of Ustilaginomycotina based on multiple gene analyses and morphological data1. *https://doi.org/101080/15572536200611832620* **98**:906–916. doi:10.1080/15572536.2006.11832620

Belanger RR, Labbe C, Jarvis WR. 1994. Commercial-scale control of rose powdery mildew with a fungal antagonist. *Plant Dis* **78**:420–424. doi:10.1094/PD-78-0420

Belhaj K, Cano LM, Prince DC, Kemen A, Yoshida K, Dagdas YF, Etherington GJ, Schoonbeek HJ, van Esse HP, Jones JDG, Kamoun S, Schornack S. 2017. Arabidopsis late blight: infection of a nonhost plant by Albugo laibachii enables full colonization by Phytophthora infestans. *Cell Microbiol*. doi:10.1111/cmi.12628

Bentley BL. 1987. Nitrogen Fixation by Epiphylls in a Tropical Rainforest. *Source: Annals of the Missouri Botanical Garden* **74**:234–241.

Benyagoub M, Willemot C, Bélanger RR. 1996. Influence of a subinhibitory dose of antifungal atty acids fromSporothrix flocculosa on cellular lipid composition in fungi. *Lipids* **31**:1077–1082. doi:10.1007/BF02522465

Berendsen RL, Vismans G, Yu K, Song Y, de Jonge R, Burgman WP, Burmølle M, Herschend J, Bakker PAHM, Pieterse CMJ. 2018. Disease-induced assemblage of a plant-beneficial bacterial consortium. *ISME J* **12**:1496–1507. doi:10.1038/s41396-018-0093-1

Berg G, Rybakova D, Fischer D, Cernava T, Vergès M-CC, Charles T, Chen X, Cocolin L, Eversole K, Corral GH, Kazou M, Kinkel L, Lange L, Lima N, Loy A, Macklin JA, Maguin E, Mauchline T, McClure R, Mitter B, Ryan M, Sarand I, Smidt H, Schelkle B, Roume H, Kiran GS, Selvin J, Souza RSC de, van Overbeek L, Singh BK, Wagner M, Walsh A, Sessitsch A, Schloter M. 2020. Microbiome definition re-visited: old concepts and new challenges. *Microbiome* **8**:103. doi:10.1186/s40168-020-00875-0

Bergna A, Cernava T, Rändler M, Grosch R, Zachow C, Berg G. 2018. Tomato seeds preferably transmit plant beneficial endophytes. *Phytobiomes J* **2**:183–193. doi:10.1094/PBIOMES-06-18-0029-R/ASSET/IMAGES/LARGE/PBIOMES-06-18-0029-RF6.JPEG

Berini F, Casartelli M, Montali A, Reguzzoni M, Tettamanti G, Marinelli F. 2019. Metagenome-Sourced Microbial Chitinases as Potential Insecticide Proteins. *Front Microbiol* **10**. doi:10.3389/FMICB.2019.01358

Bernsdorff F, Döring A-C, Gruner K, Schuck S, Bräutigam A, Zeier J. 2015. Pipecolic Acid Orchestrates Plant Systemic Acquired Resistance and Defense Priming via Salicylic Acid-Dependent and -Independent Pathways. *Plant Cell* **28**:102–129. doi:10.1105/tpc.15.00496

Bhandari DD, Lapin D, Kracher B, von Born P, Bautor J, Niefind K, Parker JE. 2019. An EDS1 heterodimer signalling surface enforces timely reprogramming of immunity genes in Arabidopsis. *Nature Communications 2019 10:1* **10**:1–13. doi:10.1038/s41467-019-08783-0

Bodenhausen N, Bortfeld-Miller M, Ackermann M, Vorholt JA. 2014. A Synthetic Community Approach Reveals Plant Genotypes Affecting the Phyllosphere Microbiota. *PLoS Genet* **10**:1–12. doi:10.1371/journal.pgen.1004283

Boekhout T. 2011. Pseudozyma Bandoni emend: Boekhout (1985) and a comparison with the yeast state of Ustilago maydis (De Candolle) Corda (1842)The Yeasts. doi:10.1016/B978-0-444-52149-1.00153-1

Bordenstein SR, Theis KR. 2015. Host Biology in Light of the Microbiome: Ten Principles of Holobionts and Hologenomes. *PLoS Biol* **13**:1–23. doi:10.1371/journal.pbio.1002226

Bradley EL, Ökmen B, Doehlemann G, Henrissat B, Bradshaw RE, Mesarich CH. 2022. Secreted Glycoside Hydrolase Proteins as Effectors and Invasion Patterns of Plant-Associated Fungi and Oomycetes. *Front Plant Sci* **13**. doi:10.3389/FPLS.2022.853106

Brito N, Espino JJ, González C. 2007. The Endo-β-1,4-Xylanase Xyn11A Is Required for Virulence in Botrytis cinerea. *https://doi.org/101094/MPMI-19-0025* **19**:25–32. doi:10.1094/MPMI-19-0025

Bulgarelli D, Schlaeppi K, Spaepen S, van Themaat EVL, Schulze-Lefert P. 2013. Structure and Functions of the Bacterial Microbiota of Plants. *Annu Rev Plant Biol*. doi:10.1146/annurev-arplant-050312-120106

Busby PE, Peay KG, Newcombe G. 2016. Common foliar fungi of Populus trichocarpa modify Melampsora rust disease severity. *New Phytologist*. doi:10.1111/nph.13742

Caballo-Ponce E, Meng X, Uzelac G, Halliday N, Cámara M, Licastro D, da Silva DP, Ramos C, Venturi V. 2018. Quorum Sensing in Pseudomonas savastanoi pv. savastanoi and Erwinia toletana: Role in Virulence and Interspecies Interactions in the Olive Knot. *Appl Environ Microbiol* **84**:e00950-18. doi:10.1128/AEM.00950-18

Calderón CE, Rotem N, Harris R, Vela-Corcía D, Levy M. 2019. Pseudozyma aphidis activates reactive oxygen species production, programmed cell death and morphological alterations in the necrotrophic fungus Botrytis cinerea. *Mol Plant Pathol* **20**:562–574. doi:10.1111/MPP.12775

CARPENTER EJ. 1992. Nitrogen fixation in the epiphyllae and root nodules of trees in the lowland tropical rainforest of Costa Rica. *Acta oecologica : (1990)* **13**:153–160.

Cesaro P, Gamalero E, Zhang J, Pivato B. 2021. Editorial: The Plant Holobiont Volume I: Microbiota as Part of the Holobiont; Challenges for Agriculture. *Front Plant Sci*. doi:10.3389/fpls.2021.799168

Chaloner TM, Gurr SJ, Bebber DP. 2021. Plant pathogen infection risk tracks global crop yields under climate change. *Nat Clim Chang* **11**:710–715. doi:10.1038/s41558-021-01104-8

Chaloner TM, Gurr SJ, Bebber DP. 2020. Geometry and evolution of the ecological niche in plant-associated microbes. *Nature Communications 2020 11:1* **11**:1–9. doi:10.1038/s41467-020-16778-5

Chaudhry V, Runge P, Sengupta P, Doehlemann G, Parker JE, Kemen E. 2021. Shaping the leaf microbiota: Plant-microbe-microbe interactions. *J Exp Bot* **72**:36–56. doi:10.1093/jxb/eraa417

Chen Y, Miyata S, Makino S, Moriyama R. 1997. Molecular characterization of a germination-specific muramidase from Clostridium perfringens S40 spores and nucleotide sequence of the corresponding gene. *J Bacteriol*. doi:10.1128/jb.179.10.3181-3187.1997

Cheng Y, McNally DJ, Labbé C, Voyer N, Belzile F, Bélanger RR. 2003. Insertional mutagenesis of a fungal biocontrol agent led to discovery of a rare cellobiose lipid with antifungal activity. *Appl Environ Microbiol*. doi:10.1128/AEM.69.5.2595-2602.2003

Choudhury SR, Traquair JA, Jarvis WR. 1994. 4-METHYL-7,11-HEPTADECADIENAL AND 4-METHYL-7.11-HEPTADECADIENOIC ACID: NEW ANTIBIOTICS FROM SPOROTHRIX FLOCCULOSA AND SPOROTHRIX RUGULOSA. *J Nat Prod* **57**:700–704.

Cooper AJ, Latunde-Dada AO, Woods-Tör A, Lynn J, Lucas JA, Crute IR, Holub EB. 2008. Basic compatibility of Albugo candida in Arabidopsis thaliana and Brassica juncea causes broad-spectrum suppression of innate immunity. *Molecular Plant-Microbe Interactions*. doi:10.1094/MPMI-21-6-0745

Cui HL, Duan GL, Zhang H, Cheng W, Zhu YG. 2019. Microbiota in non-flooded and flooded rice culms. *FEMS Microbiol Ecol* **95**. doi:10.1093/FEMSEC/FIZ036

De Angelis G, Simonetti G, Chronopoulou L, Orekhova A, Badiali C, Petruccelli V, Portoghesi F, D'Angeli S, Brasili E, Pasqua G, Palocci C. 2022. A novel approach to control Botrytis cinerea fungal infections: uptake and biological activity of antifungals encapsulated in nanoparticle based vectors. *Sci Rep* **12**:7989. doi:10.1038/s41598-022-11533-w

de Chaves MA, Reginatto P, da Costa BS, de Paschoal RI, Teixeira ML, Fuentefria AM. 2022. Fungicide Resistance in Fusarium graminearum Species Complex. *Curr Microbiol* **79**:62. doi:10.1007/s00284-021-02759-4

de Vries S, von Dahlen JK, Schnake A, Ginschel S, Schulz B, Rose LE. 2018. Broad-spectrum inhibition of Phytophthora infestans by fungal endophytes. *FEMS Microbiol Ecol* **94**. doi:10.1093/FEMSEC/FIY037

de Vrieze M, Gloor R, Codina JM, Torriani S, Gindro K, L'Haridon F, Bailly A, Weisskopf L. 2019. Biocontrol Activity of Three Pseudomonas in a Newly Assembled Collection of Phytophthora infestans Isolates. *Phytopathology* **109**:1555–1565. doi:10.1094/PHYTO-12-18-0487-R

Delgado-Baquerizo M, Guerra CA, Cano-Díaz C, Egidi E, Wang J-T, Eisenhauer N, Singh BK, Maestre FT. 2020. The proportion of soil-borne pathogens increases with warming at the global scale. *Nat Clim Chang* **10**:550–554. doi:10.1038/s41558-020-0759-3

Devarajan AK, Muthukrishanan G, Truu J, Truu M, Ostonen I, Subramanian Kizhaeral S, Panneerselvam P, Gopalasubramanian SK. 2021. The Foliar Application of Rice Phyllosphere Bacteria induces Drought-Stress Tolerance in Oryza sativa (L.). *Plants 2021, Vol 10, Page 387* **10**:387. doi:10.3390/PLANTS10020387

Djamei A, Schipper K, Rabe F, Ghosh A, Vincon V, Kahnt J, Osorio S, Tohge T, Fernie AR, Feussner I, Feussner K, Meinicke P, Stierhof YD, Schwarz H, MacEk B, Mann M, Kahmann R. 2011. Metabolic priming by a secreted fungal effector. *Nature*. doi:10.1038/nature10454

Doehlemann G, van der Linde K, Aßmann D, Schwammbach D, Hof A, Mohanty A, Jackson D, Kahmann R. 2009. Pep1, a secreted effector protein of Ustilago maydis, is required for successful invasion of plant cells. *PLoS Pathog*. doi:10.1371/journal.ppat.1000290

Doehlemann G, Wahl R, Vranes M, de Vries RP, Kämper J, Kahmann R. 2008. Establishment of compatibility in the Ustilago maydis/maize pathosystem. *J Plant Physiol* **165**:29–40. doi:10.1016/J.JPLPH.2007.05.016

Dong J, Chen C, Chen Z. 2003. Expression profiles of the Arabidopsis WRKY gene superfamily during plant defense response. *Plant Mol Biol* **51**:21–37. doi:10.1023/a:1020780022549

Dong YH, Wang LH, Xu JL, Zhang HB, Zhang XF, Zhang LH. 2001. Quenching quorum-sensing-dependent bacterial infection by an N-acyl homoserine lactonase. *Nature*. doi:10.1038/35081101

Dong YH, Xu JL, Li XZ, Zhang LH. 2000. AiiA, an enzyme that inactivates the acylhomoserine lactone quorum-sensing signal and attenuates the virulence of Erwinia carotovora. *Proc Natl Acad Sci U S A*. doi:10.1073/pnas.97.7.3526

Dongus JA, Bhandari DD, Penner E, Lapin D, Stolze SC, Harzen A, Patel M, Archer L, Dijkgraaf L, Shah J, Nakagami H, Parker JE. 2022. Cavity surface residues of PAD4 and SAG101 contribute to EDS1 dimer signaling specificity in plant immunity. *Plant Journal* **110**:1415–1432. doi:10.1111/tpj.15747

Drula E, Garron ML, Dogan S, Lombard V, Henrissat B, Terrapon N. 2022. The carbohydrate-active enzyme database: functions and literature. *Nucleic Acids Res* **50**:D571–D577. doi:10.1093/NAR/GKAB1045

Du Y, Chen X, Guo Y, Zhang X, Zhang H, Li F, Huang G, Meng Y, Shan W. 2021. Phytophthora infestans RXLR effector PITG20303 targets a potato MKK1 protein to suppress plant immunity. *New Phytologist* **229**:501–515. doi:10.1111/NPH.16861

Dunker F, Trutzenberg A, Rothenpieler JS, Kuhn S, Pröls R, Schreiber T, Tissier A, Kemen A, Kemen E, Hückelhoven R, Weiberg A. 2020. Oomycete small RNAs bind to the plant RNA-induced silencing complex for virulence. *Elife* **9**. doi:10.7554/ELIFE.56096

Fabro G. 2022. Oomycete intracellular effectors: specialised weapons targeting strategic plant processes. *New Phytologist* **233**:1074–1082. doi:10.1111/NPH.17828

Fawke S, Doumane M, Schornack S. 2015. Oomycete Interactions with Plants: Infection Strategies and Resistance Principles. *Microbiol Mol Biol Rev* **79**:263. doi:10.1128/MMBR.00010-15

Fones HN, Bebber DP, Chaloner TM, Kay WT, Steinberg G, Gurr SJ. 2020. Threats to global food security from emerging fungal and oomycete crop pathogens. *Nat Food* **1**:332–342. doi:10.1038/s43016-020-0075-0

Francioli D, Cid G, Hajirezaei MR, Kolb S. 2022. Leaf bacterial microbiota response to flooding is controlled by plant phenology in wheat (Triticum aestivum L.). *Scientific Reports 2022 12:1* **12**:1–13. doi:10.1038/s41598-022-15133-6

Frases S, Chaskes S, Dadachova E, Casadevall A. 2006. Induction by *Klebsiella aerogenes* of a Melanin-Like Pigment in *Cryptococcus neoformans*. *Appl Environ Microbiol* **72**:1542–1550. doi:10.1128/AEM.72.2.1542-1550.2006

Freiberg E. 1998. Microclimatic parameters influencing nitrogen fixation in the phyllosphere in a Costa Rican premontane rain forest. *Oecologia 1998 117:1* **117**:9–18. doi:10.1007/S004420050625

Fritz-Sheridan RP, Portecop J. 1987. Nitrogen Fixation on the Tropical Volcano, La Soufriere (Guadeloupe): I. A Survey of Nitrogen Fixation by Blue-Green Algal Microepiphytes and Lichen Endophytes **19**:194–199.

Fürnkranz M, Wanek W, Richter A, Abell G, Rasche F, Sessitsch A. 2008. Nitrogen fixation by phyllosphere bacteria associated with higher plants and their colonizing epiphytes of a tropical lowland rainforest of Costa Rica. *The ISME Journal 2008 2:5* **2**:561–570. doi:10.1038/ismej.2008.14

Furzer OJ, Cevik V, Fairhead S, Bailey K, Redkar A, Schudoma C, MacLean D, Holub EB, Jones JDG. 2022. An Improved Assembly of the Albugo candida Ac2V Genome Reveals the Expansion of the "CCG" Class of Effectors. *Molecular Plant-Microbe Interactions* **35**:39–48. doi:10.1094/MPMI-04-21-0075-R/ASSET/IMAGES/LARGE/MPMI-04-21-0075-RF4.JPEG

Gafni A, Calderon CE, Harris R, Buxdorf K, Dafa-Berger A, Zeilinger-Reichert E, Levy M. 2015. Biological control of the cucurbit powdery mildew pathogen Podosphaera xanthii by means of the epiphytic fungus Pseudozyma aphidis and parasitism as a mode of action. *Front Plant Sci*. doi:10.3389/fpls.2015.00132

Galiana E, Marais A, Mura C, Industri B, Arbiol G, Ponchet M. 2011. Ecosystem screening approach for pathogen-associated microorganisms affecting host disease. *Appl Environ Microbiol* **77**:6069–6075. doi:10.1128/AEM.05371-11

Gámez-Arjona FM, Vitale S, Voxeur A, Dora S, Müller S, Sancho-Andrés G, Montesinos JC, di Pietro A, Sánchez-Rodríguez C. 2022. Impairment of the cellulose degradation machinery enhances Fusarium oxysporum virulence but limits its reproductive fitness. *Sci Adv* **8**. doi:10.1126/SCIADV.ABL9734

Gfeller A, Fuchsmann P, de Vrieze M, Gindro K, Weisskopf L. 2022. Bacterial Volatiles Known to Inhibit Phytophthora infestans Are Emitted on Potato Leaves by Pseudomonas Strains. *Microorganisms 2022, Vol 10, Page 1510* **10**:1510. doi:10.3390/MICROORGANISMS10081510

Glazebrook J. 2005. Contrasting mechanisms of defense against biotrophic and necrotrophic pathogens. *Annu Rev Phytopathol* **43**:205–227. doi:10.1146/annurev.phyto.43.040204.135923

Gui YJ, Chen JY, Zhang DD, Li NY, Li TG, Zhang WQ, Wang XY, Short DPG, Li L, Guo W, Kong ZQ, Bao YM, Subbarao K v., Dai XF. 2017. Verticillium dahliae manipulates plant immunity by glycoside hydrolase 12 proteins in conjunction with carbohydrate-binding module 1. *Environ Microbiol* **19**:1914–1932. doi:10.1111/1462-2920.13695

Hajlaou MR, Traquair JA, Jarvis WR, Belanger RR. 2008. Antifungal activity of extracellular metabolites produced by Sporothrix flocculosa. *http://dx.doi.org/101080/09583159409355331* **4**:229–237. doi:10.1080/09583159409355331

Hajlaoui MR, Belanger RR. 2008. Antagonism of the yeast-like phylloplane fungus Sporothrix flocculosa against Erysiphe graminis var tritici. *http://dx.doi.org/101080/09583159309355297* **3**:427–434. doi:10.1080/09583159309355297

Hane JK, Paxman J, Jones DAB, Oliver RP, de Wit P. 2020. "CATAStrophy," a Genome-Informed Trophic Classification of Filamentous Plant Pathogens – How Many Different Types of Filamentous Plant Pathogens Are There? *Front Microbiol* **10**:3088. doi:10.3389/FMICB.2019.03088/BIBTEX

Helfrich EJN, Vogel CM, Ueoka R, Schäfer M, Ryffel F, Müller DB, Probst S, Kreuzer M, Piel J, Vorholt JA. 2018. Bipartite interactions, antibiotic production and biosynthetic potential of the Arabidopsis leaf microbiome. *Nat Microbiol*. doi:10.1038/s41564-018-0200-0

Hemetsberger C, Herrberger C, Zechmann B, Hillmer M, Doehlemann G. 2012. The Ustilago maydis effector Pep1 suppresses plant immunity by inhibition of host peroxidase activity. *PLoS Pathog* **8**. doi:10.1371/JOURNAL.PPAT.1002684

Henrissat B, Davies G. 1997. Structural and sequence-based classification of glycoside hydrolases. *Curr Opin Struct Biol* **7**:637–644. doi:10.1016/S0959-440X(97)80072-3

Henry LP, Bruijning M, Forsberg SKG, Ayroles JF. 2021. The microbiome extends host evolutionary potential. *Nat Commun* **12**:5141. doi:10.1038/s41467-021-25315-x

Herlihy J, Ludwig NR, Ackerveken G van den, McDowell JM. 2019. Oomycetes Used in Arabidopsis Research. *Arabidopsis Book* **2019**:1–26. doi:10.1199/tab.0188

Holub EB. 2008. Natural history of Arabidopsis thaliana and oomycete symbioses BT - The Downy Mildews - Genetics, Molecular Biology and Control In: Lebeda A, Spencer-Phillips PTN, Cooke BM, editors. Dordrecht: Springer Netherlands. pp. 91–109. doi:10.1007/978-1-4020-8973-2_8

Horner NR, Grenville-Briggs LJ, van West P. 2012. The oomycete Pythium oligandrum expresses putative effectors during mycoparasitism of Phytophthora infestans and is amenable to transformation. *Fungal Biol*. doi:10.1016/j.funbio.2011.09.004

Hyde KD, Xu J, Rapior S, Jeewon R, Lumyong S, Niego AGT, Abeywickrama PD, Aluthmuhandiram JVS, Brahamanage RS, Brooks S, Chaiyasen A, Chethana KWT, Chomnunti P, Chepkirui C, Chuankid B, de Silva NI, Doilom M, Faulds C, Gentekaki E, Gopalan V, Kakumyan P, Harishchandra D, Hemachandran H, Hongsanan S,

Karunarathna A, Karunarathna SC, Khan S, Kumla J, Jayawardena RS, Liu JK, Liu N, Luangharn T, Macabeo APG, Marasinghe DS, Meeks D, Mortimer PE, Mueller P, Nadir S, Nataraja KN, Nontachaiyapoom S, O'Brien M, Penkhrue W, Phukhamsakda C, Ramanan US, Rathnayaka AR, Sadaba RB, Sandargo B, Samarakoon BC, Tennakoon DS, Siva R, Sriprom W, Suryanarayanan TS, Sujarit K, Suwannarach N, Suwunwong T, Thongbai B, Thongklang N, Wei D, Wijesinghe SN, Winiski J, Yan J, Yasanthika E, Stadler M. 2019. The amazing potential of fungi: 50 ways we can exploit fungi industrially. *Fungal Divers*. doi:10.1007/s13225-019-00430-9

Jarvis WR, Shaw LA, Traquair JA. 1989. Factors affecting antagonism of cucumber powdery mildew by Stephanoascus flocculosus and S. rugulosus. *Mycol Res* **92**:162–165. doi:10.1016/S0953-7562(89)80006-1

Jelenska J, Davern SM, Standaert RF, Mirzadeh S, Greenberg JT. 2017. Flagellin peptide flg22 gains access to long-distance trafficking in Arabidopsis via its receptor, FLS2. *J Exp Bot* **68**:1769–1783. doi:10.1093/JXB/ERX060

Jensen D, Thrane C, Tronsmo A, Funck Jensen D. 1997. Endo-1, 3-β-glucanase and cellulase from Trichoderma harzianum: purificat ion and part ial ch… Endo-1,3-glucanase and cellulase from Trichoderma harzianum: purification and partial characterization, induction of and biological activity against plant pathogenic Pythium spp. *Eur J Plant Pathol* **103**:331–344.

Jones JDG, Dangl JL. 2006. The plant immune system. *Nature* **444**:323–329. doi:10.1038/nature05286

Jones JDG, Vance RE, Dangl JL. 2016. Intracellular innate immune surveillance devices in plants and animals. *Science* **354**. doi:10.1126/SCIENCE.AAF6395

Kamoun S, Furzer O, Jones JDG, Judelson HS, Ali GS, Dalio RJD, Roy SG, Schena L, Zambounis A, Panabières F, Cahill D, Ruocco M, Figueiredo A, Chen X-R, Hulvey J, Stam R, Lamour K, Gijzen M, Tyler BM, Grünwald NJ, Mukhtar MS, Tomé DFA, Tör M, Van Den Ackerveken G, McDowell J, Daayf F, Fry WE, Lindqvist-Kreuze H, Meijer HJG, Petre B, Ristaino J, Yoshida K, Birch PRJ, Govers F. 2015. The Top 10 oomycete pathogens in molecular plant pathology. *Mol Plant Pathol* **16**:413–434. doi:https://doi.org/10.1111/mpp.12190

Kamoun S, van West P, Vleeshouwers VGAA, de Groot KE, Govers F. 1998. Resistance of Nicotiana benthamiana to Phytophthora infestans Is Mediated by the Recognition of the Elicitor Protein INF1. *Plant Cell* **10**:1413. doi:10.2307/3870607

Kemen E. 2014. Microbe–microbe interactions determine oomycete and fungal host colonization. *Curr Opin Plant Biol* **20**:75–81. doi:https://doi.org/10.1016/j.pbi.2014.04.005

Kemen E, Jones JDG. 2012. Obligate biotroph parasitism: can we link genomes to lifestyles? *Trends Plant Sci* **17**:448–457. doi:https://doi.org/10.1016/j.tplants.2012.04.005

Köhl J, Kolnaar R, Ravensberg WJ. 2019. Mode of Action of Microbial Biological Control Agents Against Plant Diseases: Relevance Beyond Efficacy. *Front Plant Sci* **10**. doi:10.3389/fpls.2019.00845

Kojic EM, Darouiche RO. 2004. *Candida* Infections of Medical Devices. *Clin Microbiol Rev* **17**:255–267. doi:10.1128/CMR.17.2.255-267.2004

Kong P, Hong C. 2016. Soil bacteria as sources of virulence signal providers promoting plant infection by Phytophthora pathogens. *Sci Rep* **6**:33239. doi:10.1038/srep33239

Korczynska JE, Danielsen S, Schagerlöf U, Turkenburg JP, Davies GJ, Wilson KS, Taylor EJ. 2010. The structure of a family GH25 lysozyme from Aspergillus fumigatus. *Acta Crystallogr Sect F Struct Biol Cryst Commun*. doi:10.1107/S1744309110025601

Kruse J, Doehlemann G, Kemen E, Thines M. 2017. Asexual and sexual morphs of Moesziomyces revisited. *IMA Fungus*. doi:10.5598/imafungus.2017.08.01.09

Kubicek CP, Starr TL, Glass NL. 2014. Plant cell wall-degrading enzymes and their secretion in plant-pathogenic fungi. *Annu Rev Phytopathol* **52**:427–451. doi:10.1146/ANNUREV-PHYTO-102313-045831

Kumar J, Babele PK, Singh D, Kumar A. 2016. UV-B radiation stress causes alterations in whole cell protein profile and expression of certain genes in the rice phyllospheric bacterium Enterobacter cloacae. *Front Microbiol* **7**:1440. doi:10.3389/FMICB.2016.01440/BIBTEX

Kusstatscher P, Adam E, Wicaksono WA, Bernhart M, Olimi E, Müller H, Berg G. 2021. Microbiome-Assisted Breeding to Understand Cultivar-Dependent Assembly in Cucurbita pepo. *Front Plant Sci* **12**. doi:10.3389/FPLS.2021.642027

Lanver D, Berndt P, Tollot M, Naik V, Vranes M, Warmann T, Münch K, Rössel N, Kahmann R. 2014. Plant Surface Cues Prime Ustilago maydis for Biotrophic Development. *PLoS Pathog* **10**:e1004272. doi:10.1371/JOURNAL.PPAT.1004272

Lanver D, Müller AN, Happel P, Schweizer G, Haas FB, Franitza M, Pellegrin C, Reissmann S, Altmüller J, Rensing SA, Kahmann R. 2018. The Biotrophic Development of Ustilago maydis Studied by RNA-Seq Analysis. *Plant Cell* **30**:300–323. doi:10.1105/TPC.17.00764

Lanver D, Tollot M, Schweizer G, lo Presti L, Reissmann S, Ma LS, Schuster M, Tanaka S, Liang L, Ludwig N, Kahmann R. 2017. Ustilago maydis effectors and their impact on virulence. *Nature Reviews Microbiology 2017 15:7* **15**:409–421. doi:10.1038/nrmicro.2017.33

Lapin D, Bhandari DD, Parker JE. 2020. Origins and Immunity Networking Functions of EDS1 Family Proteins. *Annu Rev Phytopathol* **58**:253–276. doi:10.1146/annurev-phyto-010820-012840

Larousse M, Galiana E. 2017. Microbial Partnerships of Pathogenic Oomycetes. *PLoS Pathog* **13**:e1006028. doi:10.1371/journal.ppat.1006028

Lee G, Lee SH, Kim KM, Ryu CM. 2017. Foliar application of the leaf-colonizing yeast Pseudozyma churashimaensis elicits systemic defense of pepper against bacterial and viral pathogens. *Sci Rep*. doi:10.1038/srep39432

Lee SJ, Park SY, Lee JJ, Yum DY, Koo BT, Lee JK. 2002. Genes encoding the N-acyl homoserine lactone-degrading enzyme are widespread in many subspecies of Bacillus thuringiensis. *Appl Environ Microbiol*. doi:10.1128/AEM.68.8.3919-3924.2002

Lefevere H, Bauters L, Gheysen G. 2020. Salicylic Acid Biosynthesis in Plants. *Front Plant Sci* **11**:1–7. doi:10.3389/fpls.2020.00338

Legein M, Smets W, Vandenheuvel D, Eilers T, Muyshondt B, Prinsen E, Samson R, Lebeer S. 2020. Modes of Action of Microbial Biocontrol in the Phyllosphere. *Front Microbiol* **11**:1619. doi:10.3389/FMICB.2020.01619/BIBTEX

Léon-Kloosterziel KM, Gil MA, Ruijs GJ, Jacobsen SE, Olszewski NE, Schwartz SH, Zeevaart JAD, Koornneef M. 1996. Isolation and characterization of abscisic acid-deficient Arabidopsis mutants at two new loci. *The Plant Journal* **10**:655–661. doi:https://doi.org/10.1046/j.1365-313X.1996.10040655.x

Li PD, Zhu ZR, Zhang Y, Xu J, Wang H, Wang Z, Li H. 2022. The phyllosphere microbiome shifts toward combating melanose pathogen. *Microbiome* **10**:1–17. doi:10.1186/S40168-022-01234-X/FIGURES/8

Lindow SE, Brandl MT. 2003. Microbiology of the phyllosphere. *Appl Environ Microbiol* **69**:1875–1883. doi:10.1128/AEM.69.4.1875-1883.2003

Liu T, Song T, Zhang X, Yuan H, Su L, Li W, Xu J, Liu S, Chen L, Chen T, Zhang M, Gu L, Zhang B, Dou D. 2014. Unconventionally secreted effectors of two filamentous pathogens target plant salicylate biosynthesis. *Nat Commun* **5**:4686. doi:10.1038/ncomms5686

Lombard V, Golaconda Ramulu H, Drula E, Coutinho PM, Henrissat B. 2014. The carbohydrate-active enzymes database (CAZy) in 2013. *Nucleic Acids Res* **42**. doi:10.1093/NAR/GKT1178

Ma A, Lv D, Zhuang X, Zhuang G. 2013. Quorum quenching in culturable phyllosphere bacteria from tobacco. *Int J Mol Sci* **14**:14607–14619. doi:10.3390/IJMS140714607

Ma H, Zhang B, Gai Y, Sun X, Chung K-R, Li H. 2019. Cell-Wall-Degrading Enzymes Required for Virulence in the Host Selective Toxin-Producing Necrotroph Alternaria alternata of Citrus. *Front Microbiol* **10**. doi:10.3389/fmicb.2019.02514

Ma Z, Michailides TJ. 2005. Advances in understanding molecular mechanisms of fungicide resistance and molecular detection of resistant genotypes in phytopathogenic fungi. *Crop Protection* **24**:853–863. doi:10.1016/J.CROPRO.2005.01.011

Ma Z, Song T, Zhu L, Ye W, Wang Yang, Shao Y, Dong S, Zhang Z, Dou D, Zheng X, Tyler BM, Wang Yuanchao. 2015. A Phytophthora sojae Glycoside Hydrolase 12 Protein Is a Major Virulence Factor during Soybean Infection and Is Recognized as a PAMP. *Plant Cell* **27**:2057–2072. doi:10.1105/TPC.15.00390

Ma Z, Zhu L, Song T, Wang Yang, Zhang Q, Xia Y, Qiu M, Lin Y, Li H, Kong L, Fang Y, Ye W, Wang Yan, Dong S, Zheng X, Tyler BM, Wang Yuanchao. 2017. A paralogous decoy protects Phytophthora sojae apoplastic effector PsXEG1 from a host inhibitor. *Science* **355**:710–714. doi:10.1126/SCIENCE.AAI7919

Maignien L, DeForce EA, Chafee ME, Murat Eren A, Simmons SL. 2014. Ecological Succession and Stochastic Variation in the Assembly of Arabidopsis thaliana Phyllosphere Communities. *mBio* **5**. doi:10.1128/MBIO.00682-13

Mélida H, Sandoval-Sierra J V, Diéguez-Uribeondo J, Bulone V. 2013. Analyses of extracellular carbohydrates in oomycetes unveil the existence of three different cell wall types. *Eukaryot Cell* **12**:194–203. doi:10.1128/EC.00288-12

Migheli Q, González-Candelas L, Dealessi L, Camponogara A, Ramón-Vidal D. 1998. Transformants of Trichoderma longibrachiatum Overexpressing the beta-1,4-Endoglucanase Gene egl1 Show Enhanced Biocontrol of Pythium ultimum on Cucumber. *Phytopathology* **88**:673–677. doi:10.1094/PHYTO.1998.88.7.673

Mikiciński A, Sobiczewski P, Puławska J, Maciorowski R. 2016. Control of fire blight (Erwinia amylovora) by a novel strain 49M of Pseudomonas graminis from the phyllosphere of apple (Malus spp.). *Eur J Plant Pathol*. doi:10.1007/s10658-015-0837-y

Mimee B, Labbé C, Pelletier R, Bélanger RR. 2005. Antifungal activity of flocculosin, a novel glycolipid isolated from Pseudozyma flocculosa. *Antimicrob Agents Chemother*. doi:10.1128/AAC.49.4.1597-1599.2005

Misas Villamil JC, Mueller AN, Demir F, Meyer U, Ökmen B, Schulze Hüynck J, Breuer M, Dauben H, Win J, Huesgen PF, Doehlemann G. 2019. A fungal substrate mimicking molecule suppresses plant immunity via an inter-kingdom conserved motif. *Nature Communications 2019 10:1* **10**:1–15. doi:10.1038/s41467-019-09472-8

Morella NM, Weng FCH, Joubert PM, Jessica C, Lindow S, Koskella B. 2020. Successive passaging of a plant-associated microbiome reveals robust habitat and host genotype-dependent selection. *Proc Natl Acad Sci U S A* **117**:1148–1159. doi:10.1073/PNAS.1908600116/SUPPL_FILE/PNAS.1908600116.SAPP.PDF

Morita T, Konishi M, Fukuoka T, Imura T, Kitamoto D. 2007. Microbial conversion of glycerol into glycolipid biosurfactants, mannosylerythritol lipids, by a basidiomycete yeast, Pseudozyma antarctica JCM 10317T. *J Biosci Bioeng*. doi:10.1263/jbb.104.78

Mueller AN, Ziemann S, Treitschke S, Aßmann D, Doehlemann G. 2013a. Compatibility in the Ustilago maydis–Maize Interaction Requires Inhibition of Host Cysteine Proteases by the Fungal Effector Pit2. *PLoS Pathog* **9**:e1003177. doi:10.1371/JOURNAL.PPAT.1003177

Mueller AN, Ziemann S, Treitschke S, Aßmann D, Doehlemann G. 2013b. Compatibility in the Ustilago maydis–Maize Interaction Requires Inhibition of Host Cysteine Proteases by the Fungal Effector Pit2. *PLoS Pathog* **9**:e1003177. doi:10.1371/JOURNAL.PPAT.1003177

Nalley L, Tsiboe F, Durand-Morat A, Shew A, Thoma G. 2016. Economic and Environmental Impact of Rice Blast Pathogen (Magnaporthe oryzae) Alleviation in the United States. *PLoS One* **11**:e0167295. doi:10.1371/journal.pone.0167295

Nawrath C, Métraux J-P. 1999. Salicylic Acid Induction-Deficient Mutants of Arabidopsis Express PR-2 and PR-5 and Accumulate High Levels of Camalexin after Pathogen Inoculation. *Plant Cell* **11**:1393–1404. doi:10.2307/3870970

Ökmen B, Jaeger E, Schilling L, Finke N, Klemd A, Lee YJ, Wemhöner R, Pauly M, Neumann U, Doehlemann G. 2022. A conserved enzyme of smut fungi facilitates cell-to-cell extension in the plant bundle sheath. *Nature Communications 2022 13:1* **13**:1–13. doi:10.1038/s41467-022-33815-7

Oubaha B, Ezzanad A, Bolívar-Anillo HJ, Oubaha B, Ezzanad A, Bolívar-Anillo HJ. 2021. Plant Beneficial Microbes Controlling Late Blight Pathogen, Phytophthora

infestans. *Agro-Economic Risks of Phytophthora and an Effective Biocontrol Approach*. doi:10.5772/INTECHOPEN.99383

Padder SA, Rather RA, Bhat SA, Shah MD, Baba TR, Mubarak NM. 2022. Dynamics, phylogeny and phyto-stimulating potential of chitinase synthesizing bacterial root endosymbiosiome of North Western Himalayan Brassica rapa L. *Sci Rep* **12**. doi:10.1038/S41598-022-11030-0

Pandey SP, Somssich IE. 2009. The role of WRKY transcription factors in plant immunity. *Plant Physiol* **150**:1648–1655. doi:10.1104/PP.109.138990

Parafati L, Cirvilleri G, Restuccia C, Wisniewski M. 2017. Potential Role of Exoglucanase Genes (WaEXG1 and WaEXG2) in the Biocontrol Activity of Wickerhamomyces anomalus. *Microb Ecol* **73**:876–884. doi:10.1007/S00248-016-0887-5/FIGURES/6

Parker JE, Holub EB, Frost LN, Falk A, Gunn ND, Daniels MJ. 1996. Characterization of eds1, a mutation in Arabidopsis suppressing resistance to Peronospora parasitica specified by several different RPP genes. *Plant Cell* **8**:2033–2046. doi:10.1105/tpc.8.11.2033

Parratt SR, Laine AL. 2016. The role of hyperparasitism in microbial pathogen ecology and evolution. *ISME Journal*. doi:10.1038/ismej.2015.247

Perlin DS, Rautemaa-Richardson R, Alastruey-Izquierdo A. 2017. The global problem of antifungal resistance: prevalence, mechanisms, and management. *Lancet Infect Dis* **17**:e383–e392. doi:10.1016/S1473-3099(17)30316-X

Petre B, Contreras MP, Bozkurt TO, Schattat MH, Sklenar J, Schornack S, Abd-El-Haliem A, Castells-Graells R, Lozano-Durán R, Dagdas YF, Menke FLH, Jones AME, Vossen JH, Robatzek S, Kamoun S, Win J. 2021. Host-interactor screens of Phytophthora infestans RXLR proteins reveal vesicle trafficking as a major effector-targeted process. *Plant Cell* **33**:1447–1471. doi:10.1093/PLCELL/KOAB069

Phillips AJ, Anderson VL, Robertson EJ, Secombes CJ, van West P. 2008. New insights into animal pathogenic oomycetes. *Trends Microbiol* **16**:13–19. doi:10.1016/J.TIM.2007.10.013

Prince DC, Rallapalli G, Xu D, Schoonbeek H, Çevik V, Asai S, Kemen E, Cruz-Mireles N, Kemen A, Belhaj K, Schornack S, Kamoun S, Holub EB, Halkier BA, Jones JDG. 2017. Albugo-imposed changes to tryptophan-derived antimicrobial metabolite biosynthesis may contribute to suppression of non-host resistance to Phytophthora infestans in Arabidopsis thaliana. *BMC Biol* **15**:20. doi:10.1186/s12915-017-0360-z

Qin C, Tao J, Liu T, Liu Y, Xiao N, Li T, Gu Y, Yin H, Meng D. 2019. Responses of phyllosphere microbiota and plant health to application of two different biocontrol agents. *AMB Express* **9**:1–13. doi:10.1186/S13568-019-0765-X/FIGURES/6

Rajesh PS, Ravishankar Rai V. 2014. Quorum quenching activity in cell-free lysate of endophytic bacteria isolated from Pterocarpus santalinus Linn., and its effect on quorum sensing regulated biofilm in Pseudomonas aeruginosa PAO1. *Microbiol Res*. doi:10.1016/j.micres.2013.10.005

Rau A, Hogg T, Marquardt R, Hilgenfeld R. 2001. A new lysozyme fold. Crystal structure of the muramidase from Streptomyces coelicolor at 1.65 Å resolution. *Journal of Biological Chemistry*. doi:10.1074/jbc.M102591200

Reyre J-L, Grisel S, Haon M, Navarro D, Ropartz D, Gall S le, Record E, Sciara G, Tranquet O, Berrin J-G, Bissaro B. 2022. The maize pathogen Ustilago maydis secretes glycoside hydrolases and carbohydrate oxidases directed towards components of the fungal cell wall. *bioRxiv* 2022.09.16.508353. doi:10.1101/2022.09.16.508353

Ritpitakphong U, Falquet L, Vimoltust A, Berger A, Métraux JP, L'Haridon F. 2016. The microbiome of the leaf surface of Arabidopsis protects against a fungal pathogen. *New Phytologist*. doi:10.1111/nph.13808

Rosenberg E, Koren O, Reshef L, Efrony R, Zilber-Rosenberg I. 2007. The role of microorganisms in coral health, disease and evolution. *Nat Rev Microbiol* **5**:355–362. doi:10.1038/nrmicro1635

Ruhe J, Agler MT, Placzek A, Kramer K, Finkemeier I, Kemen EM. 2016a. Obligate Biotroph Pathogens of the Genus Albugo Are Better Adapted to Active Host Defense Compared to Niche Competitors. *Front Plant Sci* **7**. doi:10.3389/FPLS.2016.00820

Ruhe J, Agler MT, Placzek A, Kramer K, Finkemeier I, Kemen EM. 2016b. Obligate biotroph pathogens of the genus albugo are better adapted to active host defense compared to niche competitors. *Front Plant Sci*. doi:10.3389/fpls.2016.00820

Ruhe J, Agler MT, Placzek A, Kramer K, Finkemeier I, Kemen EM. 2016c. Obligate biotroph pathogens of the genus albugo are better adapted to active host defense compared to niche competitors. *Front Plant Sci*. doi:10.3389/fpls.2016.00820

Saravanakumar K, Dou K, Lu Z, Wang X, Li Y, Chen J. 2018. Enhanced biocontrol activity of cellulase from Trichoderma harzianum against Fusarium graminearum through activation of defense-related genes in maize. *Physiol Mol Plant Pathol* **103**:130–136. doi:10.1016/J.PMPP.2018.05.004

Savary S, Bregaglio S, Willocquet L, Gustafson D, Mason D'Croz D, Sparks A, Castilla N, Djurle A, Allinne C, Sharma M, Rossi V, Amorim L, Bergamin A, Yuen J, Esker P, McRoberts N, Avelino J, Duveiller E, Koo J, Garrett K. 2017. Crop health and its global impacts on the components of food security. *Food Secur* **9**:311–327. doi:10.1007/s12571-017-0659-1

Savary S, Willocquet L, Pethybridge SJ, Esker P, McRoberts N, Nelson A. 2019. The global burden of pathogens and pests on major food crops. *Nat Ecol Evol* **3**:430–439. doi:10.1038/s41559-018-0793-y

Saville BJ, Donaldson ME, Doyle CE. n.d. Investigating Host Induced Meiosis in a Fungal Plant Pathogen.

Sengupta B, Nandi AS, Samanta RK, Pal D, Sengupta DN, Sen SP. 1981. Nitrogen Fixation in the Phyllosphere of Tropical Plants: Occurrence of Phyllosphere Nitrogen-Fixing Micro-organisms in Eastern India and their Utility for the Growth and Nitrogen Nutrition of Host Plants. *Ann Bot* **48**:705–716. doi:10.1093/OXFORDJOURNALS.AOB.A086177

Shaffique S, Khan MA, Wani SH, Pande A, Imran M, Kang SM, Rahim W, Khan SA, Bhatta D, Kwon EH, Lee IJ. 2022. A Review on the Role of Endophytes and Plant Growth Promoting Rhizobacteria in Mitigating Heat Stress in Plants. *Microorganisms 2022, Vol 10, Page 1286* **10**:1286. doi:10.3390/MICROORGANISMS10071286

Shakir S, Zaidi SS-E-A, de Vries FT, Mansoor S. 2021. Plant Genetic Networks Shaping Phyllosphere Microbial Community. *Trends Genet* **37**:306–316. doi:10.1016/j.tig.2020.09.010

Shalev O, Ashkenazy H, Neumann M, Weigel D. 2021. Commensal Pseudomonas protect Arabidopsis thaliana from a coexisting pathogen via multiple lineage-dependent mechanisms. *The ISME Journal 2021 16:5* **16**:1235–1244. doi:10.1038/s41396-021-01168-6

Simon J-C, Marchesi JR, Mougel C, Selosse M-A. 2019. Host-microbiota interactions: from holobiont theory to analysis. *Microbiome* **7**:5. doi:10.1186/s40168-019-0619-4

Skamnioti P, Gurr SJ. 2009. Against the grain: safeguarding rice from rice blast disease. *Trends Biotechnol* **27**:141–150. doi:10.1016/J.TIBTECH.2008.12.002

Skibbe DS, Doehlemann G, Fernandes J, Walbot V. 2010. Maize tumors caused by Ustilago maydis require organ-specific genes in host and pathogen. *Science* **328**:89–92. doi:10.1126/SCIENCE.1185775

Stein M, Dittgen J, Sánchez-Rodríguez C, Hou B-H, Molina A, Schulze-Lefert P, Lipka V, Somerville S. 2006. Arabidopsis PEN3/PDR8, an ATP binding cassette transporter, contributes to nonhost resistance to inappropriate pathogens that enter by direct penetration. *Plant Cell* **18**:731–746. doi:10.1105/tpc.105.038372

Stevenson EM, Gaze WH, Gow NAR, Hart A, Schmidt W, Usher J, Warris A, Wilkinson H, Murray AK. 2022. Antifungal Exposure and Resistance Development: Defining Minimal Selective Antifungal Concentrations and Testing Methodologies. *Frontiers in Fungal Biology* **0**:28. doi:10.3389/FFUNB.2022.918717

Stone BWG, Weingarten EA, Jackson CR. 2018. The Role of the Phyllosphere Microbiome in Plant Health and FunctionAnnual Plant Reviews Online. doi:10.1002/9781119312994.apr0614

Tanaka S, Brefort T, Neidig N, Djamei A, Kahnt J, Vermerris W, Koenig S, Feussner K, Feussner I, Kahmann R. 2014. A secreted Ustilago maydis effector promotes virulence by targeting anthocyanin biosynthesis in maize. *Elife* **2014**. doi:10.7554/ELIFE.01355.001

Teichmann B, Linne U, Hewald S, Marahiel MA, Bölker M. 2007. A biosynthetic gene cluster for a secreted cellobiose lipid with antifungal activity from Ustilago maydis. *Mol Microbiol*. doi:10.1111/j.1365-2958.2007.05941.x

Thines M. 2014. Phylogeny and evolution of plant pathogenic oomycetes-a global overview. *Eur J Plant Pathol*. doi:10.1007/s10658-013-0366-5

Trivedi P, Batista BD, Bazany KE, Singh BK. 2022. Plant–microbiome interactions under a changing world: responses, consequences and perspectives. *New Phytologist* **234**:1951–1959. doi:10.1111/NPH.18016

Trivedi P, Leach JE, Tringe SG, Sa T, Singh BK. 2020a. Plant–microbiome interactions: from community assembly to plant health. *Nat Rev Microbiol* **18**:607–621. doi:10.1038/s41579-020-0412-1

Trivedi P, Leach JE, Tringe SG, Sa T, Singh BK. 2020b. Plant–microbiome interactions: from community assembly to plant health. *Nature Reviews Microbiology 2020 18:11* **18**:607–621. doi:10.1038/s41579-020-0412-1

Ulrich RL. 2004. Quorum quenching: Enzymatic disruption of N-acylhomoserine lactone-mediated bacterial communication in Burkholderia thailandensis. *Appl Environ Microbiol*. doi:10.1128/AEM.70.10.6173-6180.2004

Valdes AM, Walter J, Segal E, Spector TD. 2018. Role of the gut microbiota in nutrition and health. *BMJ* **361**. doi:10.1136/bmj.k2179

van Vu B, Itoh K, Nguyen QB, Tosa Y, Nakayashiki H. 2012. Cellulases Belonging to Glycoside Hydrolase Families 6 and 7 Contribute to the Virulence of Magnaporthe oryzae. */ 1135 MPMI* **25**. doi:10.1094/MPMI

Veliz EA, Martínez-Hidalgo P, Hirsch AM. 2017. Chitinase-producing bacteria and their role in biocontrol. *AIMS Microbiol* **3**:689–705. doi:10.3934/MICROBIOL.2017.3.689

Vergnes S, Gayrard D, Veyssière M, Toulotte J, Martinez Y, Dumont V, Bouchez O, Rey T, Dumas B. 2020. Phyllosphere Colonization by a Soil Streptomyces sp. Promotes Plant Defense Responses Against Fungal Infection. *Mol Plant Microbe Interact* **33**:223–234. doi:10.1094/MPMI-05-19-0142-R

Vorholt JA. 2012. Microbial life in the phyllosphere. *Nat Rev Microbiol*. doi:10.1038/nrmicro2910

Walker TS, Bais HP, Grotewold E, Vivanco JM. 2003. Root exudation and rhizosphere biology. *Plant Physiol*. doi:10.1104/pp.102.019661

Wan J, He M, Hou Q, Zou L, Yang Y, Wei Y, Chen X. 2021. Cell wall associated immunity in plants. *Stress Biology 2021 1:1* **1**:1–15. doi:10.1007/S44154-021-00003-4

Wang K, Auzane A, Overmyer K. 2022. The immunity priming effect of the Arabidopsis phyllosphere resident yeast Protomyces arabidopsidicola strain C29. *Front Microbiol* **13**. doi:10.3389/fmicb.2022.956018

Wang QM, Begerow D, Groenewald M, Liu XZ, Theelen B, Bai FY, Boekhout T. 2015. Multigene phylogeny and taxonomic revision of yeasts and related fungi in the Ustilaginomycotina. *Stud Mycol* **81**:55–83. doi:10.1016/j.simyco.2015.10.004

Wang Y, Zhao Y, Wang X, Zhong L, Fan Q, Lan Z, Ye X, Huang Y, Li Z, Cui Z. 2021. Functional Characterization of the Novel Laminaripentaose-Producing β-1,3-Glucanase MoGluB and Its Biocontrol of Magnaporthe oryzae. *J Agric Food Chem* **69**:9571–9584. doi:10.1021/acs.jafc.1c03072

Weiberg A, Wang M, Lin FM, Zhao H, Zhang Z, Kaloshian I, Huang H Da, Jin H. 2013. Fungal small RNAs suppress plant immunity by hijacking host RNA interference pathways. *Science (1979)* **342**:118–123. doi:10.1126/SCIENCE.1239705/SUPPL_FILE/WEIBERG-SM.PDF

Whipps J, Lewis K CR. 1988. Mycoparasitism and plant disease control. *Fungi Biol Control Syst* 161–187.

Xu N, Zhao Q, Zhang Z, Zhang Q, Wang Y, Qin G, Ke M, Qiu D, Peijnenburg WJGM, Lu T, Qian H. 2022. Phyllosphere Microorganisms: Sources, Drivers, and Their Interactions

with Plant Hosts. *J Agric Food Chem* **70**:4860–4870. doi:10.1021/ACS.JAFC.2C01113/ASSET/IMAGES/LARGE/JF2C01113_0003.JPEG

Yerkovich N, Cantoro R, Palazzini JM, Torres A, Chulze SN. 2020. Fusarium head blight in Argentina: Pathogen aggressiveness, triazole tolerance and biocontrol-cultivar combined strategy to reduce disease and deoxynivalenol in wheat. *Crop Protection* **137**:105300. doi:https://doi.org/10.1016/j.cropro.2020.105300

Yoshida S, Hiradate S, Koitabashi M, Kamo T, Tsushima S. 2017. Phyllosphere Methylobacterium bacteria contain UVA-absorbing compounds. *J Photochem Photobiol B* **167**:168–175. doi:10.1016/J.JPHOTOBIOL.2016.12.019

Yu D, Chen C, Chen Z. 2001. Evidence for an important role of WRKY DNA binding proteins in the regulation of NPR1 gene expression. *Plant Cell* **13**:1527–1540. doi:10.1105/tpc.010115

Zaychikov VA, Potekhina N V, Dmitrenok AS, Fan D, Tul'skaya EM, Dorofeeva L V, Evtushenko LI. 2021. Cell Wall Rhamnan in Actinobacteria of the Genus Curtobacterium. *Microbiology (N Y)* **90**:343–348. doi:10.1134/S0026261721030139

Zentgraf U, Doll J. 2019. Arabidopsis WRKY53, a Node of Multi-Layer Regulation in the Network of Senescence. *Plants (Basel)* **8**. doi:10.3390/plants8120578

Zhang L, Yan J, Fu Z, Shi W, Ninkuu V, Li G, Yang X, Zeng H. 2021. FoEG1, a secreted glycoside hydrolase family 12 protein from Fusarium oxysporum, triggers cell death and modulates plant immunity. *Mol Plant Pathol* **22**:522–538. doi:10.1111/MPP.13041

Zheng Z, Qamar SA, Chen Z, Mengiste T. 2006. Arabidopsis WRKY33 transcription factor is required for resistance to necrotrophic fungal pathogens. *Plant J* **48**:592–605. doi:10.1111/j.1365-313X.2006.02901.x

Zilber-Rosenberg I, Rosenberg E. 2008. Role of microorganisms in the evolution of animals and plants: the hologenome theory of evolution. *FEMS Microbiol Rev* **32**:723–735. doi:10.1111/j.1574-6976.2008.00123.x

Zou L, Yang F, Ma Y, Wu Q, Yi K, Zhang D. 2019. Transcription factor WRKY30 mediates resistance to Cucumber mosaic virus in Arabidopsis. *Biochem Biophys Res Commun* **517**:118–124. doi:https://doi.org/10.1016/j.bbrc.2019.07.030

Zulak KG, Cox BA, Tucker MA, Oliver RP, Lopez-Ruiz FJ. 2018. Improved Detection and Monitoring of Fungicide Resistance in Blumeria graminis f. sp. hordei With High-Throughput Genotype Quantification by Digital PCR. *Front Microbiol* **9**. doi:10.3389/fmicb.2018.00706

Zuluaga AP, Vega-Arreguín JC, Fei Z, Ponnala L, Lee SJ, Matas AJ, Patev S, Fry WE, Rose JKC. 2016. Transcriptional dynamics of Phytophthora infestans during sequential stages of hemibiotrophic infection of tomato. *Mol Plant Pathol* **17**:29–41. doi:https://doi.org/10.1111/mpp.12263

Zuo W, Ökmen B, Depotter JRL, Ebert MK, Redkar A, Misas Villamil J, Doehlemann G. 2019. Molecular Interactions Between Smut Fungi and Their Host Plants. *Annu Rev Phytopathol*. doi:10.1146/annurev-phyto-082718-100139

6. Appendix:

6.1 GH25 sequences with accession number:

>*Moesziomyces bullatus* ex *Albugo* on *Arabidopsis* (*MbA*)

MKFSATALIGTLAGLASLSVGAPLEKRVSGTPGFDISGYQPNPNYSSAVANGAKFVII
KATEGTTFKSSSFSSQYTGATNAGLIRGAYHFAHPDSSSGATQAKFFLANGGGWSGD
GRTLPGMIDLESVSGSPTCYGLSQSALVSWIKDFGNTYKASTGRYPMIYTSSGWWNQ
CVASSAFAADYPLVVANYGVSSPKIPTGFSYYSFWQYADSGTYPGDQDTWNGDLAS
LKKFATG

>*Moesziomyces antarcticus* T-34 _GAC71720.1

MKFSATALIGTLAGLASLSVGAPLEKRVSGTPGFDISGYQPNPNYSSAVANGAKFVII
KATEGTTFKSSSFSSQYTGATNAGLIRGAYHFAHPDSSSGATQAKFFLANGGGWSGD
GRTLPGMIDLESVSGSPTCYGLSQSALVSWIKDFGNTYKASTGRYPMIYTSSGWWNQ
CVASSAFAADYPLVVANYGVSSPKIPTGFSYYSFWQYADSGTYPGDQDTWNGDLAS
LKKFATG

>*Moesziomyces aphidis* _ETS64701.1

MRFSATALIGTLAGLASLSVGAPLEKRVSGTPGFDISGYQPNPNYSSAVANGAKFVIIK
ATEGTTFKSSS
FSSQYTGATNAGLIRGAYHFAHPDSSSGATQAKFFLANGGGWSGDGRTLPGMIDLES
VSGSPTCYGLSQSALVSWIKDFGNTYKASTGRYPMIYTSSGWWNQCVASSAFAADY
PLVVANYGVSSPKIPTGFSYYSFWQYADSGTYPGDQDTWNGDLASLKKFATG

>*Ustilago_trichophora*_SPO25525.1

MKFFTTALVGSLAALASCIQAAPLVKRVSGTPGFDISGYQPNPNYSSAVANGAKFVII
KATEGTTFKSSSFSSQYTGATNAGLIRGAYHFAHPDSSSGSAQAKFFLANGGGWSSD
GRTLPGMLDLESVSGSSTCYGLSRSALVSWIQDFGNTYKSATGRYPMIYTNAGWWN
QCVASSAFAADYPLVVANYGVSSPKIPTGFTYYSFWQYADSGTYPGDQDTWNGSLD
SLKTFARG

>*Sporisorium_graminicola*_XP_029737830.1

MKFSGVAIVGTLAALASVSRSAPLEKRVSGVPGFDISGYQPNPNYSSDVANGAKFVVI
KATEGTTYKNPDFSSQYNGATNAGLIRGGYHFAHPDKSSGATQAKFFLANGGGWSN
DGRTLPGALDLESSSGSATCYGLSQSSMVSWIKDFGNTYHASTGRYPTLYCSSGWW
NQCVDSSAFASDYALWIANYGVSSPKIANGFSYYTFWQYADSGKFDGDQDVFNGSY
DNLKKFATGG

>*Sporisorium_reilianum*_f.sp.*reilianum*_SJX62959.1

MKFSGTAIVGTLAALASCIQAAPLEKRVSGVPGFDISGYQPNPNYSSDVANGAKFVVI
KATEGTSYKNPYFSSQYNGATNAGLIRGAYHFARPDKSSGAAQAKYFLANGGGWSN
DGITLPGSLDMESSSGVATCYGLSQSGMVSWIKDFSNTYYSSTGRYPTIYCSSGWWN
QCVASSAFSSTNALWIANYGVSSPKIPTGWDYYTFWQYADSGTYDGDQDTFNGSLD
NLKKFARGG

>*Sporisorium_reilianum*_SRZ2_CBQ73122.1

MKFSGTAIVGTLAALASCIQAAPLEKRVSGVPGFDISGYQPNPNYSSDVANGAKFVVI
KATEGTSYKNPY
FSSQYNGATNAGLIRGAYHFARPDKSSGAAQAKYFLANGGGWSNDGITLPGSLDME
SSSGVATCYGLSQSGMVSWVKDFSNTYYSSTGRYPTIYCSSGWWNQCVASSAFKSSS
ALWVANYGVSSPKIPTGWDYYTFWQYADSGTYDGDQDTFNGSLDNLKKFARGG

>*Kalmanozyma_brasiliensis_* XP_016290453.1

MKFSIATLVGAVAALAACTQAAPLEKRVSGVPGFDISRYQSNVDFNQAKANGARFVI
IKATEGTTVKSSAFSSQYTGATNAGLIRGAYHFARPDSSGGAAQANFFLNNGGGWSS
DGRTLPGMLDLESSSGVATCYGLSRSQLVSWISDFGETYRSSTGRYPMIYTNSGWWN
QCVASSAFASNYPLVVASYSSSPKIPTGFSTYSFWQYADSGTYPGDQDTWNGNLDNL
QKFASG

>*Sporisorium_scitamineum_*CDR99711.1

MKFSGVAIVGFLAALAYSTQAAPLEKRVSGVPGFDISGYQPNPDYSRDVANGAKFVV
IKATEGTSYKNPYFSSQYNRATNAGLIRGAYHFAHPDRSSGSAQANFFLANGGGWSN
DGITLPGSLDLESSSGSATCYGLSQSGMVSWIKDFGNTYYASTGRYPTLYASSGWWN
QCVASSAFADLYALWVANYGVSSPRIPTGFSYYTFWQYADSGTFDGDQDVFNGSFD
NLQKFARGG

>*Ustilago_hordei_*CCF52975.1

MVIVNSVFNRQLIEPVPLPNLEQYNYTQSCSLTTAGTNQIKLATTTILAAVASLATLID
ASPIDKRVSGVRGQDVSAYQPNVNFNTEASKGCKFVYIKATERTTFKSCTFSSQYNG
ATSAGLIRGAYHFARPNSSSGSAQAKFFLANGGGWSNDGRTLPGVVDLESVSGQPTC
YGLSKSQLISWLQDFGSTYYSATGRWPTIYTSSGWWNECVASSAFAADYLLWIANY
VLSCPKMPTGFSYYSFWQYADSVDLSGDQDVWNGSLESLKAYARG

>*Ganoderma_boninense_*VWP02528

MKFPTASLLALAVAAVSASPTPELEARASKPKGIDVSNWQGTVNFSTAKSHGVEFAY
IKATEGTTYVDPTFSSHWESATKAGILRGAYHFAHPAGSSGAAQAEYFIAHGGGWSK
DGRTLPGALDIEYNPSGSECYGMTHGQIVAFVKDFSDTYHKKTSVYPIIYTTTDWWK
TCTGNSAEFGKTNPLWLADWSSSIGELPAGWKYATFWQYADKGSLGPGDQDEFNGT
YDGLKKIASG

>*Trichophyton_interdigitale_* EZF33479.1

MKLSLLTVAAAAGAAVAAPAAEIDTRAGSVQGFDISGYQPNVDFRAAYNGGARFV
MIKATEGTTFKSSTFNSQYTGATNNKFIRGGYHFAHPDGSATAQCDYFLANGGGWS
NDGITLPGMIDLEGTSGKPKCYGLSASSMIAWIKAFSDRYRAKTGRYPMIYTSPDWW
QSCTGNTKSFGTTNPLVLARWASSPGTAPGGWPYHTFWQNADTYRFGGDSEIFNGG
MDQLQRFAKGG

>*Metarhizium_anisopliae_*KFG85189.1

MKRSGAISLGFAALVSSAAASPVQLEQRAATVKGFDISSYQPNVDFHKAYADGARFV
IIKATEGTTYTDKTFSKHYTGATEAKLIRGAYHFAHPGQNQASAEADFFVKNGGGWS
GDGITLPGMVDLESEKGHPQCWGLSHSAMVAWIRDFADTYHEKTTRWPMLYTNPS
WWSSCTGNSQAFKDTCPLVLARYAGSPGAIPGGWPAQTIWQNSDKSPWGGDSDVFN
GDLARLKKLATG

>*Pochonia_chlamydosporia*_RZR65980.1

MKTTAISLGLAALIGSVAASPIEIEERAATVKGFDISSYQPNVDFAKAYAGGARFVIIK
ATEGISYTDKTFSKHYTGATKAKLIRGAYHFAHPGQNKASAEAEFFVKHGGGWSKD
GITLPGMVDLESEQGHPQCWGLSHSAMVAWIKEFADTYHKKTTRYPMLYTNPSWW
SSCTGNSKAFKDTCPLVLARYASSPGTIPGGWPAQTIWQNSDKSPWSGDSDIFNGDLT
RLKKLATG

>*Dichomitus_squalens*_TBU22184.1

MKFATASVFVLVATAATALPVLQKRANPKGIDISSYQGTVNFNTVKANGISFVYIKAT
EGTTFKDPNFSSHYEGATNAGLIRGGYHFAHPGSSSGATQAKYFLAHGGGWSSDGIT
LPGALDIEYNPSGAECYGLSASEMVSWIKDFSNTYHSSTGVYPVIYTTTDWWKTCTG
NSAAFASTNPLWIARYSSSIGALPAGWSYTTFWQYADSGSNPGDQDEFNGTLDGLKK
LALG

>*Aspergillus_fumigatus*_ XP_001481415.1

MKFSIVAIATIAGLASALPSQPEARATTVQGFDISNHQKSVNFEAAKKDGAQFVMIKA
TEGTTYKDTVFNSHYTGATKAGLLRGGYHFARPDKSTGSTQAKFFLKNGGGWSDDN
RTLPGMLDIEYNPYGATCYGLSHSQMVAWIHDFVNEYHHATSRWPMIYTTADWWN
RCTGNAKGFGDKCPLVLAAYSSSPPKTIPGDWKTWTIWQNSDKYKHGGDSDKFNGP
MTQLRKLASG

>*Pseudogymnoascus_verrucosus*_XP_018132300.1

MKLSALAVASILGFAAATPAPLEKRATVQGFDISGYQPSVNFAAAYASGARFVIIKAT
EGTTFISSTFSSQYTGATNAGFIRGGYHFAHPGSSTGAAQANYFLAHGGGWSKDGITL
PGMLDIEYNPSGATCYGLSAASMVAWIHDFVNTYHTKTGVYPMIYTTTDWWTQCT
GNSAAFASTCPLVLARYASSPGTMPAGWPYQTIWQNSDAYAYGGDSDVFNGSLDQL
KKIALG

>*Talaromyces_marneffei*_XP_002145760.1

MNMLVSTLAVSASLFGLAKATVQGFDISSYQPNVNFNAAYSAGARFVIIKATEGTTYI
DSTFSNHYIGATNAGFIRGGYHFAHPSVSSGATQAKYFIAHGGGWSGDGITLPGMLDI
EYNPNGATCYGLSASQMVSWIHDFVNTYYASEGVYPMIYTTNDWWTTCTGDSTAFS
TTCPLVLARYASSPGTIPGGWGYQTIWQNTDSYAYGGDSDVFNGALSQLKAIALG

>*Fusarium*_sp._ KAF5012743.1

MNMLVSTLAVSASLVGLAKATVQGFDISSYQPSVDFSAAYDSGARFVIIKATEGTDYI
DSTFSSHYTGATNAGFSRGGYHFAHPDSSSGATQAKYFIAHGGGWSGDGITLPGMLD
IEYNPSGATCYGLSASAMVSWISDFVNTYHASEGVYPLIYTTNDWWTTCTGDSTAFS
STCPLVLARYGSSPGTIPGNWGYQTFWQNADSYTYGGDSDIFNGGLSQLKAIASG

>*Thermothielavioides_terrestris*_NRRL8126_XP_003650266.1

MLTSALLASLALAAGVKATVQGFDISHYQPNVDFAAAYNAGARFVIIKATEGTSYID
PSFSSHYTGATKAGLIRGGYHFAHPGETTGAAQADYFIAHGGGWTPDGITLPGMLDL
ESESNGECWGLSASAMVAWIRDFSDRYHERVGVYPMLYTNPSWWQTCTGNSNAFV
NTNPLVLAHYSSSVGTIPGGWPYQTIWQNSDSYKYGGDSDIFNGSLDRLQALAKGS

>*Coniochaeta*_sp_KAB5536330.1

MKSTIAAVLGLAATAQATVQGFDISHYQSSVNFAAAYSAGARFVIIKATEGTTYTDP
AFSSHYTGATNAGLIRGGYHFAHPGETTGAAQADYFIAHGGGWSGDGITLPGMLDLE
SEGGATCWGLSASAMVAWIKAFSDRYHSRTGRYPMLYTNPSWWSSCTGNSNAFVN
TNPLVLARYSSSPGTIPGGWPYQTIWQNSDSYAYGGDSDIFNGDIAGLRRLATG

>*Cordyceps_militaris*_ATY65680

MKSFSSIITGIAGLASVASATVQGFDVSGYQPTVNWGAAYSSGARFVMIKATEGTGYI
SPSFNSQYPGATNAGFIRGGYHFALPDRSSGSTQADYFIAHGGGWSGDGITLPGMLDI
EYNPYGATCYGLSQSAMVNWISDFLERYKAKTTQYPIIYTTTDWWKTCTGNSPAFG
QKSPLSLARYASSVGEIPNGWSYQTFWQNSDKYAYGGDSQIFNGAYTQLQKIARGG

>*Neurospora_crassa*_XP_964535.1

MKSFVLTALAGLVGAVQATVQGFDISHYQGSVNFARAYSSGARFVIIKATEGTNYID
PKFSSHYTGATSAGLIRGGYHFAHPDSSSGAAQADYFLAHGGGWSKDGITLPGMIDL
ESSSGKATCYGLSTSAMVSWIKAFSDRYHSKTGRYPMIYTNYSWWSKCTGNSKSFAT
TNPLVLARWSSSVGTIPGGWSYQTIWQNADTYTYGGDSDIFNGSLDRLKALAKGS

>*Sordaria_macrospora*_XP_003352547.1

MKSFSVLTALAGLIGAAQATVQGFDISHYQSSVNFAGAYSSGARFVIIKATEGTTYTD
PKFSSHYTGATSAGLIRGGYHFAHPDSSTGAAQADYFLAHGGGWSNDGITLPGMIDL
ESVSGKATCFGLSTSAMVSWIKSFSDRYHTKTGRYPMIYTNYSWWNQCTGNSKTFA
TTNPLVLARWSSTIGTLPGGWSVHTIWQNADTYTYGGDSDVFNGSLDRLKALAKGS
G

>*Penicillium_rubens*_Wisconsin_54-1255_ XP_002564022.1

MKINALPLLFATAASASVQGFDISGYQPKVDFAGAYAAGARFVMIKATEGTSFISSSF
SSQYQGATSAGLIRGGYHFAHPDSSTGAAQAKYFIAHGGGWSDDGLTLPGMLDIEYN
PSGATCYGLSHSAMVSWIKDFGETYKSAAGRYPMIYTTADWWNTCTGGSTAFSQDY
PLVLARYSTSVGTIPGGWPFQSFWQNSDAYSFGGDSEIWNGSEASLKTFAKTAA

>*Peltaster_fructicola*_ QIW99810.1

MHNIVATTLAIAGTAYAAVQGFDISHYQPNFDYNSAAASGARFGIVKCTEGISVVDE
KFSDHYNGVTNAGMYRGAYHFARPQRSSGTDQANFFLNYGGGWTPDGITLPGMLD
LENNPGSGGQCYGLSQASMVQWVSDFIETYGATTGRYPMIYTTNNWWRTCTGNTG
AFNQKSPLVLARYSSSAGTVPGGWPYHTIWQNSANYAYGGDSDFFNGDENGLARLA
SG

>*Phialemoniopsis_curvata*_XP_030995322.1

MKVTIASALTLAATAQAAVQGFDISHYQPNVDFAAAKASGARFVIIKATEGTSYIDPS
FSSHYTGATNAGLIRGGYHFAHPGQTTGAAQADYFLAHGGGWSGDGITLPGMLDLE
SEGSSGECWGLSASAMVAWIKAFSDRYHSKTGRYPMLYTNPSWWKDCTGNSNAFV
STNPLVLARYSSSPGTIPGGWPYQTIWQNSDSYKYGGDSDIFNGSEDNLRKLATG

>*Aspergillus_nidulans*_ XP_664074.1

MKGISLLALPGLAYAAVQGFDISNWQPTVDYKGAYASGARFVMIKATEGTSFIDPLF
NTHYPGATSAGLIRGGYHFAHPDSSSGSAQAKYFLAHGGGWSGDGITLPGMLDLEA
GCYGLSATAMVSWISDFGETYKSATGRYPMIYTTTSWWQECTGNNDGFGEYPLVLA
RWASTPGTLPASWDYYSFWQNSDSYAYGGDSQLWNGSEERLRIFASG

>*Aspergillus_nidulans_* XP_682238.1

MKFISVLALPGLAYAAVQGFDISHYQETVDYQGAYDSGARFVMIKATEGTSYTDPKF
STHYSGATSAGLIRGGYHFAQPGSSSGADQASYFIEHGGGWSGDGQTLPGMLDLEAG
CYGLSTSAMSSWIKDFGETYKAATGRYPMIYTTTSWWQECTGNDSGFGEYPLVVAR
WGSSVGTLPASWSTHSFWQNADTYEFGGDSEVWNGSEDSLKTFAK

>*Xylaria_grammica*_RWA07563.1

MKASLVSLLGLANGALATVQGFDISHYQSSVNFAAAYSAGARFVIIKATEGTTYLDPS
FSSHYTGATNAGFIRGGYHFAHLDTSSGATQANYFLAHGGGWSGDGITLPGMLDLE
GSCVLSASATVAWIKDFSNTYHSKTGVYPLLYTNPSWWSSCTGNSNAFVNTNPLVLA
RYSSSAGTPPGGWPYYTFWQYNDAYTYGGDSEVFNGDMAGLLRIAKG

>*Piromyces* _sp_ AWI66961.1

MRLNIKSILSLITVPVVLGIPCVSPDGDRDLCINDDDSGAPIPIFESFEESSNDFSDFEFET
PDVEIEKPVIEIETTEIEIETPDLEIETSKTPEIEVRTPEIEVRTPEIEESIIHNIIDISKFNTVK
DYELAASEPDVEGVIMRVGGRGWGSGAIYDDTLFETHYKNFAATKKVKIGYYFYSQ
AINEEEAIEEAQYVLDNIKGKQCDFPIYWDTELADSENHEGRADLLSVSERMKVGLA
FIKHIQSNGYRAGVYSNDSWYNNQLNFKQFVDAGASIWVARYVSDLSITPTQPSYDA
WQYTSSGKVNGIQGNVDKSFVFTNLAGWEIETPEDEIKTPEVEIKTPEIEESVIHNIIDIS
K

> *Piromyces_ finnis_* ORX43133.1

MRLNLKCLLTLLVPLALAKVEDPCTAPGGEGVCIDKSLCKMSSGQKGTATTYTGYC
KNDPANILCCVKKVTQLTNGTNLSKAGVCKNVSKCPTNSNTLYSNQCPGSSNVKLC
VPKVTTTTKKTTTTKKTTTTTKKTTTTKKATTIIKPTTFKQKEIIDLSKWNVVNDYSA
AAKEIDGVILRCGYRGYGSSGSLAKDDKLETHYNGFKGKTKIGYYFFTQAKTTAEAE
AEATYVVNTLLKGKTNNFPIFWDSELSGASGNTGRADGLSKTTRTNCAVAFIKKIKA
LGYKAGVYASESWFRDNLDLKKLTDAGAYIWVAKYSNNSPSTSSYDAWQYSSSGSV
KGINGNVDKSHVYKNIAGW

>*Chalaropsis*_sp_P00721.1

TVQGFDISSYQPSVNFAGAYSAGARFVIIKATEGTSYTNPSFSSQYNGATTATGNYFIR
GGYHFAHPGETTGAAQADYFIAHGGGWSGDGITLPGMLDLESEGSNPACWGLSAAS
MVAWIKAFSDRYHAVTGRYPMLYTNPSWWSSCTGNSNAFVNTNPLVLANRYASAP
GTIPGGWPYQTIWQNSDAYAYGGSNNFINGSIDNLKKLATG

>*Botrytis_cinerea*_XP_001558643.2

MSFSKIFIAFAGIIAVASSNPLVPRASTACSTSSGPGFCQSTSSSCSGGKYIAGACPGGV
DNQCCVATCSSGKGVCQATSVACSGGSFSSGLCPGPADVQCCIKSGGGTTPPSSGAG
SLGIDISQLGTPAFFECAKKTKDIVAIRGYQQACGTGGQVDKNFVASYKNAKAAGFT
RIDSYIFPCTGTPTGSEPKCKSVDTQMAEYLKVISDNNMDIHTLWLDLEPTSVSNSPCN
AWNLGAAANEKLAKQWVTAMKATGLKWGIYANGNQWSGIFASRSTDIGSDLPLWA
VQEDYKEGVNTVTTFMGGWTKAVAKQYSLDTTLCGLGVDLDSFA

>*Sclerotinia_sclerotiorum*_XP_001597807.1

MSLSKIFIAFTGIIAVASSNPLIPRASTACSTSSGPGFCQSTSTSCTNGKYIAGACPGAAN
NQCCVATCSSGQGTCQATSVSCSGGTFKSGLCPGPSDIECCIKSSGSTGSLGFDISQLG

STTFFQCAKKTKDVVVIRGYEQACGSGGQVDSNFVTSYKNAKAAGFTRIDSYLFPCT
GTPTGNEPQCKSISTQISEYLQVISSNNMDITMLWLDIEPTSASTSACNAWNLGAAAN
EKLAKQWVAAIKATGLKWGIYANGNQWSGMFASRSTDVGSELPLWAVQDDFEAGV
NTVDTFMGGWTEAVAKQYYLDTTLCGLGVDLDSFS

>*Lichtheimia_ramosa*_CDS02619.1

MKNLLVGLSLLASAFVSTQAANTGVDVSALTSTSAWSCAKNYGYSHAIIRCYFEAW
GGNPGGALDSSCAQNYANAVAGGFNQIDLYMFPCTGRSTCKSPATQVNEMVAHMN
KNKMKIGTLWLDVEVDPQSNNWPSASQAQSTLKQFKQAFDATGLKWGVYASQSQ
WTSITGSKDWVLDSSVPLWYAHYDEALNFNDFSPFGGWTKPTIKQYAGSQSFCSGN
WDKNFYG

6.2 Appendix Figures

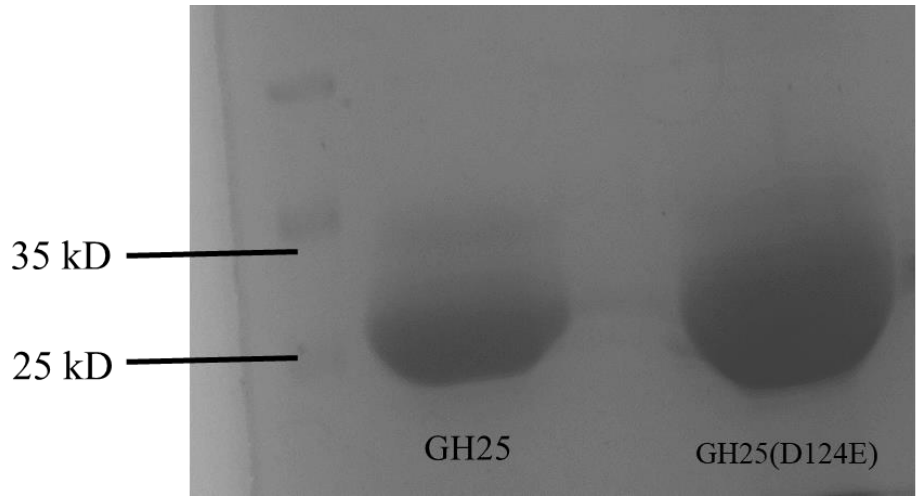

Figure 6.2. 1 Visualization of purified *MbA*_GH25

*MbA*_GH25 and *MbA*_GH25(D124E) purified by Ni-NTA affinity chromatography visualized on 12%SDS gel; expected band size- 27KDa.

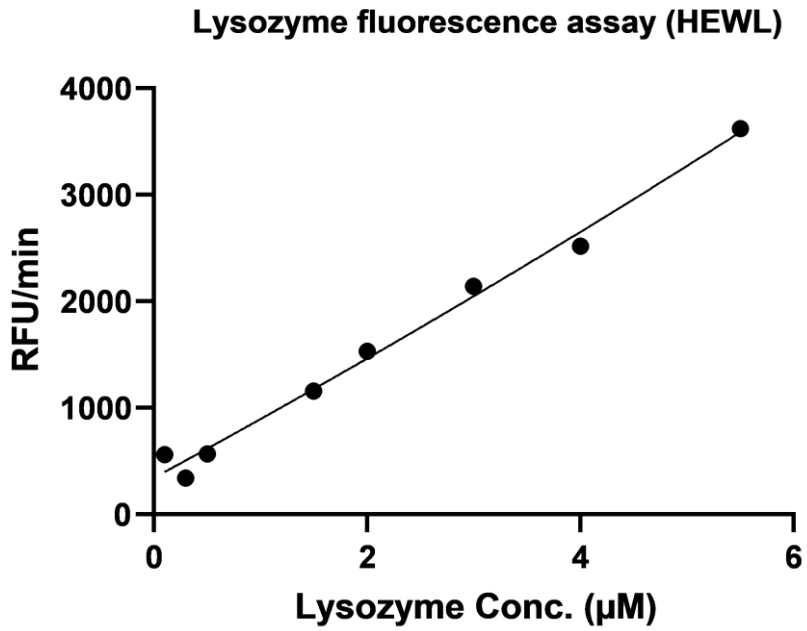

Figure 6.2. 2 Detection of lysozyme activity for commercial Hen-egg white lysozyme (HEWL)

HEWL (stock solution, 11 µM) was tested for activity using the EnzChek Lysozyme Assay Kit. The fluorescence was recorded every minute in a fluorescence microplate reader using excitation/emission of 485/530 nm in increasing concentrations from 0.1 µM to 5.5 µM. Finally, relative fluorescence unit (RFU)/min was calculated for each concentration and plotted on the graph.

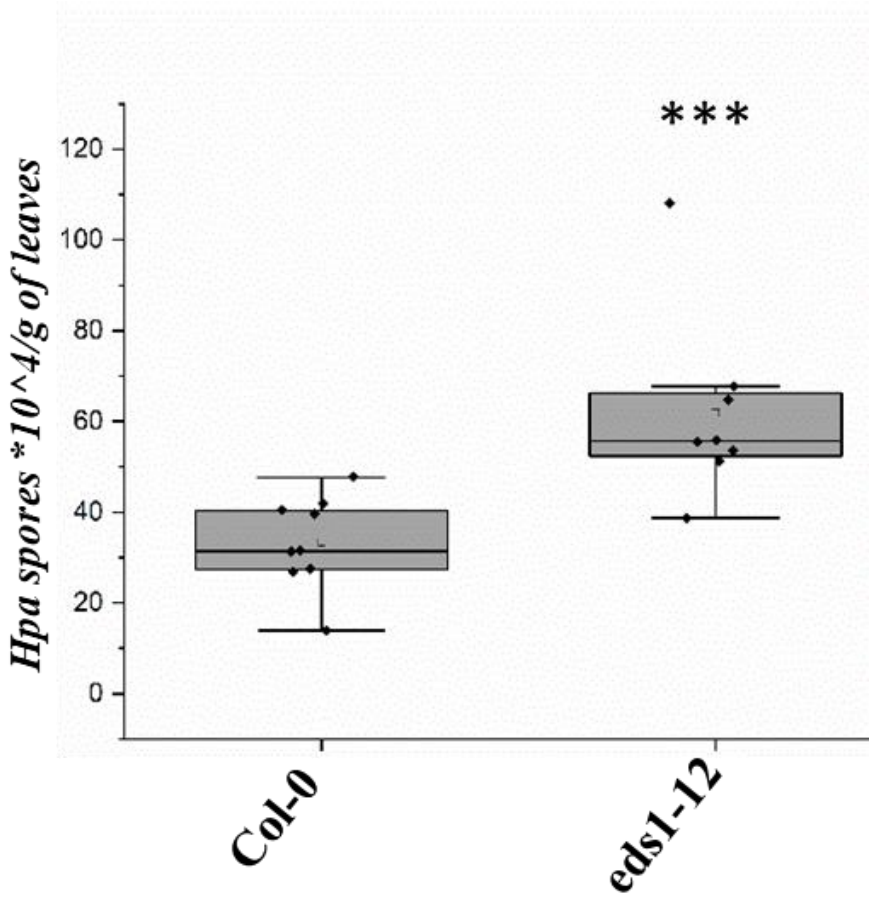

Figure 6.2. 3 *Hpa* infection in Col-0 vs *eds1-12*

Quantification of *Hpa* spores *10^4 / g of leaves was performed at 5 dpi on Col-0 and eds1-12 mutant (in Col-0 background) A. thaliana seedlings Experiments conducted in three biological replicates (consisting of three technical replicates). One-way ANOVA was performed to find significant difference between treatments.

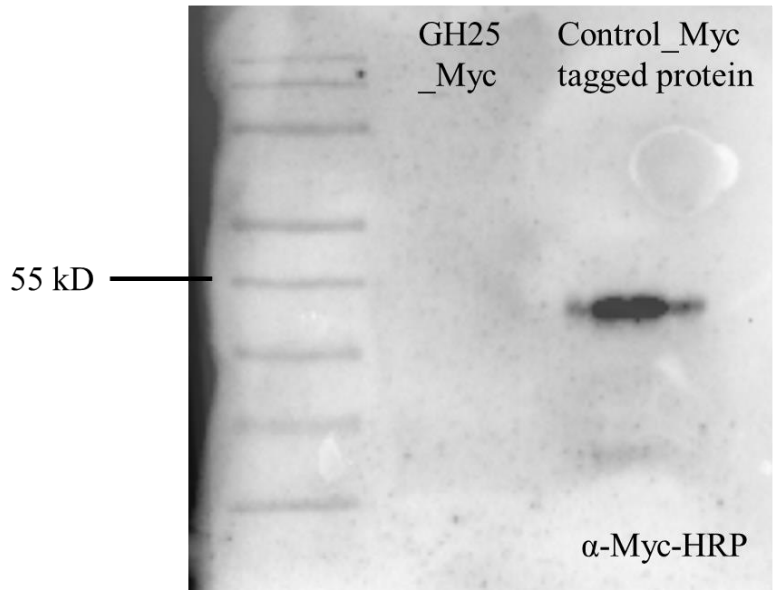

Figure 6.2. 4 Transient expression of *MbA*_GH25 using Myc-epitope

Agrobacterium vector expressing Myc tagged GH25 was infiltrated into 5 weeks old *N. benthamiana*. 3 days post infiltration, total protein extracted and western blot performed with α-Myc antibody, however no expression of GH25_Myc protein was detected.

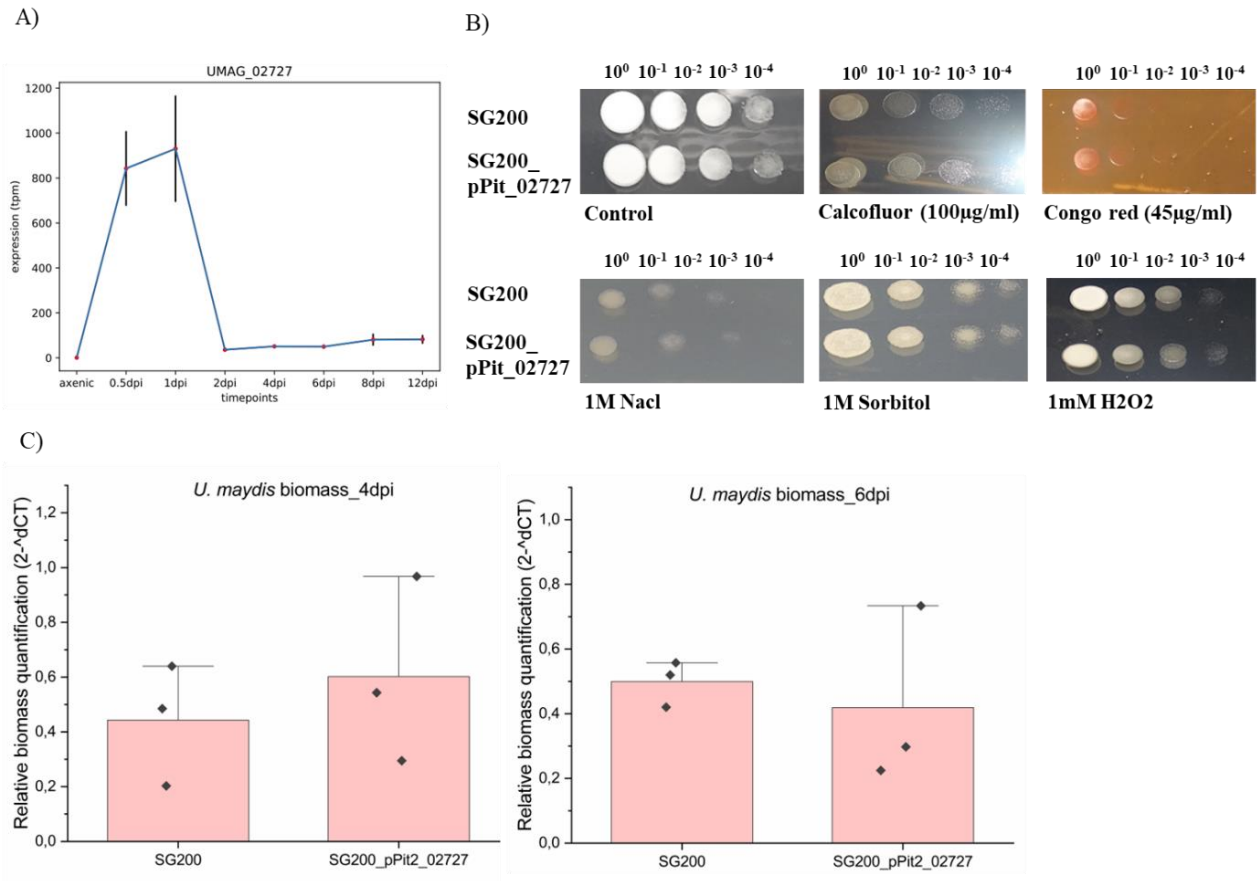

Figure 6.2. 5 Functional characterization of UMAG_02727

A) Gene expression analysis of *Ustilago maydis* GH25 gene (UMAG_02727) in axenic culture and *in planta* (*Zea mays*) with highest level of expression between 0.5 and 1 dpi. B)- Stress assay of SG200 and SG200_pPit2_02727, on CM medium and 2% glucose (Control) and different conditions such as 100 µg/ml calcofluor, 45 µg/ml Congo-red, 1 M NaCl, 1 M sorbitol and 1 mM H2O2. The strains were dropped on the CM plates containing different stress supplements in a dilution series from 10^0 to 10^{-4}. C)- Relative biomass quantification of *U. maydis* at 4dpi and 6dpi with *U. maydis* housekeeping gene ppi normalized to maize housekeeping gene gapdh. Experiment performed in three biological replicates; error bar represents outlier (co-eff.-1.5). No significant difference in biomass observed with unpaired t-test.

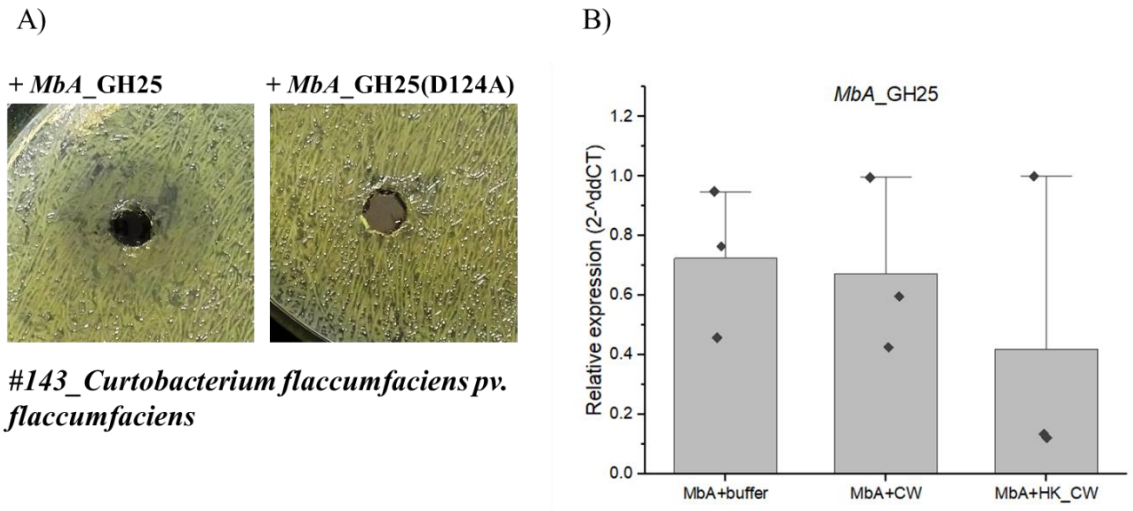

Figure 6.2. 6 Mechanism of *MbA*_GH25 antagonism

A)-*Curtobacterium flaccumfaciens pv. flaccumfaciens* inhibited by *MbA*_GH25 protein as indicated by halo formation as opposed to purified *MbA*_GH25(D124A). B)- *MbA* gh25 expression analyzed in response to extracted *Albugo* cell wall (CW) and Heat-killed (HK) *Albugo* CW in three biological replicates. *MbA* housekeeping gene ppi was used; error bars indicate outlier -coeff-1.5. Unpaired t-test was performed but no significant difference in between treatments or *MbA* in axenic culture was observed.

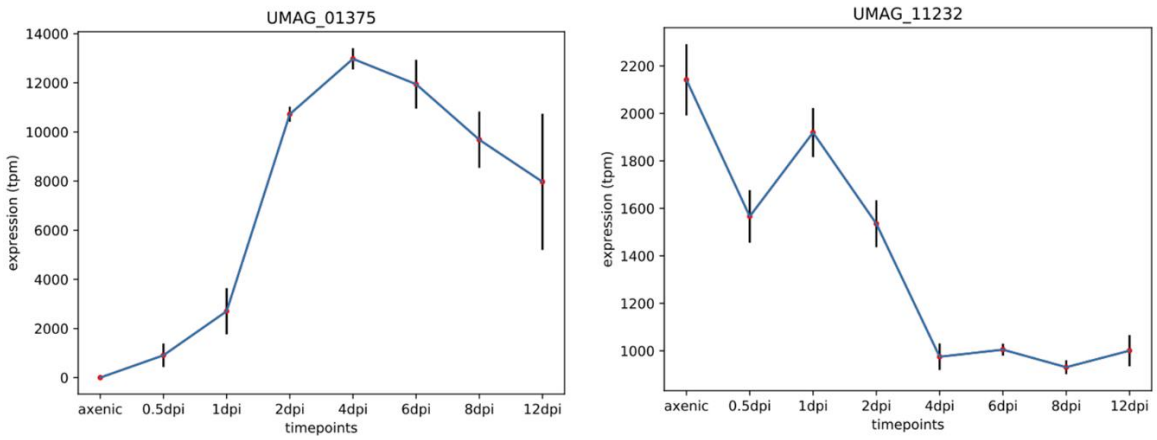

Figure 6.2. 7 Difference in gene expression pattern between Pit2 and Actin

Gene expression analysis of *Ustilago maydis* Pit2 (UMAG_01375) and Actin (UMAG_11232) in axenic culture and in planta (*Zea mays*) at different time points. Pit2 has much higher in planta expression levels.

Table 6. 1 Maize disease index calculation

Calculation of the tumor formation index in seedling (13dpi), p-value ≤ 0.05 = significant)

Strains	Replicate	Heavy tumors	Tumors	Small tumors	Index	Index relative to SG200	p-value (compared to SG200)
SG200	1	5	10	36	2.246753	1	
	2	7	6	30	2.568966	1	
	3	7	11	29	2.553846	1	
SG200_pPit2_02727	1	0	0	38	1.628571429	0.72485	0.001
	2	0	0	37	1.881355932	0.73234	
	3	0	0	33	1.455882353	0.570074	
SG200_pActin_02727	1	3	11	26	2.245902	0.999621	0.22
	2	5	8	23	2.625	1.021812	
	3	5	4	19	2.085106	0.816457	

Erklärung zur Dissertation:

gemäß der Promotionsordnung vom 12. März 2020

Hiermit versichere ich an Eides statt, dass ich die vorliegende Dissertation selbstständig und ohne die Benutzung anderer als der angegebenen Hilfsmittel und Literatur angefertigt habe. Alle Stellen, die wörtlich oder sinngemäß aus veröffentlichten und nicht veröffentlichten Werken dem Wortlaut oder dem Sinn nach entnommen wurden, sind als solche kenntlich gemacht. Ich versichere an Eides statt, dass diese Dissertation noch keiner anderen Fakultät oder Universität zur Prüfung vorgelegen hat; dass sie - abgesehen von unten angegebenen Teilpublikationen und eingebundenen Artikeln und Manuskripten - noch nicht veröffentlicht worden ist sowie, dass ich eine Veröffentlichung der Dissertation vor Abschluss der Promotion nicht ohne Genehmigung des Promotionsausschusses vornehmen werde. Die Bestimmungen dieser Ordnung sind mir bekannt. Darüber hinaus erkläre ich hiermit, dass ich die Ordnung zur Sicherung guter wissenschaftlicher Praxis und zum Umgang mit wissenschaftlichem Fehlverhalten der Universität zu Köln gelesen und sie bei der Durchführung der Dissertation zugrundeliegenden Arbeiten und der schriftlich verfassten Dissertation beachtet habe und verpflichte mich hiermit, die dort genannten Vorgaben bei allen wissenschaftlichen Tätigkeiten zu beachten und umzusetzen. Ich versichere, dass die eingereichte elektronische Fassung der eingereichten Druckfassung vollständig entspricht.

Teilpublikationen:

Chaudhry V, Runge P, Sengupta P, Doehlemann G, Parker JE, Kemen E. 2021. Shaping the leaf microbiota: Plant-microbe-microbe interactions. *J Exp Bot* **72**:36–56. doi:10.1093/jxb/eraa417

Eitzen K, Sengupta P, Kroll S, Kemen E, Doehlemann G. 2021. A fungal member of the Arabidopsis thaliana phyllosphere antagonizes Albugo laibachii via a GH25 lysozyme. *Elife* **10**:e65306. doi:10.7554/eLife.65306

17.10.2022	Priyamedha Sengupta	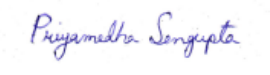
Datum	Name	Unterschrift

Delimitation of own contribution:

I have conducted all the results in this study independently and without other assistance than stated here. Part of my results have already been published in "A fungal member of the *Arabidopsis thaliana* phyllosphere antagonizes *Albugo laibachii* via a GH25 lysozyme" was written in collaboration with Dr. Katharina Eitzen, Prof. Dr. Gunther Doehlemann, and Prof. Dr. Eric Kemen.

The experimental contributions of other persons that participated in this study are listed below:

Katharina Eitzen together with her student helper Franca Arndt constructed the *Pichia pastoris* strain expressing *MbA*_GH25. Katharina also generated the MbA_GH25 knockout strain - *MbA*_Δg2490.

Teres Mary Jacob performed the stress assay with *Ustilago maydis* SG200 and SG200_pPit2_02727 strains as a part of her 6 weeks Masters' module.

Acknowledgements:

It is commonly said that it takes a village to raise a child. I feel that it also takes a village to get a PhD. Therefore, I would like to acknowledge everyone who has supported during my time here as a PhD student at Universität zu Köln. Firstly, I would like to thank Prof. Gunther Doehlemann for giving me the opportunity to pursue my PhD in his group. Thank you, Gunther, for your scientific guidance, for giving me the space and independence to develop my own ideas and always supporting me for my scientific outreach activities.

I would like to thank my thesis advisory Committee members, Prof. Jane Parker and Prof. Eric Kemen for great scientific discussions on my project and helping me to navigate smoothly through my PhD years. I am grateful to Prof. Bart Thomma for being the second reviewer in my thesis defense committee. I am thankful to be a part of the SPP DECRyPT consortium for funding, workshops and establishing strong collaborations within research groups engaged in Plant-microbe interactions. I am thankful to CEPLAS graduate school for providing me with an amazing scientific community and promoting networking and exchange between Cologne, Düsseldorf and Jülich. Thank you to Graduate school coordinators Dr. Nadine Rademacher and Dr. Isabell Witt for their support and organizing workshops and symposia which have benefitted me greatly as a doctoral researcher. I would like to acknowledge Petra Bracht and Claudia Balan from CEPLAS for their encouragement and support in various science communication activities that I have been part of.

Coming to the people with whom I have spent the most amount of time during PhD-all the members of AG Doehlemann. I would start off by thanking Katharina, for taking me under her wings and introducing me to the holy trinity *Moesziomyces-Albugo-Arabidopsis*. Kathi has been an amazing colleague, lab mate and above all, a friend with whom I hope to be in contact with all my life. Huge thanks to Weiliang and Bilal for their guidance and discussion during any experimental hiccups. Sina and Janina are two of the kindest people, I have ever met, who have always been there, whether it is a work-related matter, my wisdom teeth extraction or just for chatting over coffee. I want to thank Yoon Joo and Phillip for being great lab mates, and for all the non(scientific) talks about maize cobs and beyond. Speaking of maize, thanks to Plant-side boys Maurice and Daniel for all the fun conversations in the lab. Thanks to Andrea for being a helpful next-door neighbour and a fellow potterhead. Anna and Luyao, I am so happy to have started my PhD journey with you and wish you both great successes ahead. Thank you so much Johana for all the helpful suggestions and I will miss having random interactions with

you on topics ranging from calculating molarity to Indian food and weddings. Ute, Rapha and Jan, thank you for your incredible support in keeping the AG together. Ute, thank you for helping me avoid two beschaffungsantrag and lending me Murakami for reading. Rapha, I will surely miss the fantasy film festival reminders from you, although I can't bear to watch any of them. I am happy to see the new generation of PhD students Zarah and Laura settling in the AG, who will also take the science communication tradition forward. Zarah, you have been brilliant in adapting to the GH25 project and I am sure you are going to take it to new heights. Thank you, Gudrun, for your support and making me feel at home during my first Christmas vacation here. Cheers to the amazing alumni of AG Doehlemann, Jan (Schulze Hünyck), Selma, Elaine, and Jasper for all the nice time in the lab. Best wishes to Georgios, who is now carrying on with the bioinformatics legacy after Jasper. We have had some great students in the AG, of which I would like to thank Teres for a very productive 6 weeks module. Thanks to Henni, Sena and Fernanda for all the fun interactions. I am very grateful to Jaqueline Bautor for helping me adapt in Prof. Parker's lab at the MPI, the *Hpa* assays would not have been possible without her. Best wishes to Dr. Isabel Saur and members of AG Saur for the coming years.

I would like to thank my friends Jazmin, Sweta and Anjana for making my stay in Cologne very enjoyable. Thanks to Ria and Harshita for all the Bengali food and adda. Finally, I am thankful to my family and friends back in India for their love and support. Thanks to my father, for being a great scientist and introducing me to the academic world from an early age. Thanks to my mother who is a great source of positivity in my life aside from being an amazing scientist turned author. I may have convinced my mom to call germs as microbes, but she gave me the strength to achieve my dreams and continues to do so.

Curriculam vitae:

Priyamedha Sengupta

Born on 31.12.1994 in Kolkata, India

Education:

01/2019-09/2022	**Doctoral research** CEPLAS/University of Cologne, Germany Elucidating the role of Gylcoside Hydrolase family 25 in microbial antagonism (Prof. Dr. Gunther Doehlemann)
07/2018-12/2018	**Research internship** CEPLAS/University of Cologne, Germany Molecular analysis of epiphytic yeasts (Prof. Dr. Gunther Doehlemann)
07/2015-07/2017	**Master of Science in Botany** University of Calcutta, Kolkata, India Post-harvest management of green mould using Biocontrol Agent and Sulphur Nanoparticle with special reference to Mandarin and Indian Gooseberry. (Prof. Dr. Krishnendu Acharya)
07/2012-07/2015	**Bachelor of Science in Botany** Lady Brabourne College, University of Calcutta, Kolkata, India
2012	**School Final Examination (12+)** West Bengal Council of Higher Sceondary Education Carmel High School, Kolkata, India

Honors and Awards

- FEMS Early Career Researcher Travel Grant for miCROPe conference, July 2022, Vienna, Austria.
- Poster award for presentation titled ' Elucidating the role of Glycoside Hydrolase 25 in microbial antagonism' at the SPP DECRyPT conference, Cologne, March 2022.
- First place in Falling walls lab Rhineland for 3 minutes pitch on 'Breaking the wall of Microbial Interactions for Plant protection', Cologne, September 2019.
- Qualified lectureship in CSIR-UGC NET examination, India, December 2017.
- UGC Post-Graduate Indira Gandhi National Scholarship, India from 2015-2017.

Publications

- Eitzen K, **Sengupta P**, Kroll S, Kemen E, Doehlemann G. A fungal member of the *Arabidopsis thaliana* phyllosphere antagonizes *Albugo laibachii* via a GH25 lysozyme. elife 2021 Jan 11; 10. doi: 10.7554/eLife.65306
- Chaudhry V, Runge P, **Sengupta P**, Doehlemann G, Parker JE, Kemen E. Shaping the leaf microbiota: plant-microbe-microbe interactions. J Exp Bot. 2020 Sept 10; 72(1):36-56. doi:10.1093/jxb/eraa417
- **Sengupta, P**., Sen, S., Mukherjee, K., and Acharya, K. Postharvest Diseases of Indian Gooseberry, and Their Management: A Review, International Journal of Fruit Science, 2019 Apr 27; doi: 10.1080/15538362.2019.1608889.
- Sen, S., **Sengupta, P**., Molla, J., Mukherjee, K., and Acharya, K. Management of postharvest green mold decay in common mandarin and Indian gooseberry with Bacillus licheniformis SR-14. Journal of Applied Horticulture, 2018 Mar DOI: 10.37855/jah.2018.v20i02.23.

Scientific communication activities

- Speaker at Pint of Science, Germany, May 9, 2022, on the topic 'Plants and microbes: Keep your friends close, but your enemies even closer'.
- Speaker at Soapbox Science Rheinland, August 21, 2021, Cologne, Germany on the topic 'Frontline workers: How microbes protect plants'.
- Presented a 3-minute pitch 'Breaking the Wall of Pathogenic Invasion for Plant Protection' at Falling walls Lab November 8, 2019, Berlin, Germany.